GIMA
Geographical Information Management and Applications

Improvement of Land Subsidence Communication through Point Cloud Visualizations

Final thesis

Nienke Vogelzang

g.d.vogelzang@students.uu.nl

Supervisor: Edward Verbree

Responsible professor: Peter van Oosterom

February 2021

Universiteit Utrecht

TU Delft

University of Twente

Wageningen UR

Preface

In front of you lies the thesis 'Improvement of Land Subsidence Communication through Point Cloud Visualizations'. This thesis was written as part of my graduation from the master Geographical Information Management and Application within the faculty of Geosciences of the University of Utrecht. I was engaged in this research from September 2020 to February 2021. Together with my supervisor Edward Verbree from TU Delft I was able to finish this thesis, while at the same time enjoy writing it.

The year 2020 was different than the other years of both my bachelor and my master, due to the coronavirus (COVID-2019). It was a challenge to stay connected with my fellow students, but I am happy to say that I managed this challenge due to the online meetings both planned by Edward Verbree and my fellow students. I look back on my thesis as a period in which I learned so many new things. The road to my final thesis did however not go without setbacks, as due to the different topics covered, I sometimes lost the overall picture of my thesis. Edward Verbree always managed to help me see the overall picture again, so I could continue writing my thesis. In short, I look back to this period of study with pride.

I would like to thank Edward Verbree, Peter van Oosterom, Ramon Hanssen and Niels van der Vaart for their feedback on this thesis. Edward Verbree provided feedback on this thesis throughout the whole process of writing it. His knowledge of a broad range of insightful studies and his experience with point clouds helped me writing. Peter van Oosterom and his expertise in point clouds predominantly helped me to formulate my research questions, and to determine the scope of this thesis. The knowledge of Ramon Hanssen of PS-InSAR data helped me to write the chapters of this thesis regarding the technical background of PS-InSAR. Niels van der Vaart was not involved in the complete process of writing this thesis, but Niels provided feedback on the final draft. His insights regarding geographical interfaces were especially valuable for this thesis. Additionally, I would like to thank the company SkyGeo. Their current form of land subsidence communication was fundamental for this thesis, and thanks to SkyGeo the PS-InSAR data is made available. At last, I would like to thank my family and friends for supporting me during the whole process of writing this thesis. I have considered the support of all people involved as incredibly valuable, and I am very grateful for that.

I sincerely hope you enjoy reading this thesis.

Nienke Vogelzang

'S Hertogenbosch, 22 February 2021

Abstract

The land of the Netherlands is significantly moving each year, in both a horizontal and vertical direction. The focus of this study is on vertical deformation, as it is becoming harder for the Dutch society to deal with the adverse effect of vertical deformation. The adverse effects of vertical deformation are not only a problem of the present but also of the future, as with the increase in land subsidence, population and urban land use the adverse effects are also increasing. The adverse effects of the vertical movement of the land of the Netherlands include damage to infrastructure and water management, change in flooding-risks, CO2 emission and changing water quality. Measures and policies that can aid the Dutch society in dealing with the adverse effects of land subsidence or land rise have been, and still are being developed. By giving the society impartial and public access to up-to-date data regarding the rate of land deformation, the processes causing land deformation, and geographical data related to land deformation, public authorities will be able to make better informed decisions regarding measures and policies that are suitable for a large-area level rather than an ad-hoc level. In short, there is a significant need for land subsidence communication in the Netherlands.

Currently, land subsidence in the Netherlands is being communication with the use of Bodemdalingskaart 1.0 and 2.0. Both maps make use of Persistent Scattered Interferometric Synthetic Aperture Radar (PS-InSAR) data, which represents the deformation in the Netherlands at a millimeter level. This thesis analyzed to what extent the current communication of land subsidence in the Netherlands can be improved with the use of adding the two aspects spatio-temporal visualization and Laser Imaging Detection and Ranging (LiDAR) point clouds. The added value of these two aspects has been analyzed based on five sub-process: (1) analyzing the interpretability of the current form of land subsidence communication, (2) defining how the spatio-temporal aspects and LiDAR point clouds can improve the interpretability of the current communication, (3) evaluating and selecting techniques to combine and graphically represent PS-InSAR with LiDAR, (4) creating the prototype and (5) testing the prototype. The results from this thesis highlight the added value of a spatio-temporal visualization of PS-InSAR points that are combined with LiDAR point clouds.

Acronyms

2D-NDT	Two-Dimensional Normal Distribution Transform
3D-NDT	Three-Dimensional Normal Distribution Transform
AHN	Actual Height model of the Netherlands
ALS	Airborne Laser Scanning
BAG	Basisregistratie Adressen en Gebouwen
BDK1.0	Bodemdalingskaart 1.0
BDK2.0	Bodemdalingskaart 2.0
cLoD	Continuous Level-Of-Detail
D-InSAR	Differential Interferometric Synthetic Aperture Radar
DSM	Digital Surface model
DTM	Digital Terrain Model
ETRS 89	European Terrestrial Reference System 1989
ICP	Iterative Closest Point
InSAR	Interferometric Synthetic Aperture Radar
LiDAR	Laser Imaging Detection and Ranging
LoD	Level-Of-Detail
NAP	Normaal Amsterdams Peil
PDF	Probability Density Function
PS	Persistent Scatters
PS-InSAR	Persistent Scattered Interferometric Synthetic Aperture Radar
SAR	Synthetic Aperture Radar
SDI	Spatial Data Infrastructure
SLR	Side-Looking Radar
SPCI	Smart Point Cloud Infrastructure
TIN	Triangular irregular network
TLS	Terrestrial Laser Scanning
UML	Unified Modeling Language
VLS	Vehicle Laser Scanning

Contents

1

Introduction

1.1 Context

The land of the Netherlands is moving significantly each year, and it is becoming harder for the Dutch society to deal with the adverse effects of this movement. The land is not only moving horizontally, affecting the geographic position of areas, it is also moving vertically, affecting the elevation of areas. The horizontal movement has often been referred to as continental drift, which is predominantly caused by plate tectonics. This study will however only focus on the vertical movement, which consists out of both descending and rising of the land. Causes of the vertical movement of land in the Netherlands are mining, groundwater extraction, oxidation of peat, compaction due to building on soft soils, water level management, subsidence due to the weight of the Earth's crust, compaction due to extra load, isostasy (the out- or inflow of liquid mantle rock), tectonics and sediment deposition and sand suppletion (NCG, 2020). These causes of land subsidence can be categorized into two classes: natural causes and anthropogenic causes. Van Gils et al. (2020) and Stouthamer et al. (2020) refer to the anthropogenic causes as human induced drivers of land subsidence, and categorize it into three sub-classes: (1) the drainage of peatland and reclaiming areas from the sea, (2) the expansion of the infrastructural network and built-up areas in soft soil, and (3) gas extraction and salt mining. These three sub-classes of anthropogenic causes are responsible for a sinking rate of approximately 0,5 to 10 centimeters per year in the Netherlands. The natural causes concern the subsidence due to the weight of the Earth's crust, compaction, isostasy, tectonics, and sedimentation (NCG, 2020).

The process of land subsidence in the Netherlands is not new, the country has a rather long history of subsidence (Van de Ven, 1993; Vos and Van Heeringen, 1997; Erkens et al., 2016, in Van Gils et al., 2020). To get an understanding of what is meant with a 'long history', Van Gils et al. (2020) refer to the start of large-scale drainage of peatlands in the Netherlands, which started approximately 1.000 years ago.

Unfortunately, with the increase in subsidence, population and urban land use, the adverse effects are also increasing. Both NCG (Netherlands Centre for Geodesy and Geo-informatics) (2020) and Stouthamer et al. (2020) state that land subsidence can lead to damage to infrastructure and water management and change in flooding-risks. In addition, the subsidence of the shallow subsurface, which contains a relatively high percentage of organic matter in the Netherlands, results in CO2 emission and changing water quality. To give an indication of the costs for the Netherlands: the associated social costs of the adverse effects of land subsidence in only soft soils can amount to €22.000 million until the year 2050 (€5.200 million for urban infrastructure, €16.000 million for foundations and €1.200 million for the rural area) (NCG, 2020).

To mitigate and adapt to the adverse effects of land subsidence in the Netherlands, measures have been developed. Scientists have critically analyzed these measures, two of these critics will be shortly discussed as they reflect the need for communication of spatial data regarding land subsidence. First, due to little understanding of the implementation and effectiveness of large-area measures, most of the measures have been developed ad-hoc at the local level, while the problem is occurring at the large-area level. According to Stouthamer et al. (2020), to increase the understanding of the effectiveness and implementations of large-area measures, an understanding of the exact rates and processes causing subsidence is required. Second, measures that result from public decision making are considered to be ineffective due to the fragmentation of competences and the lack of specific policy focusing on soil subsidence in the Dutch legal system. A suggested improvement is impartial and public access to up-to-date data on for example groundwater levels, subsurface properties and surface elevation represented in a standardized sufficient temporal and spatial resolution. According to Van Gils et al. (2020), this improvement can aid public authorities in taking better decisions and developing more informed measures and policies.

The criticism of both Stouthamer (2020) and Van Gils et al. (2020) can be merged in one overall criticism regarding the current measures against the adverse effects of land subsidence: improvement is desired in the form of data communication. To improve the current measures, the Dutch society needs impartial and public access to up-to-date data regarding the rate of land subsidence, the processes causing land subsidence and geographical data related to land subsidence.

Persistent Scattered Interferometric Synthetic Aperture Radar (PS-InSAR) has been successfully used to monitor the deformation in the Netherlands at a millimeter level (Van Natijne et al. 2018). In 2018, in cooperation with universities, knowledge institutes, and companies, the PS-InSAR data has been used to develop the first land subsidence map of the Netherlands: BDK1.0 (Bodemdalingskaart 1.0), covering the time period of 2015-2018.

In 2019, the Dutch Government, as contracting party of the land subsidence maps, advocated for making the land subsidence data with a higher Level-of-Detail (LoD) open. The reasoning behind the Dutch Government's advocation for opening the deformation data of the Netherlands was to stimulate innovation, and to aid society in dealing with land subsidence. However, in order to allow market parties to bring products of quality to the market, the Dutch Government decided to only open up the data with a limited spatial resolution, and a temporal resolution of just six months (de Rechtspraak, 2019). The Dutch Government won the case, and as a result deformation data was published on geoportals of the Netherlands and hence became more open. One can however question to what extent the data has become more open, as deriving application specific deformation information from PS-InSAR data is a time consuming and knowledge intensive process. As a result, not everyone is able to use the data as one might not understand how to process it

In September 2020, the second version of the land subsidence map was launched: BDK2.0 (Bodemdalingskaart 2.0). The deformation data of the second version has a higher LoD compared to the first version: BDK1.0 uses a cell size of 2x2km, and there are only five given areas for which the measure points have been visualized (layer: detail analyse (voorbeelden)), whereas BDK2.0 uses a cell size of 300x300m, and measure points have been visualized for the majority of built-up areas (NCG, 2020). The data of the BDK2.0 covers the time period of 2015-2019, whereas the first version covers the time period of 2015-2018. Both BDK1.0 and BDK2.0 can however not be used for application specific purposes, as expertise knowledge is required for the interpretation and validation of the data.

1.2 Problem Statement

Even though land subsidence data in the Netherlands is being communicated with the use of BDK1.0 and BDK2.0 in a relatively open way, it is not self-evident that this communication has reached its full potential regarding interpretability of the data. Gehlot and Verbree (2006) state that an interactive and dynamic three-dimensional visualization of a data set of public interest, as for example land subsidence, will allow more and more users to easier disseminate scientific information from the visualization. Next to that, they state that the value of scientific information is being increased when linked to other geo-information sources of which users are already familiar with.

With eight height measurements per square meter, the AHN (Algemene Hoogtekaart Nederland; Actual Height Model of the Netherlands) LiDAR (Laser Imaging Detection and Ranging) point cloud dataset is frequently being used for generating three-dimensional visualizations of (parts of) the Netherlands (PDOK, 2020). The study of Van Natijne (2018) extends the usage of AHN to PS-InSAR, and states that AHN is a suitable basis for visualizing PS-InSAR data in a three-dimensional way. There are currently four types of AHN datasets publicly accessible: AHN1, AHN2, AHN3 and parts of AHN4.

The integration of PS-InSAR deformation data with other geo-information sources is not new (Van Natijne et al., 2018; Gehlot et al., 2005). Research regarding the combination of PS-InSAR data with LiDAR point clouds has been done by van Natijne et al. (2018). The scope of their study did however not include an analysis of how users disseminate information from their final data representation. Next to that, the purpose of their study was deliberately limited to the underlying technique of combining the two datasets, lacking the (potential) integration of a user needs analysis, design principles or graphical visualizations.

Gehlot et al. (2005) investigated how other geo-information sources can be integrated with PS-InSAR deformation data to increase the interpretability of deformation data. They describe this integration as a need to improve the interpretability of deformation information. Their study underlines that the AHN datasets of the Netherlands are an important source of information that can be integrated into PS-InSAR deformation data. Their research is however limited to preliminary results.

This section has discussed why combining PS-InSAR deformation data with a geo-information source with which users are familiar with, adds value to the representation of deformation data. A three-dimensional visualization includes elements users are familiar with: for example, individual buildings or the organization of multiple buildings. Literature has already discussed the possibility to link LiDAR point cloud data, which is three-dimensional data, to PS-InSAR data. Linking these two datasets has however not been done yet in the perspective of communicating deformation information to the public. This study will add the novelty of integrating a user needs analysis, design principles and graphical visualizations in the realization of a combined visualization of PS-InSAR with LiDAR point clouds, to enhance the interpretability of the PS-InSAR data.

1.3 Objective and Research Questions

The objective of this research is to investigate to what extent a combination of PS-InSAR deformation data with LiDAR point clouds in a spatio-temporal visualization can support the communication of land subsidence by improving the interpretability of spatio-temporal deformation data.

A conceptual interface will be developed, and will go beyond a visualization that is purely focused on the combination of PS-InSAR deformation data and LiDAR point clouds: it will also integrate design principles and graphical visualizations to ensure a better interpretability of the data. The concept will therefore be an interface in which the necessary design principles and graphical visualizations are integrated, to allow users (Section 2.1.1) to relatively easy interpret PS-InSAR deformation data.

The central research question of this research is:

To what extent can a spatio-temporal visualization of a combination of PS-InSAR deformation data with LiDAR point clouds improve the interpretability of the communication of land subsidence in the Netherlands?

In order to formulate an answer on the central research question, an understanding of the components of the research objective is needed. Therefore, the central question is supported by the following five sub-questions:

1. To what extent is the PS-InSAR deformation data visualization, used for the current communication of land subsidence in the Netherlands, interpretable?
2. What aspects of PS-InSAR deformation data visualization can be improved by linking it to LiDAR point clouds?
3. To what extent can PS-InSAR data and LiDAR point clouds be combined into one visualization?
4. Which design principles and graphical visualizations can be applied to the visualization to ensure interpretability?
5. To what extent is the spatio-temporal visualization of the combination of PS-InSAR and LiDAR point clouds interpretable?

1.4 Scope of the Research

This section will discuss the limitations of this research regarding topics that will not be discussed in this research.

Land subsidence

This study will not discuss the causes, consequences and solutions of land subsidence in the Netherlands.

Underlying (processing) techniques

This research will be limited to the underlying technique of PS-InSAR, the underlying technique of Distributed Scattered Synthetic Aperture Radar (DS-InSAR) will not be discussed. Besides, the underlying technique of PS-InSAR will not be discussed in depth, but only to the extent of what is needed to reach the objective of this research. Similar, the LiDAR technique will not be discussed in depth, but only to the extent of what is needed to reach the objective of this study.

Scope of LiDAR point clouds

It is not within the scope of this research to combine multiple LiDAR datasets that have been collected with different systems: the focus is on AHN3.

Area covered by conceptual interface

Due to the need for intensive computation power and intensive storage space when working with both the PS-InSAR data and the LiDAR point clouds, the conceptual interface will not be developed for the complete land of the Netherlands. In this research, the conceptual interface will be developed for the area of Groningen, where land subsidence is a serious issue due to gas extraction. There will however not be a section dedicated to a description of the study area, as this is not relevant for realizing the conceptual interface.

Testing the conceptual interface

It is not within the scope of this research to extensively test the conceptual interface. The concept will however be tested, but only with a non-extensive testing theory (Section 3.5.4).

Open data

In this research it is assumed that open data leads to innovation and allows a well-informed public. The externalities of making data open, or to what extent the used data can actually be defined as open will not be further discussed in this research.

Horizontal and vertical deformation
This research will be limited to visualizing vertical deformation. Techniques used to derive horizontal deformation, relating to ascending and descending orbits of the satellite, will therefore not be discussed.

User identification
Not all users of the land subsidence communication will have the same purpose of use for the data. These different purposes will however not be taken into consideration in the development process of the concept. The users are identified as the public, and are assumed to not have geospatial knowledge and to desire a form of communication that is relatively easy to interpret. Section 2.1.1 will elaborate on the users of land subsidence communication.

1.5 Relevance

The scientific relevance of this study is associated to its contribution to communication with the use of point clouds, which is currently still in its infancy. By illustrating the effect of communicating land subsidence with the use of point clouds on data interpretability, this study contributes to the exploration of the potential of point cloud visualization for communication purposes with the public.

Apart from the scientific relevance of this study, an increased interpretability of land subsidence data is also valuable for the society: (1) it increases the effectiveness and implementations of large-area measures regarding the adverse effects of land subsidence, which is useful as land subsidence is a process occurring at a large-area level (Stouthamer et al., 2020), (2) it can aid public authorities in making better decisions, and develop more informed measures and policies (Van Gils et al., 2020), and (3) it stimulates innovation, and aids society in dealing with subsidence (de Rechtspraak, 2019).

1.6 Reading Guide

This research consists of six components. The first component is a general introduction to the topic of communicating land subsidence in the Netherlands, and why an improvement of the current communication of land subsidence is valuable. This first components can be found in the previous chapter: Chapter 1. The second component concerns the theoretical groundwork on which this study will build forward, and is presented in Chapter 2. Subsequently, Chapter 3 describes what method will be used to achieve and test an enhanced form of land subsidence communication. The fourth component of this research are the findings of this study, and are represented in Chapter 4. The fifth component can be found in Chapter 5, and discusses the results of this study. The last component of this study concerns the conclusions that are drawn from the findings of this research, which are presented in Chapter 6.

2

Theoretical Framework

2.1 Interpretability of the Current Land Subsidence Communication in the Netherlands

This chapter will discuss the current land subsidence communication in the Netherlands. First the users of the communication will be identified. Subsequently, it will be discussed how open data should be communicated and what the roles of land subsidence communication are. After the explanation of the roles, it will be assessed to what extent the current land subsidence communication integrates the key components required to fulfill these roles. Based on this assessment, it will be discussed how the current land subsidence communication can be improved. The chapter will end with an examination of the potential role that point clouds can play in improving the current land subsidence communication.

2.1.1 User Identification

The land subsidence maps have been visualized to communicate spatial patterns of deformation in the Netherlands to the public. The maps are considered to be less suitable for professionals and experts, as the visualizations have not been optimized and are therefore not suitable for specific applications (NCG, 2020). The public can thus be defined as the targeted audience of the land subsidence communication. It can be rather hard to define the needs of the public as a user, as the public consist of unique individuals that can each have a different purpose of use for the data. In this research it is assumed that the public, and therefore the users, desire a form of communication that is relatively easy to interpretate, as this allows the users to derive the information they desire from the communication.

2.1.2 Communication of Open Data

As explained in Section 1.1, deformation data has become more open since its publication on the geoportals of the Netherlands. The principle of open data is that data should be available to all who have a use for the information, and that the data can be re-used and accesses for any purpose (Goldsmith & Crawford, 2014; OKF, 2012 in Gagliardi et al., 2016). Donker and Van Loenen (2016) add to this that open data is often associated with realizing ambitions, such as a more efficient and transparent government, increased economic value and solving societal problems. The movement of opening land subsidence data enables citizens to engage in a well-informed way in governance processes regarding measures against the adverse effects of land subsidence. However, the fact that the data is now openly published, does not mean that everyone can explore the data. Exploring the open land subsidence data requires users to download the data, which in turn requires 10 to 20 gigabytes space of storage to store the data, and (knowledge of) a storage-intensive software (for example ArcGIS Pro or QGIS) to view geographic data. Users are thus only able to explore the data when their hardware meets the needs required for the exploration, and when the users have knowledge of a software that is able to display the geographic data. In this study it is assumed that not all individuals of the Dutch society conform to the previously described hardware and knowledge requirements. Solely public access to the data will therefore not suffice in fulfilling the need of the Dutch society for open data related to land subsidence.

As a result of solely public access to the data not being sufficient, the need of society for a proper form of data communication remains relevant. Gagliardi et al. (2016) underline this by stating that in order to stimulate the engagement of citizens in governance processes, offering open data alone is not sufficient;

it needs to be well communicated, elaborated and used. Currently, the only portals that are offering the exploration of land subsidence data of the Netherlands, without having to download the data, are BDK1.0 and BDK2.0. When applying the theory of Gagliardi et al. (2016) to BDK1.0 and BDK2.0, one can state that this current form of communication needs to be well elaborated and used. An infrastructure that facilitates communication, elaboration and usage of data is therefore desired. Grus et al. (2007) refer to this as an SDI (Spatial Data Infrastructure), which is a network-based national solution to provide effective, easy and consistent access to geographic information and services by public agencies and other. The intention of an SDI is to support social, economic, personal, and political development, and include the policies, technology, human resources, related activities, and standards necessary to support these intentions (Grus et al., 2007).

An SDI consists out of three key components: a geoportal, metadata, and a search function. A geoportal is used to access and find the spatial data, metadata consists of documentations on the production process and content of the spatial data, and the search function allows users to find data by an interactive interface (Hu & Li, 2017). Following the argumentation of this paragraph, it can be assumed that the three key components of an SDI indirectly contribute to the previously described engagement role of BDK1.0 and BDK2.0

2.1.3 The Role of the Communication of Land Subsidence Data

As stated in Section 2.1.1, the land subsidence maps have been visualized to communicate spatial patterns of deformation in the Netherlands to the public. According to the defined roles of maps by DiBiase (1990), the role associated to the goal of the land subsidence maps, as described before by NCG (2020), is to present geographic data (Figure 1a), as the maps are a means of a visual communication to the public. The three other map roles defined by DiBiase (1990) are: exploration, confirmation or analysis and synthesis. In order to compare the goals of the different map use roles with each other, MacEachren and Kraak (1997) visualized the roles defined by DiBiase (1990) of a map in a cube (Figure 1b), referred to as the map use cube.

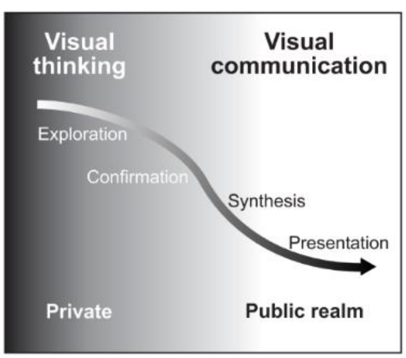

Figure 1a Roles of maps (DiBiase, 1990)

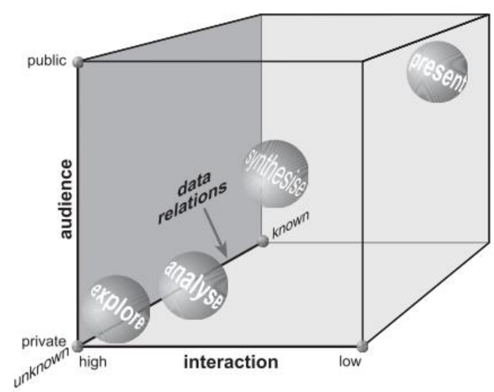

Figure 1b Goals of roles in the map use cube (MacEachren and Kraak,1997)

The study of Van Elzakker et al. (2003) provides components that should be integrated into a visualization when its role is to serve as a geographical interface to find and retrieve data. This role is seen as a general role, that forms the basis of the other four roles in the map use cube. In addition to describing the components of a map with a general role, Van Elzakker et al. (2003) also describe what key components a map with a presenting and exploration role should have. The study describes from a user perspective what they desire in a map with a certain role, and translate this into required components related to that role. It is relevant to discuss the components of the general and presenting role, as the land subsidence maps of the Netherlands have both a general and a presenting role.

The desired components of a map with a general role can be categorized into five key components: administrative levels, layer configuration, a selection tool, drawing boxes and visual graphs (Van Elzakker et al., 2003):

- The functionality to use different *administrative levels* (Figure 2) enables users to analyze the data for different aggregation levels; a drop-down list of administrative units (geographical unit) is preferred rather than a search bar, as users may not always know the correct spelling.
- In some cases, different administrative levels are offered with the use of different layers, that can be turned off and on and change in overlay order, this is referred to as *layer configuration*.
- A *selection tool* (Figure 2) enables users to select just one administrative unit by for example clicking on the unit of concern on the map, this is convenient for users that are particularly interested in a certain area.
- Administrative boundaries are usually artificial and arbitrary, the functionality of *drawing boxes* (Figure 2), containing the area of interest of users, enables users to discover spatial patterns independent from administrative units.
- *Visual graphs* like tables and diagrams allows users to retrieve data from the administrative units.

Similar to the general role of maps, the desired components of a map with a presenting role can be categorized into four key components: retrieval of data in different formats, additional facilities, comparison of maps, and dynamic time-series (Van Elzakker et al, 2003):

- Users desire to *retrieve data in different formats* (Figure 2), such as tables and charts.
- *Facilities* such as a locator map and printing and downloading facilities are desired by the users
- The functionality to *compare maps* can be useful for users to understand the differences between different map layers.
- *Dynamic time-series* of maps enables users to compare the same theme of a map at different times.

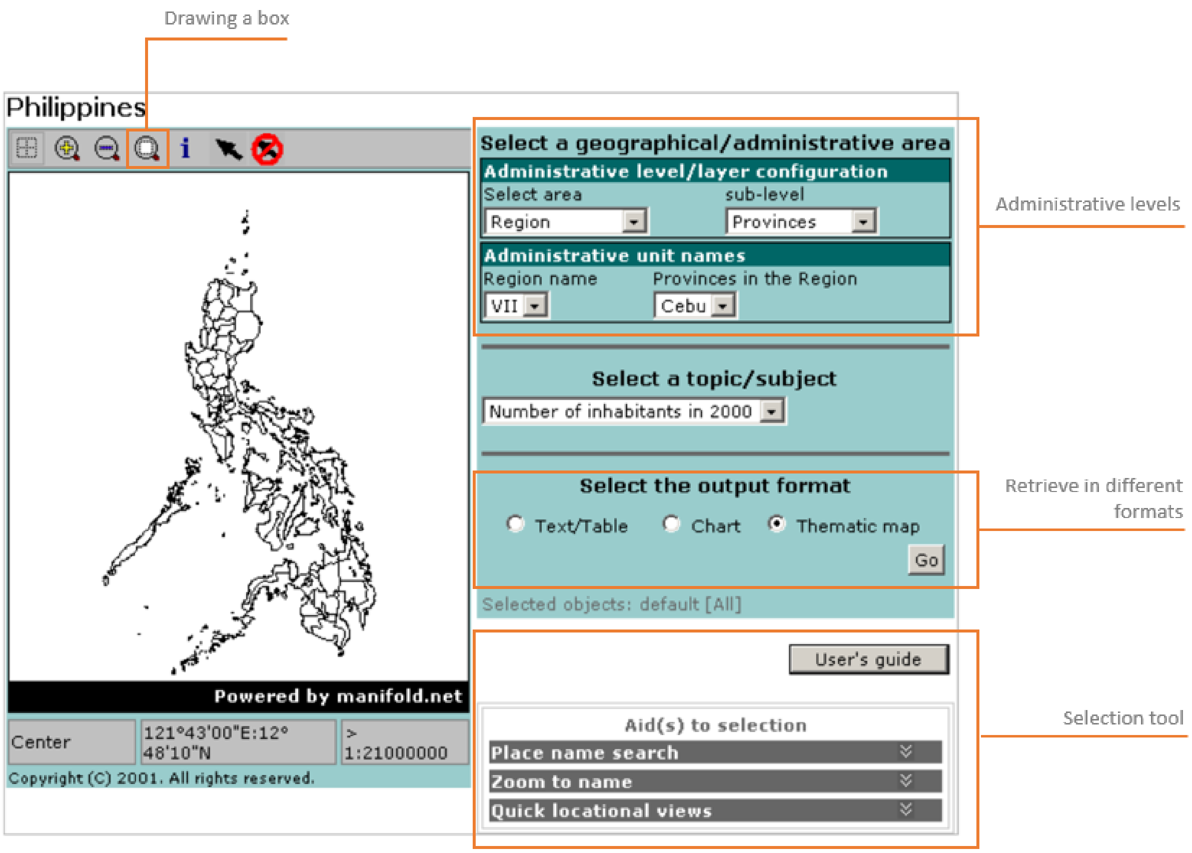

Figure 2 Example of an interface with a selection of the key components (based on Van Elzakker et al., 2003)

Three different roles of the land subsidence map of the Netherlands have been discussed in this section: the general role to serve as an interface to find and retrieve data, the role of presenting data, and the final role of engaging citizens in the governance processes regarding measures against the adverse effects of land subsidence. Associated to the general and presenting role are the previously discussed key components based on the study of Van Elzakker et al. (2003). The engagement role is associated to the key components of an SDI, as discussed previously discussed by Hu and Li (2017). The three roles are sub-roles of the overall goal of the land subsidence map: communicate land subsidence to the public (NCG, 2020). Figure 3 illustrates what key components of a map are associated to the three roles necessary to realize the overall goal of the land subsidence map.

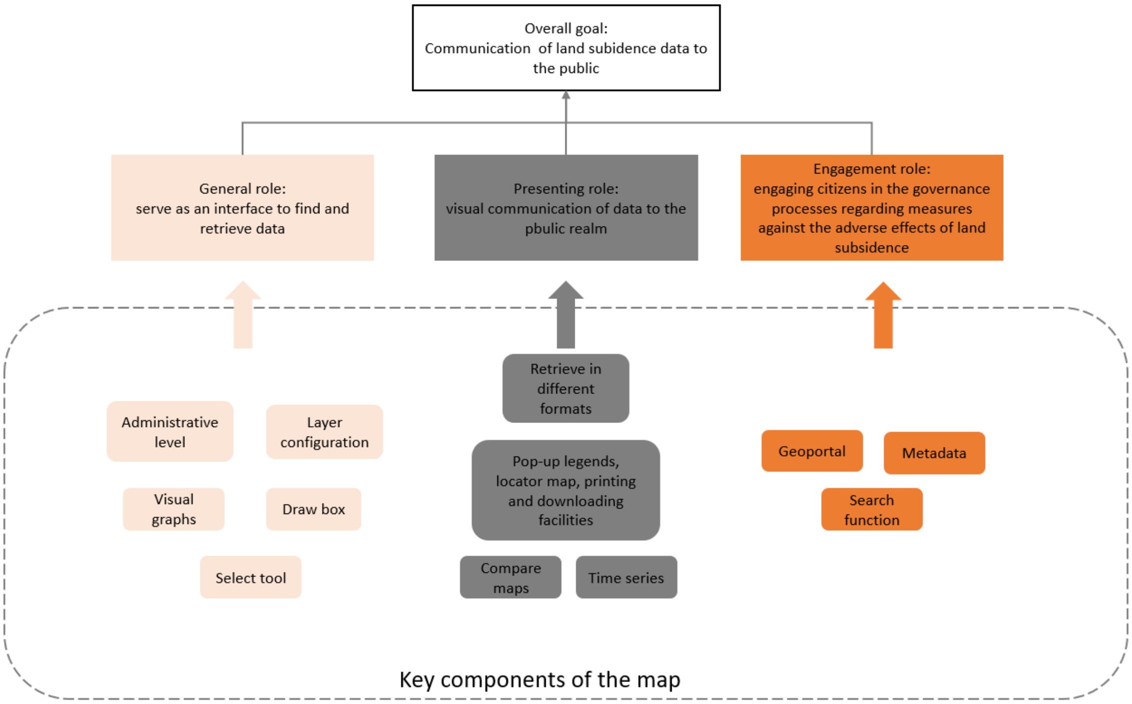

Figure 3 Structure of the key components and roles of the goal of the map used for land subsidence communication

2.1.4 Assessing the Key Components of the Current form of Communication

Figure 3 illustrates that the key components play a fundamental role in achieving the overall goal of the land subsidence map. An analysis of the current state of the key components of BDK2.0 will therefore provide a relevant assessment framework to critically look at the current communication of land subsidence in the Netherlands. The results of the assessment are shown in Table 1.

Table 1 Assessment format

Engagement role	
Geoportal	- The BDK1.0 and BDK2.0 are both freely accessible via a website, which can be accessed without any restrictions - Users can share their findings on 'het gebruikersforum', a platform for users of the BDK2.0. - The interface to access the data is partly in English and partly in Dutch - When one wants to compare deep with shallow subsidence, one has to go to the geoportal of BDK1.0 in a new tab
Metadata	- There is no explanation of what is shown in the graphical visualization after selecting a point, and how this can be interpreted - It is stated that the scale of the color scheme can be changed, but there is no information on where this can be done - There is no explanation on that the order of layers can be changed, while this might not be clear for users that are unfamiliar with an interface that has different map layers - Relatively elaborated and clear explanation on the underlying technique and visualization methods - There is a brief explanation of when certain pixels have no value, but not why they have no value - There is no explanation on where the transparency switch is located in the interface, or what it can be used for

	- There are layers West-1/2, Midden-1/2 and Oost-1/2 which are associated to the different positions of the satellite. However, there is a limited explanation on how version 1 differs from version 2, and how to deal with these differences - On the website it is stated that as a consequence of the different positions of the satellite, contradicting results might occur. However, there is no explanation on what sort of contradicting results, and how to deal with these - Extra information in the form of tables can be retrieved for each of the layers containing measure points, and when panning over one of the cells of the table, extra information for that specific cell is given - The marker cannot be placed randomly, only at a measure point. There is however no explanation on what can be selected and what not - There is no explanation for why only measure points in urban areas have been visualized, and not in rural areas - There is no information about the used coordinate system and map projection - There is no information on the update frequency of the data
Search function	- There is a search bar, with which one can search an address - Users can pan and zoom in and out

1a Engagement role: assessment of key components (based on Hu & Li, 2017)

General role	
Administrative levels	- Users cannot select the administrative level they want to view the data for
Selection tool	- Only measure points can be selected
Drawing boxes	- An area of interest cannot be defined by drawing a box on the map
Visual graphs	- The tables are partly in English and partly in Dutch - There is no explanation concerning the charts and tables after selecting a measure point
Layer configuration	- Layers can be turned off and on, and layers can be dragged to change their order of overlay - Only when selecting a layer from the list 'afgeleide laag' in the 'kaartlagen' pane, the layer shows up in the 'bodemdalingskaart' list and can be dragged to change the order of layers. When a layer is not selected in 'afgeleide lagen', it can also not be visualized on the map. The list of 'afgeleide lagen' does not offer any functionalities, but only creates an additional step to visualize a certain layer - The 'aardgasvelden' layer is used in this interface as a background layer. As only one background can be selected at a time, one is not able to see the contour lines of the Netherlands when combining 'aardgasvelden' with the land subsidence data points. - There is one specific layer for the marker on one of the measure points, making it easier to drag the marker in top of layers and to turn it off and on

1b General role: assessment of key components (based on Van Elzakker et al., 2003)

Presenting role	
Retrieve in different formats	- Users can view the data on a map - Displacement rates data of the measure points, municipalities and water authorities can be viewed in a table - Temporal data of measure points can be viewed in a graph
Pop-up legends, locator map, printing and downloading facilities	- The legend of the stability factor does not show labels for individual classes, only for the upper and lower class. This is not advised, as discrete classes have been used, and users are now not able to associate a label to the middle colors. Next to this, apart from the upper and lower class, no values can be assigned to the labels of the color ramp (e.g. High stability = a difference smaller than 2 mm/year) - There is no legend for the layer 'grondsoortenkaart'

	- There is no legend for the layer 'aardgasvelden' - The land subsidence data has not been classified, but the user is able to change the minimum and maximum value linked to the color ramp (legend) of the land subsidence layers - The explanation panel on the left side of the map cannot be minimized - There is no print functionality - It is not possible to download any data. There is a download tool, but it is not working - The tables and charts are also not downloadable - There is no locator map
Compare maps	- Maps can be compared with the use of an overlay function, maps can however not be visualized simultaneously without an overlay - Layers can be made transparent - Visual graphs cannot be visualized simultaneously, and can thus not be compared
Time-series	- When selecting a certain measure point one can see the time-series of deformation of that location of 2015-2019 in the form of a graph, where displacement measures have been plotted against time - The maps itself are not being visualized with the use of dynamic time-series

1c Presenting role: assessment of key components of BDK2.0 (based on Van Elzakker et al., 2003)

In the next section it will be discussed how the results of this assessment can be used to improve the current communication of land subsidence in the Netherlands.

2.1.5 Improvement of the Current Communication of Land Subsidence

In the previous section the map used for the communication of land subsidence in the Netherlands has been discussed. The current form of communication was not only discussed, but also critically analyzed from the perspective of its three roles: general role, presenting role and engagement role. Using this critique to improve the current communication of land subsidence is relevant, as these three roles contribute to achieving the final goal of the map (Figure 3). Improving the key components will help to reach the full potential of the map. Next to that, improving the key components will increase the user satisfaction, as it will make the maps easier to interpret for its users.

In this section, the assessment performed in Section 2.1.4 (Table 1) will be translated into recommendations that will contribute to an improvement of the key components. The recommendations have been established based on the user perspective, meaning from the perspective of what the public would desire. In this user perspective it is assumed that the public is the standard non-critical public.

Geoportal

According to the critical analysis, there are two ways to make the land subsidence data more accessible. The first way concerns the language of the geoportal, which is currently partly in English and partly in Dutch. It is recommended to give users the possibility to choose their language of preference, to avoid possible language barriers. The second way concerns both BDK1.0 and BDK2.0: it is relatively inconvenient to switch from the geoportal of 2.0 to the geoportal of 1.0. Therefore, it is recommended to also offer the two layers showing both deep and shallow subsidence in BDK2.0, this way users do not have to change between the geoportals to view the shallow and deep layers.

Metadata

An interactive visual interface supports the activity of analytical reasoning of a map, and therefore supports the interpretability of patterns of the visualized information (Andrienko et al., 2020). However, in order to assure that users make use of the interface, features of the user interface need to be well explained. Therefore, the interface of the land subsidence map would support the activity of analytical reasoning more if there is an explanation provided on how to use the interface, for example: where to change the transparency of layers, where to change the scale of the color scheme, how to change the order of layers, or where a marker can be placed and where not.

A second recommendation regarding metadata would be adding an explanation on how to interpret the graphical visualizations (graphs and charts). It is important that the users know how to interpret the graphical visualizations, as they provide a richer visual display and can facilitate comparisons (Andrienko et al., 2020).

There are two possible meanings of when cells do not have a value: either some value exists in principle but could not be determined, or no value exists. It is important to help users understand what the absence of a value means (Andrienko et al., 2020). Therefore, it is recommended to add an explanation of why certain areas are left with no cell value or measure points.

An additional suggested change is to add a more extended explanation of the differences between the two versions of each direction: Midden 1/2, West 1/2, and Oost 1/2, and how to deal with the contradicting results as a result from these different versions. A last suggestion is to add information regarding the used coordinate system and projection, and the update frequency of the data.

Search function

The interface of BDK2.0 already provides users with a search function. Making users able to perform a text-based search for specific locations. During writing in the search bar, suggestions of addresses are shown based on what is already written.

Administrative levels

A selection functionality in the form of a drop-down box can be added, to enable users to choose an administrative level of their preference. A drop-down box is recommended, as users may not know the exact spelling or name of a location, and thus are in need for something different than a text-based search.

Selection tool

It is recommended to enable users to select a certain object or administrative unit, different than only a measure point, on the map. This way it is easier for users to derive data of a unit or object of preference.

Drawing boxes

In order to make users select an area independent from given administrative boundaries, the functionality to draw a box is recommended.

The functionality of the search function, administrative levels, selection tool and drawing boxes are data-reduction techniques that allows users to select a small number of representative points when all the data items are visualized in the display space. Data-reduction techniques are useful, as this allows users to visually distinguish points that are visually clustered. As a result, the attention of the user can go beyond the obvious patterns of a visualization (Andrienko et al., 2020).

Layer configuration

The layers are currently divided into two lists, adding no extra functionality but only creating one additional step to visualize layers from the list 'afgeleide lagen'. It is recommended to not have steps needed for a visualization that do not have a form of added value. An additional improvement for the layer configuration is to enable users to combine background layers (as currently only one background layer can be selected), or to add an outline of the Netherlands to the layer showing natural gas fields.

Retrieve in different formats

Currently, data can already be retrieved in three different formats: map, chart and table. However, charts can only be retrieved for measure points, not for municipalities and water authorities. Only the displacement rates for the municipalities and water authorities are given. It would however be more transparent to illustrate to the users the distribution of the measure points and their attributes from which the displacement rates have been derived. It is therefore recommended to also add charts for the administrative units, which in this case are the municipalities and water authorities.

Additional facilities

Interpretation of patterns depend strongly on appropriate labelling of the data components and an explanation of how they are encoded by visual means (Andrienko et al., 2020). Therefore, the first recommendation concerns titles, labels and legends. An addition of labels to the legends would make it easier for the users to derive information from the visualization, as users can currently only see the maximum and minimum value of the color ramps. Users are currently not able to derive values from the 'afgeleide lagen'. A legend with labels representing the range of the associated class would enable users to derive and compare values from the 'afgeleide lagen'. A second recommendation concerning the legends of the current interface, is the addition of a legend for both the 'grondsoortenkaart' and the 'aardgasvelden' layers.

The layers showing subsidence in millimeter per year have not been classified. However, human eyes are not able to distinguish the small variations of shade. Classification assigns colors to classes, allowing users to better distinguish the variations of shade. Additionally, the use of classes provides the possibility to reduce the impact of outliers (Andrienko et al., 2020).

The option to minimize the explanation panel is recommended as it allows users to get a better view of the map (Figure 4). Additionally, a locator map is recommended to make users aware of the relative location when zoomed to a certain area. Two last recommended facilities are tools for printing and downloading the data of (a selection of) the map, charts and tables.

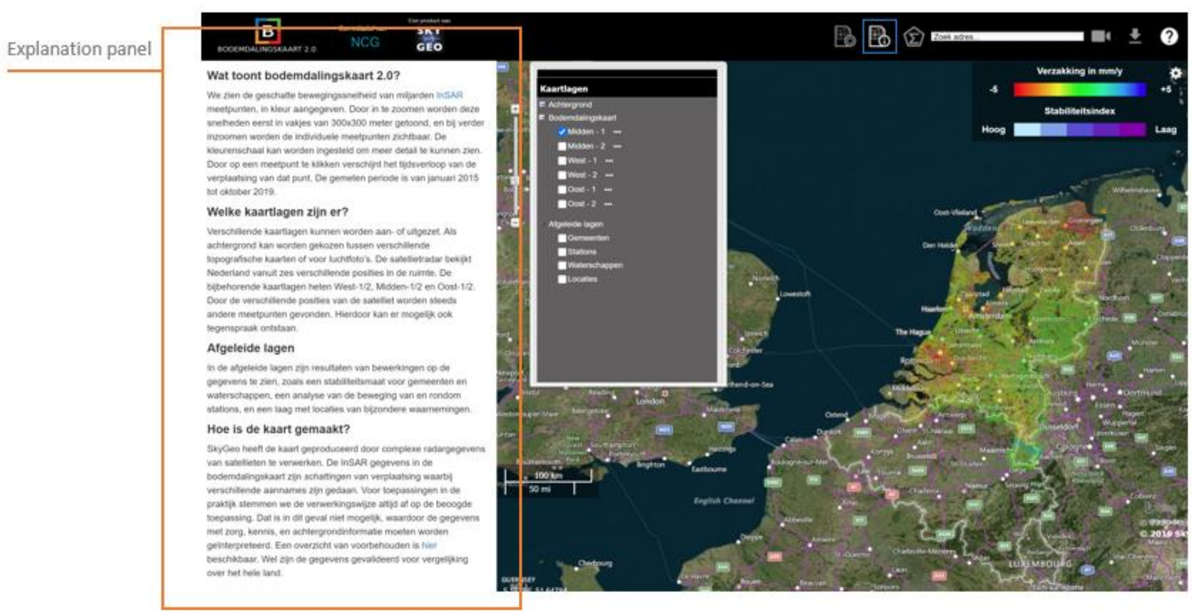

Figure 4 Explanation panel cannot be minimalized (NCG, 2020)

Compare maps

When selecting a point or an area, the visual graph of the selection cannot be compared with the visual graph of another selection. Creating separate displays for the selected points or areas and juxtapose these displays for comparison is a viable approach to allow comparison (Andrienko et al., 2020).

Time-series

Currently, only time-series of measure points in the form of graphs can be requested by the user. This allows users to understand how the event of deformation is varying over time, per measure point. Understanding this variation is a general task of time-series (Andrienko et al., 2020). However, a graphical form of time-series does not allow users to easily understand how the event of deformation is varying over space, as the time-series graphs cannot be viewed simultaneously, and if they could be viewed simultaneously there can only be viewed a limited number of graphs simultaneously dependent on the display space. Andrienko et al. (2020) state that it is important to choose an appropriate modelling method to visualize the data, so that it is suitable to understand the temporal variation of the time-series. Therefore, it is recommended to find an appropriate modelling method to visualize the time-series of deformation data that is able to show variations in time and space in one display space, allowing a detailed exploration of differences and commonalities in the data.

The previously discussed recommendations for each of the key components can be divided into four main categories of change: an increase of the user friendliness of the interface, improving the accessibility, adding metadata and an improvement of data visualization (Table 2).

Table 2. The four categories of recommended changes

Category of change	Associated recommendation per key component
Increase user friendliness of interface	Administrative levels: - Add a dropdown box in which users can select an administrative level of interest Selection tool: - Add a tool with which users can select one object or administrative unit Drawing boxes: - Add the functionality of making a selection by drawing a polygon Layer configuration: - Merge the two lists of layers into one in the layer contents pane Retrieve in different formats: - Make the data of each administrative unit available in the format of a chart Additional facilities: - Add labels to legends, instead of only showing the minimum and maximum value of the color ramp: • The stability index legend: use labels representing the range of the subsidence rate of the associated class • Only when classifying the subsidence layers: use labels representing the range of the subsidence rate of the associated class - Add a legend to the ‘grondsoortenkaart’ and the ‘aardgasvelden’ layers - Add a printing tool in the interface - Add a download tool in the interface - Add a minimize functionality to the explanation panel - Add locator map Compare maps: - Add the functionality to view visual graphs of different selections simultaneously
Improve accessibility	Geoportal: - Give users the choice to view the interface in English or Dutch
Add metadata	Metadata: - Add an instruction of how to use the interface - Add an explanation of how to interpret the graphical visualizations (charts and tables) - Add an explanation of areas that have no cell value or measure points

	- Add an explanation of the two different versions of Midden, Oost and West, and how to deal with the contradicting results - Add information of the used coordinate system and projection - Add information of the update frequency of the data
Enhancement of visualization of the data	Geoportal: - Provide the layers of shallow and deep subsidence in the geoportal of Bodemdalingskaart 2.0 Layer configuration: - Add an outline of the Netherlands to the layer 'aardgasvelden' Additional facilities: - Classify the 'subsidence in millimeters per year' data layer Time-series: - Find an appropriate modelling method to visualize the time-series of deformation data

2.1.6 The Potential Role of Point Clouds in the Improvement of the Current Form of Communication

With the development of three-dimensional laser scanning techniques, point cloud visualizations have attracted increased attention. Point cloud visualizations are currently the focus of studies in many applications (Azari et al., 2012). Next to that, point cloud visualizations have a significant added value for applications in which the end user can gain insights of the visualized phenomenon with the use of interactive, explorative, visualization methods and techniques (Verbree & Van Oosterom, 2015). A point cloud is a set of points that is represented by the three-dimensional coordinates and the associated attributes of the points, such as color, reflectance and normals (Javaheri et al., 2019). One of the examples of a point cloud visualization application that is provided in the study of Azari et al. (2012) is the simulation of dynamic behaviors using three-dimensional deformation methods. This example is one of the indications that point cloud visualizations might be an appropriate modelling method to visualize the time-series of deformation data. A second indication that underlines the appropriateness of point clouds in this perspective, is that point cloud visualizations can evolve along time, allowing users to derive trends in temporal changes of the visualized data. A third indication concerns the three-dimensional nature of point cloud visualizations, which underlines how promising point cloud visualization can be in visualizing PS-InSAR deformation data: it is currently relatively hard to recognize the human environment with only PS-InSAR deformation data. As a result, the ability to link deformation trends to objects is limited. Linking PS-InSAR data, used for visualizing BDK2.0, to three-dimensional point cloud data will enable users to attach deformation trends to objects, and hence improve the recognizability of the human environment of the PS-InSAR data.

Van Natijne et al. (2018) explain that linking PS-InSAR data to point clouds will be beneficial as it provides (1) linking of the deformation trends to particular parts of the infrastructure, for early warning and maintenance planning, (2) mitigation and detection of (regional) trends and errors in the radar processing, (3) assessment of differential deformation trends, as a signal can now be attached to the geometry of a building. Ackere et al. (2017) underline the beneficial nature of three-dimensional visualizations, by stating that three-dimensional visualization result in an enormous added value due to the fact that these visualizations are more vivid and therefore more understandable.

Before the integration of PS-InSAR data with point clouds can be developed, an understanding of the underlying techniques of both datasets is necessary and will therefore be discussed in the subsequent two chapters.

2.2 PS-InSAR

The PS-InSAR technique makes it possible to monitor deformations of urban areas with a precision level of millimeters per year (Gehlot et al., 2005). This technique is an extension of regular PS-InSAR, and adds the advantage of overcoming the problems of temporal and geometrical decorrelation of PS-InSAR. The aim of this chapter is to get an understanding of how PS-InSAR data is being collected and processed to finally be used for visualizing deformation data. To get an understanding of the possible obstacles of working with PS-InSAR data, this chapter will end with an error analysis of PS-InSAR deformation data.

2.2.1 Data Collection Method

PS-InSAR data is being measured with active satellites, the Sentinel-1, TerraSAR-X, COSMO-SkyMed and RadarSat-2 satellites are commonly used to collect the PS-InSAR data (SkyGeo, 2020). These satellites are referred to as active as they have a transmitter on board that transmits radiation, and a receiver that measures the backscattered radiation by the Earth's surface (Clevers, 2017). The principle of the operation of an active satellite has been visualized in Figure 5. Successive short pulses of microwave radiation are generated by the transmitter (A) at regular intervals, which are focused by the antenna into a beam (B). The radar beam illuminates the surface obliquely at a right angle to the motion of the platform. The antenna receives a fraction of the transmitted energy that is being backscattered by various objects within the illuminated beam (C).

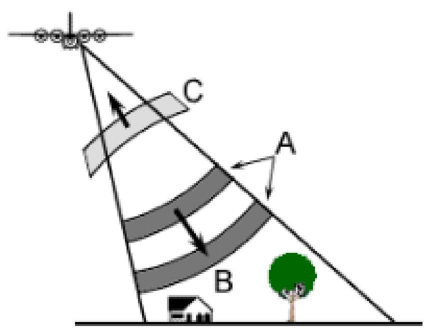

Figure 5 The principle of the operation of an active satellite (Clevers, 2017)

This type of system is generally referred to as an active remote sensing system which is operating in the microwave part of the electromagnetic spectrum (Figure 6).

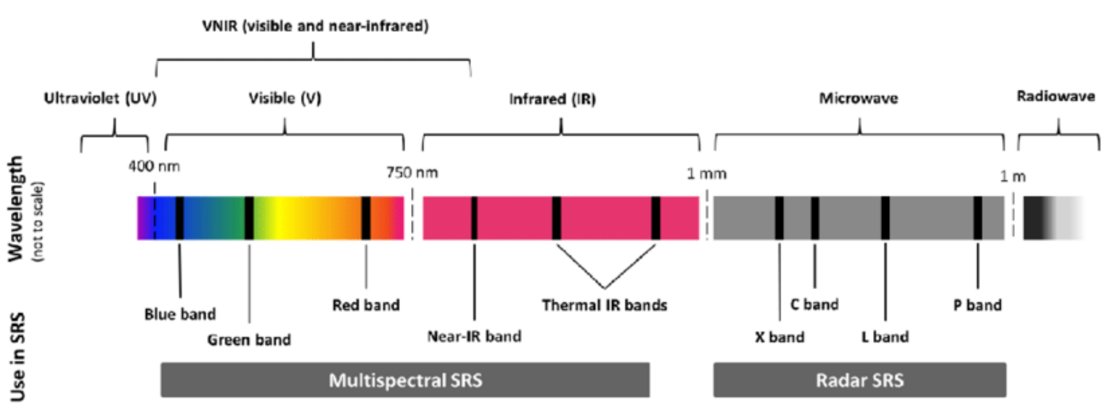

Figure 6 Electromagnetic spectrum (Pettorelli, 2018)

The opposite of an active remote sensing system is a passive remote sensing system, which does not transmit radiation but measures the backscattered radiation of the Earth's crust originating from the sun. Passive remote sensing systems operate in the infrared and visible part of the electromagnetic spectrum (Figure 6). An advantage of active satellites with respect to passive satellites is that active satellites are independent from the sun, and are able to transmit their radiation through clouds.

The backscattered signal that is measured by active satellites depends on the properties of both the satellite (for example frequency, polarization and viewing geometry) and the object that is reflecting the radiation (for example roughness and electrical properties). Therefore, active remote systems can be used to derive information from objects, such as terrain topography, height and moisture levels (dependent on electrical properties) (Clevers, 2017).

The minimal detectable object of PS-InSAR depends on the radar cross section, and the coherence of an object over time. A higher resolution of the SAR system typically results in a larger number of measure points (Figure 7). Only the x, y location and the height z of the dominant reflection of each pixel will be estimated. SkyGeo (2020) discusses three advantages of a higher SAR resolution over a lower resolution: (1) smaller cells result in less room for noise, making it more likely that the satellite shows a consistent reflection throughout time, leading to more measure points (2) the values of measured displacement are more precise (3) the points' absolute position are more precise.

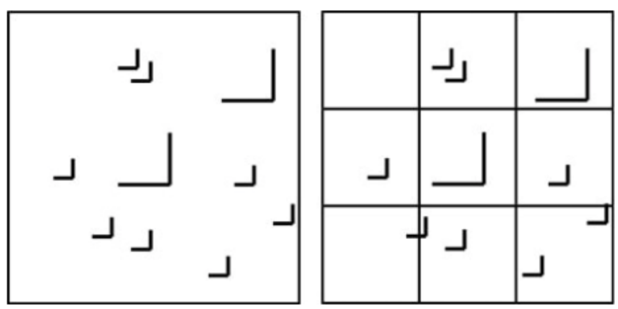

Figure 7 Lower resolution versus higher resolution (SkyGeo, 2020)

2.2.2 The Components of PS-InSAR

As the name of the technique suggest, PS-InSAR is composed of three elements: Synthetic Aperture Radar, Interferometry, and persistent scatterers.

Synthetic Aperture Radar

Synthetic Aperture Radar (SAR) is a radar system that belongs to the class of imaging radars, which are side-looking radars (SLR) as the radar instrument would not function if it was nadir-looking (Hanssen, 2001). SAR systems do differ from conventional SLR systems as SAR systems have circumvented the limited azimuth or along-track resolution (dependent on the size and height of the antenna) and range or across-track resolution (dependent on the length of the transmitted pulses) of SLR systems. In SLR systems these resolutions are limited due to the dependence on practical limitations regarding for example high energy requirements of short pulses, maximum practical size of an antenna and the minimum orbit height. The practical limitations influencing the azimuth resolution can be circumvented by a SAR system, as it artificially enlarges the antenna by using multiple acquisitions to form one image (Van Natijne, 2018). Additionally, the practical limitations influencing the range resolution can be circumvented by shortening the transmitted pulse by means of signal processing (Rees, 2001 in Van Natijne, 2018). With an increase in the azimuth resolution, the ability of an imaging radar to distinguish two closely spaced scatterers in the direction parallel to the motion vector of the sensor increases as well (Earth Esa, 2020). With an increase in the range resolution, the transmitted pulse will be shortened and the ability to distinguish between different targets will increase.

Interferometry

It is impossible for SAR systems to distinguish between two objects that are at the same range, but at different angles to the instrument. By integrating interferometry with a SAR system, it becomes possible to measure distances as well as angles. This integration can be realized by using the phase information and by combining two SAR images obtained by two different antennas or by using repeated acquisitions. Phase measurements enable the observation of relative distances as a fraction of the radar wavelength. Using two different images results in a difference in sensor locations that enable the observation of differences in angles. Phase measurements are obtained by multiplicative interferometry, a technique that makes use of coherent cross-multiplication of the two input signals. Considering that it is relatively easy to determine the fraction of a phase-cycle, phase data and therefore the phase measurements are considered to be relatively precise (Hanssen, 2001). How these phase measurements are precisely being used to measure displacement will be elaborated upon in Section 2.2.3.

Persistent Scatterers

The transmitted signal by radars is being backscattered by objects on the Earth's surface. The number of points that can be obtained by a satellite is dependent on its spatial resolution. Before explaining what is meant with persistent scatterers, it is important to first grasp the notion of scatterers: not all locations are suitable for scatter measurements, as this is dependent on how well the concerned objects reflect the transmitted signal and on its consistency over time (SkyGeo, 2020). Man-made structures have particularly convenient backscatter characteristics in this perspective: they are consistent over longer time periods, and the signal is dominated by a single scatterer or an ensemble of scatterers (Van Natijne, 2018). Scatterers that comprise this consistent behavior are referred to as Persistent Scatterers (PS) (Van Leijen, 2014 in Van Natijne, 2018). The consistent nature of PS allows the derivation of the same feature in successive radar images. As a result, a compilation of time-series can be made of the movement of a specific feature.

The combination of the three previously explained techniques allows mapping deformation trends with millimeter per year precision.

2.2.3 Measuring displacement with PS-InSAR

For the PS-InSAR technique, satellites measure the phase and the amplitude of the backscattered radiation. The phase is the fraction of a complete cycle of a wave that reaches the sensor and is associated to the displacement of an object. The amplitude is associated to the strength of the recorded signal. A difference in the phases of two sequential measurements can indicate a displacement of the corresponding measured location. An example is shown in Figure 8: the measured location in Figure 8B has subsided relative to the measured location in Figure 8B. Therefore, the backscattered signal in Figure 8B has to travel a longer distance compared to the backscattered signal in Figure 8A.

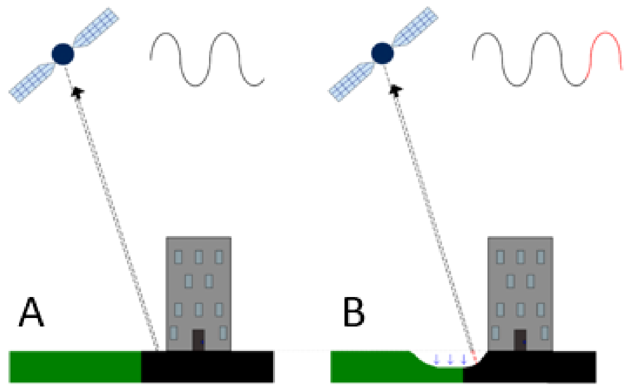

Figure 8 Measuring displacement with the use of phases (SkyGeo, 2020)

The difference in the signals is referred to as the phase difference (red part of the wave in Figure 8B), and can be used to measure the displacement that has occurred with millimeter precision, as the length of a complete wave cycle of the concerned satellite is known in the order of centimeters (SkyGeo, 2020). As a result, the relative displacement of a location can be measured relatively accurate. The absolute displacement can however not be measured with the same level of accuracy: the measured absolute displacement is typically in the order of meters. The uncertainty of the absolute displacement of an individual measure point is dependent on the resolution of the satellite and the weather at the moment of the data collection. The estimated linear trend, derived from the individual measure points, depends on the number of measurements: an increase in measure points results in an increase in the level of precision of the trend line. The associated uncertainty of the linear trendline is relatively low. The uncertainty of the absolute position (x, y, z) of a measure point is however relatively high (SkyGeo, 2020).

To overcome the problem of uncertainty of absolute measurements, the measurements are taken with respect to a reference point. Therefore, displacement estimates should always be interpreted relative to other the reference level. As a result, PS-InSAR deformation data is suitable to provide time-series for each measured location.

The satellite passes a location from both an ascending orbit and descending orbit (Figure 9). A combination of the measure points from these two orbits, and at least one independent assumption allows the decomposition of the displacement in both the vertical and horizontal direction of this measure point. The scope of this study is however limited to vertical displacement (Section 1.4).

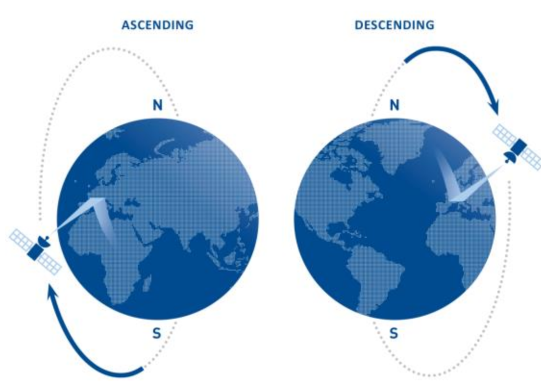

Figure 9 Ascending and descending orbit of the satellite (Tre Altamira, 2020)

The process of unwrapping refers to the process of resolving the 2π -ambiguities in the phase observations. To gain an understanding of the displacement value, the number of full wave cycles (0-2π) associated to phase measurements needs to be known. There however need to be made assumptions to estimate the actual displacement, these assumptions concern correlations in time and/or space (for example the displacement is linear during the measurement period, or the displacement rate change is smooth in space). It is important to use correct assumptions, as a wrong assumption may lead to an unwrapping error (SkyGeo, 2020).

From the collected SAR images, the PS-InSAR images need to be extracted. An algorithm is used to detect PS in the SAR data (for example the PSI algorithm developed by Delft University of Technology). The phase dispersion over time and the consistency in amplitude of targets allows the identification of presumably coherent targets. The identification of coherent targets is done both before and after the estimation of topographic, atmospheric and displacement phase contributions (Gehlot et al., 2005). These phase contributions can be separated with the use of time-series, as they allow the separation of noise sources from the deformation signal (Van Natijne, 2018). The time or ensemble coherence is estimated for the individual PS, and is used as a rough quality parameter of the measure points. A coherence threshold value determines the number of detected PS: an increase in threshold results in a decrease in the number of detected PS measure points.

2.2.4 Error Analysis

The study of Hanssen (2001) discusses the error sources that have an effect on the processing of PS-InSAR data. The error sources that will be discussed in this section are ambiguity resolution and the atmosphere.

Ambiguity resolution

The PDF of the unwrapped interferometric phase is only known for its shape, but not for different $k2\pi$ ambiguity numbers (its absolute position) (Figure 10). As a result, the integer nature of the phase PDF cannot be determined. Without non-verifiable assumptions concerning the maximum phase gradient, the absolute location of the phase PDF remains unknown.

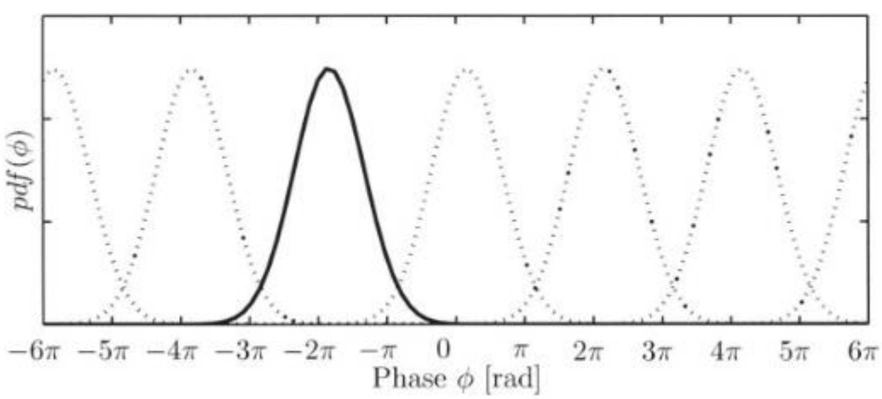

Figure 10 A section of the PDF of the unwrapped interferometric phase, for different $k2\pi$ ambiguity numbers (Hanssen, 2001)

The effect of errors in the orbit or baseline (Figure 11) of the radar can result in a scaling error when deriving topographic height differences and long-wavelength characteristics for the reference phase. This is however radar dependent.

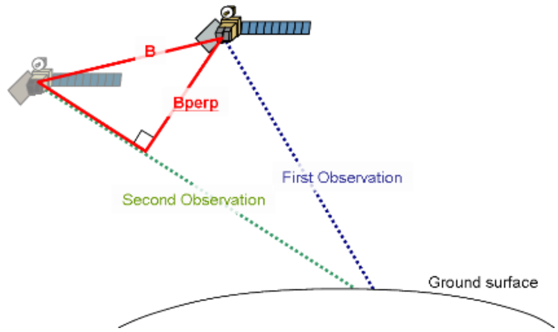

Figure 11 Baseline of a satellite illustrated by B (GSI, 2020)

Atmosphere
Due to the distribution of atmospheric refractivity, errors occur in the interferometric phase. The effects of the distribution can be distinguished into two categories: vertical stratification and turbulent mixing. Vertical stratification is the result of differences in the vertical refractivity profiles during both SAR acquisitions, assuming that there are no heterogeneities in the horizontal layers. This does however only affect mountainous terrain, and is correlated with geography (Massonet & Feigl, 1998 in Hanssen 2001). Turbulent mixing is a result from turbulent processes in the atmosphere and cause spatial heterogeneity in the refractivity during two SAR acquisitions. This affects both flat terrain and mountainous terrain.

2.2.5 Summary
This chapter discussed how PS-InSAR data is being collected with active remote sensing systems, that consist of a transmitter that transmits radiation, and a receiver that measures the radiation that is backscattered by the surface of the Earth. It has been discussed what role of the components: SAR, interferometry and PS are in the PS-InSAR technique. SAR is the radar instrument that is side looking. It differs from traditional SLR as it has circumvented the limited along-track and range-track resolution, and is therefore able to better distinguish between different targets. Interferometry allows to measure distances as well as angles by using phase measurements. As a result, relative distances can be derived from two radar images. Persistent scatterers are scatterers that comprise a consistent behavior, allowing to derive the same feature in successive radar images.

The PS-InSAR technique measures displacement by using the phase and the amplitude of the backscattered signal. The amplitude refers to the strength of the recorded signal, and the phase indicates the displacement of the corresponding location. Given the precision of phase measurements, the displacement can be relatively precisely derived from the distance a certain signal has travelled. The precision of the phase measurement is not dependent on the resolution or the weather. The precision of the estimated double-difference displacements is dependent on the weather, but not on the resolution. One has to keep in mind that the absolute position of measurements of PS-InSAR depends on the satellite system. Additionally, when working with PS-InSAR data one has to keep the error sources that can have an effect on the data in mind.

2.3 LiDAR Point Clouds
The LiDAR technique makes it possible to acquire three-dimensional point data of surface objects in a cost-effective and rapid manner (Cheng et al., 2015). The remote sensing technique of LiDAR is similar to the technique of radar, and is therefore similar to the technique of PS-InSAR. The techniques are however not identical, which will become clear in this chapter. To mitigate the understanding of the difference between the two techniques, this chapter will have a similar structure as the chapter regarding PS-InSAR (Section

2.2), and has been divided into three sections regarding: (1) how is LiDAR data being collected and processed to (2) finally be used for visualizing the point clouds and to get familiar with the possible obstacles of working with LiDAR data, this chapter will end with (3) an error analysis of LiDAR point cloud data.

2.3.1 Collection Method

Similar to PS-InSAR, the LiDAR is an active remote sensing technique (McCormick and Leavor, 2013). The active radiation source of the lidar technique is a laser. Dissimilar to the PS-InSAR technique, LiDAR is operating in the near-infrared, visible or ultraviolet part of the electromagnetic spectrum (Figure 6) rather than in the microwave window. The differences between these two parts of the spectrum are the wavelengths: the wavelengths in the ultraviolet, visible or near-infrared are much shorter compared to the microwave part (Clevers, 2017). A result of having a shorter wavelength is the ability to image smaller objects or features, as the smallest object than can be imaged is similar to the size of the wavelength. The LiDAR technique is therefore often applied in atmospheric physics and meteorology.

There are three types of laser scanning systems: (1) an airborne laser scanning system (ALS), (2) a terrestrial laser scanning system (TLS) and (3) a vehicle laser scanning system (VLS). Figure 12 illustrates a typical example of the three complementary parts of an ALS: a kinematic global positioning system (GPS), a laser for measuring the distance to the targets and an inertial measurement unit (IMU) to record the pitch, yaw and roll of the platform. A TLS system replaces the airborne helicopter and the GPS with a TLS scanner and a surveyor located on the ground, similar a VLS system replaces the airborne helicopter and the GPS with a vehicle, for example a car. The fundamentals of the different systems are however the same: the lasers are an optical source that emit photons in a coherent beam or pulse, these laser pulses typically consist of one wavelength. Subsequently, the distance between a target and a sensor is calculated by measuring the time interval between the emission of a pulse, and the detection of its reflection (Pradhan & Sameen, 2020). However, there may be multiple objects of different ranges in the travel path of a pulse, resulting in a series of echoes of the incoming signals. Conventional LiDAR systems therefore record only the first and the last incoming signal. The more advanced LiDAR systems are however able to record signals between the first and the last incoming signals. The technique of LiDAR systems is therefore able to collect elevation data. This is however not the only measured variable by LiDAR systems: most systems are also able to measure the amplitude of the incoming signal, which allows the derivation of attributes of the particle or object that causes the backscattering (Chen, 2016).

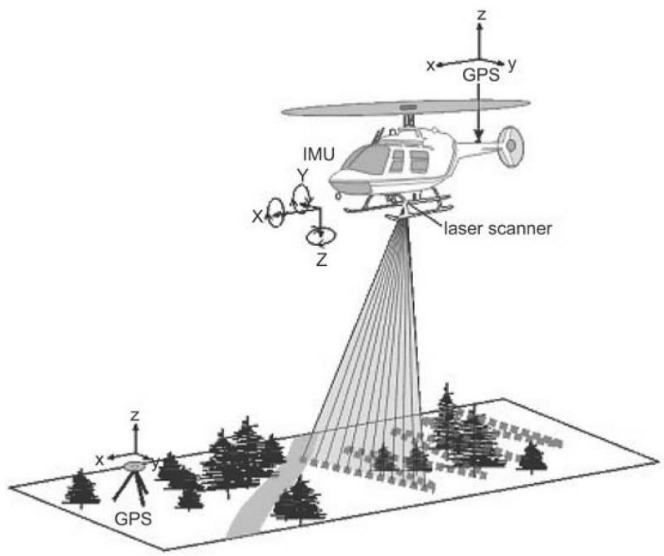

*Figure 12 ALS system (*Webster and Forbes, 2006)

With the use of georeferencing techniques the distance measurements retrieved by a LiDAR system are commonly transformed into three-dimensional point clouds. The resolution and the horizontal and vertical accuracy of the point clouds are dependent on the IMU and GPS components of the concerned laser system (Chen, 2016).

2.3.2 Making Three-dimensional Representations with LiDAR

A LiDAR point cloud consists of points that each have x, y, and z positional information. Next to that, a point cloud contains ground points (representing the terrain) and non-ground points (representing objects). A point cloud consisting of both ground and non-ground points is referred to as a Digital Surface Model (DSM), whereas a point cloud consisting of only ground points is referred to as a Digital Terrain Model (DTM) (Chen, 2016).

As the name suggests, point clouds are literally a cloud of points. Geometry can only be derived from certain perspectives, but not from all. Techniques to reconstruct the surface of the area covered by the point clouds do therefore exist. These techniques allow the transformation of a point cloud into a three-dimensional model. Poux (2020) divided these techniques into two categories: solids (Figure 13) and shells or boundaries (Figure 13). Solid representations represent the volume of the concerned object. A shell or boundary representation does not represent the volume, but only the surface or boundary of the concerned object.

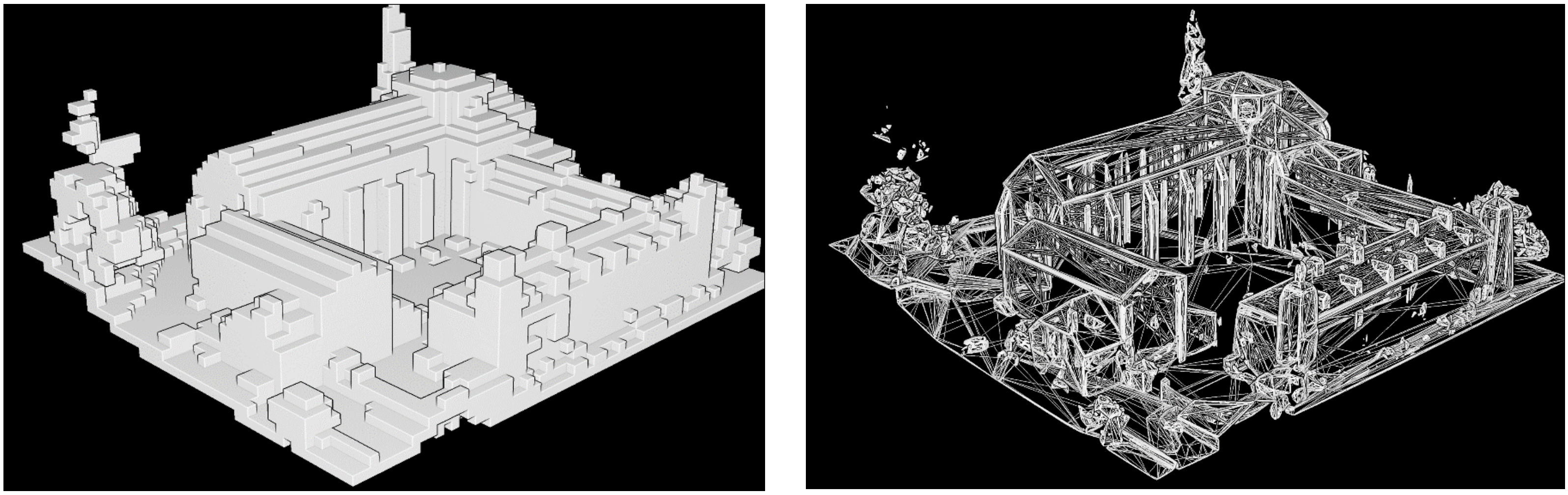

Figure 13 left: solid representation, right: shells and boundaries representation (Poux, 2020)

A boundary representation as a three-dimensional mesh is the most common model to describe point clouds through a three-dimensional model. A three-dimensional mesh uses a certain set of polygons to represent a geometric structure. They are typically used to represent surface subdivisions, allowing the discretization of a continuous surface. A mesh consists of vertices that are connected by edges, resulting in faces (Figure 14).

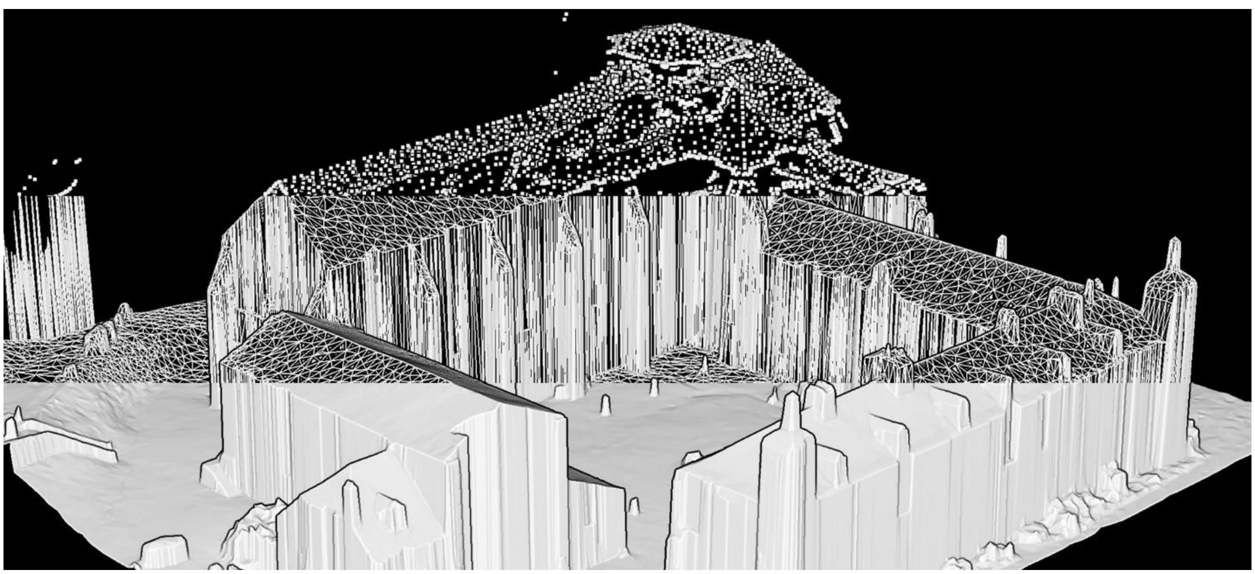

Figure 14 from top to bottom: The vertices of the mesh; the edges linking vertices together; the faces filling formed by vertices and edges, mostly triangular (Poux, 2020)

Boundary representation three-dimensional models have two main components. Next to the geometry of the point clouds, the topology or the organization of elements is a significant component of boundary representation three-dimensional models. Whereas the geometry refers to points, curves and surfaces, topology refers to the organization of the edges, faces and vertices. There are however numerous types of topological models. Figure 15 illustrates an example of a topological model: the three-dimensional formal data structure, which is in fact the first topological model that considers an explicit representation of objects (Zlatanova, 2004).

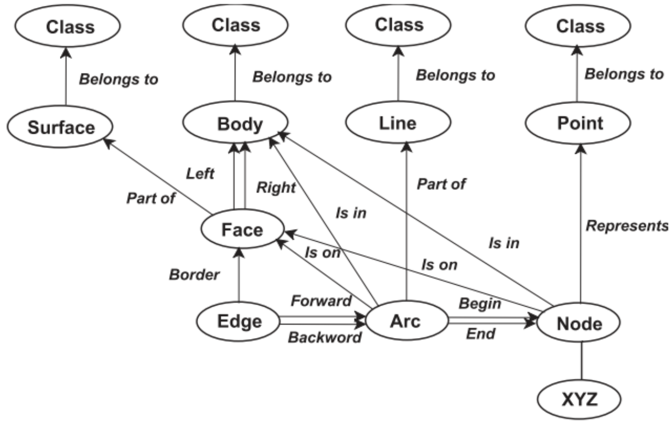

Figure 15 The three-dimensional formal data structure (Zlatanova, 2004)

Topological three-dimensional models are more complex than geometry three-dimensional models. This is because there is not one specific three-dimensional topological model suitable for all applications. The appropriate model is closely related to particular categories of applications (Zlatanova, 2003). To maximize effectiveness and efficiency of operations, it is suggested to maintain multiple topological models in one database by describing for each model the constraints, rules and objects in a metadata table (Van Oosterom et al., 2002 in Zlatanova., 2004).

Meshes are particularly suited for both representing the geometry and topology of a point cloud. One however has to keep in mind that a mesh can only represent point cloud data to a certain degree, as it interpolates the base point cloud geometry. According to Poux (2020), the mesh method that results in the highest added value when representing three-dimensional point cloud data is the parametric model. This is due to its massive enrichment of semantics, allowing to define classes of shapes, instead of particular instances. With the parametric model, the underlying geometry of classes of shapes can be modified with a parameter to a targeted value. A framework used for generating a parametric model is that of the Smart Point Cloud Infrastructure (SPCI). SPCI aims to represent the real world, spatially described by point clouds in a digital form, to serve as an intelligent environment for the concerned users. Representing point clouds in an intelligent environment is derived from our cognitive system: the recognition of an object means access to symbolic units that are stored in a semantic memory and that are abstract from earlier experiences while they are independent from any context. (Poux, 2019).

Figure 16 is a hierarchical representation of the 'semantic memory' of a SPCI: point cloud data can be divided into semantic patches (upper layer), these semantic patches are composed by connected elements (middle layer), and these elements can in turn be decomposed into domain specific elements (bottom layer). The top of the pyramid represents the highest level of domain representation. Each layer of the pyramid has its own meta-model, in which the components and the relations between them have been visualized with the use of a Unified Modeling Language (UML) diagram, an example of the UML diagram of the Patch layer is shown in Figure 17.

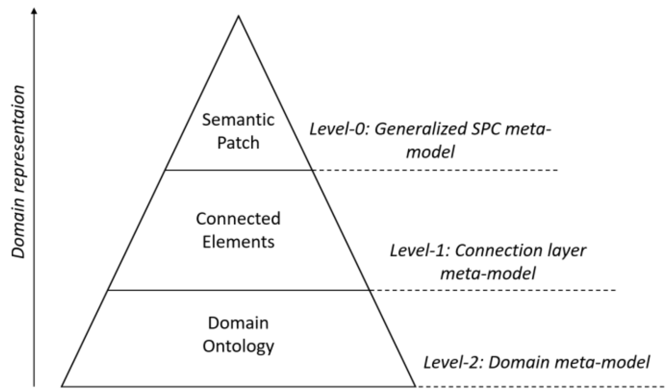

Figure 16 Hierarchical structure of the semantic memory of a SPCI

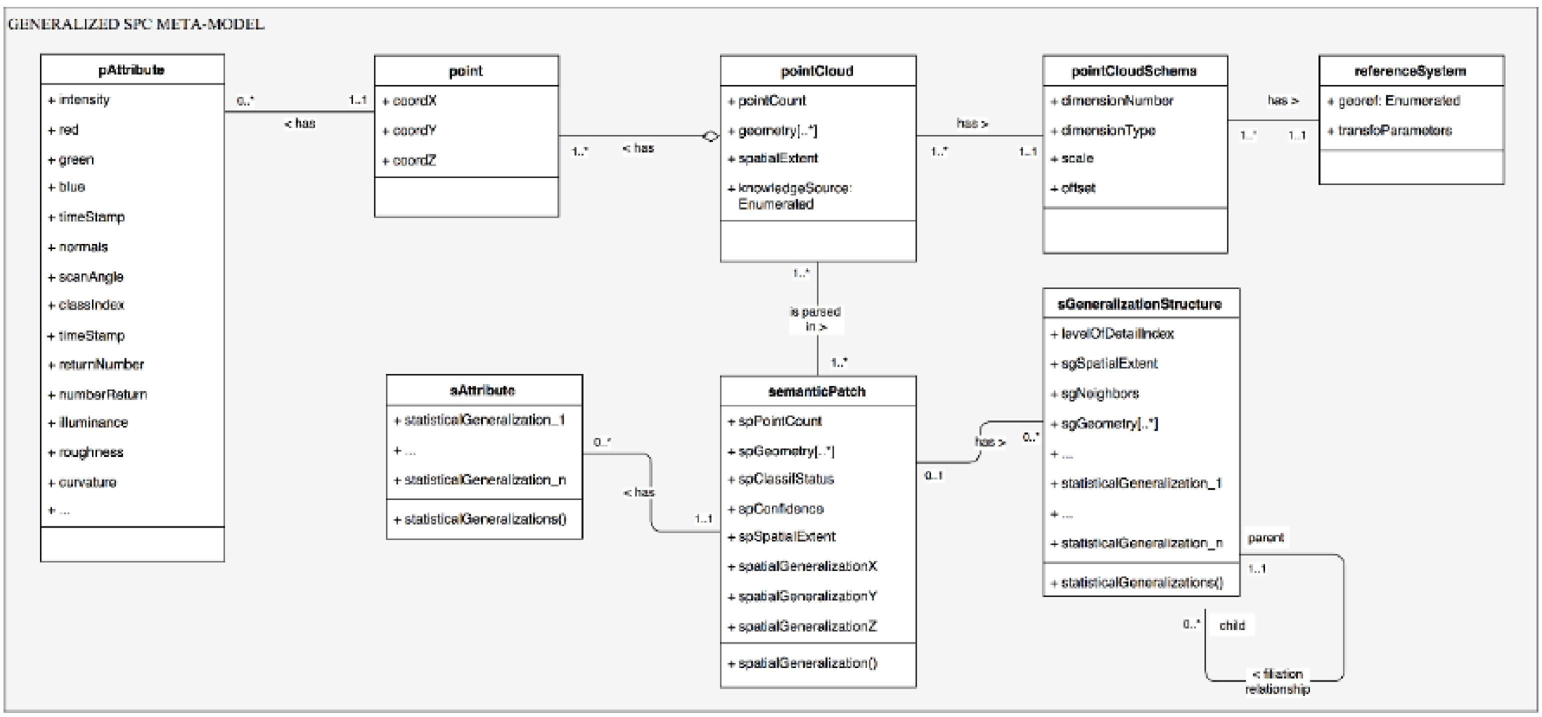

Figure 17 Meta-model of Level-0 Generalized SPC meta-model (Poux, 2019)

The semantic segmentation and classification allow users to extract or mine relevant information concerning a specific application domain (Poux, 2019). Figure 18 illustrates the difference between a three-dimensional point cloud representation and a three-dimensional semantic representation of an SPCI.

Figure 18 left: 3D point cloud representation vs right: 3D semantic representation (Poux, 2019)

2.3.3 Error Analysis

The error of a point cloud dataset is dependent on the laser scanning system used to gather the data points. The study of Pradhan and Sameen (2020) provided a performance comparison of the three different systems ALS, MLS and TLS. However, the comparisons of their study were specifically designed for road extraction and modelling. Therefore, the general comparisons, independently of road extraction and modelling, of the three systems have been filtered out and are shown in Table 3.

ALS	MLS	TLS
Direct view of pavement and building tops	Good view of pavement, unable to capture building tops	Good view of pavement with details
Oblique view of vertical faces	Direct view of vertical faces	Direct view of vertical faces with more flexibility
Fast coverage	Slow coverage	Slower coverage
Large laser footprint	Small laser footprint	Small laser footprint
Far-range travel	Short-range travel	Short-to-moderate range travel
Low point density (1–60 point/m^2)	High point density (100 points/m^2)	Very high point density (500 points/m^2)
Limited options for setup locations	Good options for setup locations	Better options for setup locations
Difficult to operate and requires adequate training	Difficult to operate, but easier than ALS as a pilot is not needed	Easy to operate with less training
Provides a low level of details	Provides a high level of details	Provides the highest level of details
Highest cost-effectiveness	High cost-effectiveness	Low cost-effectiveness

Table 3 Comparison of ALS, MLS and TLS

From Table 3 it can be derived that the datasets retrieved from the different systems differ. Therefore, it is important to consider what method is the most suitable for a specific application. To reduce the inaccuracies of the dataset, the different datasets gathered by the different systems can be combined (Cheng et al., 2015). While the different datasets have different inaccuracies, the datasets do share the commonality of being unsuitable to monitor deformation at a millimeter level (Van Natijne, 2018).

As the aim of this study is to visualize land deformation with the use of LiDAR point clouds, the next chapter will discuss how PS-InSAR deformation data can be combined with the LiDAR point clouds.

2.3.4 Summary

This chapter discussed how LiDAR data is being collection with active remote sensing systems that make use of a laser. There are three types of remote sensing systems for LiDAR point cloud collection: ALS, VLS and TLS. A boundary representation as a three-dimensional mesh is a convenient way to represent point clouds, as it is able to represent surface subdivisions, and allows for the discretization of a continuous surface. The main components of boundary representation three-dimensional models are geometry and topology. A topological model captures the organization of edges, faces and vertices whereas a geometric model refers to points curves and surfaces. A convenient infrastructure that can be used for realizing a boundary representation three-dimensional model is SPCI. SPCI makes use of a semantic memory, allowing users to extract relevant information concerning a specific application domain. Each type of system (ALS, MLS or TLS) comes with its own errors. To reduce the errors of a representation it is suggested to combine the point clouds gathered by different systems.

2.4 Combining PS-InSAR with LiDAR point clouds

Given the uncertainty of the absolute positioning of PS-InSAR measure points, and the inability of LiDAR point clouds to measure deformation at a millimeter scale precision, the individual datasets are assumed to be inadequate to provide an interpretable or accurate three-dimensional representation of deformation. Therefore, to realize an interpretable and accurate three-dimensional representation of deformation data a combination of the two datasets is desired. Essentially, both the PS-InSAR dataset and LiDAR point clouds consist of point features. Additionally, all points of both datasets have a x, y and z coordinate, both datasets can therefore be referred to as three-dimensional point features. This chapter will look into existing techniques that allow the combination of three-dimensional point features. The basics of three techniques will be discussed: the Three-Dimensional Normal Distribution Transform (3D-NDT) technique, the Iterative Closest Point (ICP) algorithm, and the method used in the study of Van Natijne et al., (2018). The 3D-NDT technique and the ICP algorithm have been designed to align point features, whereas the study of Van Natijne (2018) specifically focused on combining PS-InSAR data with LiDAR point clouds. The aim of the techniques is to find the locations in both datasets that refer to the same entity of a particular underlying object.

2.4.1 3D-NDT Technique

Magnusson (2009) studied the 2D-NDT technique, and transformed it to the 3D-NDT technique, which can also be used for scan (point cloud) registration. The goal of this registration is to find the pose of one scan (A), represented as point cloud $\mathcal{X} = \{\vec{x}_1, \ldots, \vec{x}_n\}$,that maximizes the likelihood that its points lie on the surface of a reference scan (B). The first step of this technique is the subdivision of the point cloud of scan (A) in cubes, that preferably have more than five points. In order to achieve that the points of scan A lie on the surface of the reference scan B, the rotation and translation of the pose estimate (p) of the points in the cubes of scan A needs to be optimized. Let us assume that there is a spatial transformation function $T(\vec{p}, \vec{x})$ that moves a point from the point cloud of scan A in space by the pose ($\vec{p}$). Given a PDF $p(\vec{x})$ (mixture of normal distribution and uniform distribution is suggested) that is robust to outliers and captures the local structures of the surface points (of scan B), the best pose ($\vec{p}$) of the points in a certain cube of scan A should maximize the likelihood function (Function 1), or minimize the log-likelihood function (Function 2).

$$\Psi = \prod_{k=1}^{n} p(T(\vec{p}, \vec{x}_k))$$

Function 1

$$-\log \Psi = -\sum_{k=1}^{n} \log \left(p(T(\vec{p}, \vec{x}_k))\right)$$ *Function 2*

Based on a scoring function that corresponds to the likelihood, the parameters of the pose $\vec{p}$ (the rotation and translation) that optimize the likelihood that the points of scan A are located on the surface of reference scan B can be determined (Magnusson, 2009).

Implementation issues of the 3D-NDT technique
Magnussen (2009) discusses the issue on determining the correct size of cubes, in which the point cloud to be referenced will be divided. This suitable size depends on the amount of structure in the scans and the scale of the scans. Using oversized cells predominantly affects the translation estimate. Next to that, using a fixed cube size may not be optimal, as it cannot always satisfyingly capture the underlying structure of the surface. There are however other discretization methods suitable for the 3D-NDT technique. This does however increase the complexity of the technique.

2.4.2 ICP Algorithm

The ICP algorithm matches two surfaces and determines the closest corresponding points. Subsequently, the two surfaces are aligned so that the distance between the corresponding points is minimized. This process is iterated until convergence. Baerentzen et al. (2012) refers to the ICP algorithm as a simple but rather successful technique for aligning point datasets. The algorithm does however rely on an adequate initialization, the two surfaces should for example not be too far located from each other.

The IPC algorithm aligns one mesh (M_1) to a second mesh (M_2). The algorithm assumes that the two meshes are a discretization of the same underlying surface, with possible noise, and that M_1 has been rotated and translated which is referred to as a rigid transformation. The rigid transformation can be divided into four iterative steps:

1. For all vertices of M_1, the closest vertex of M_2 has to be found
2. Determine the rotation and translation that minimized the distance between the closest vertices of M_1 and M_2
3. Apply the rotation and translation to M_1
4. Check if convergence has been reached, if not: go back to step 1. Convergence has been reached when for example the closest vertices in step 1 are the same as in the previous cycle

An example of the iteration of these steps has been visualized in Figure 19, where the red points are being aligned to the blue. In this example, the two data sets needed four iterations to be aligned.

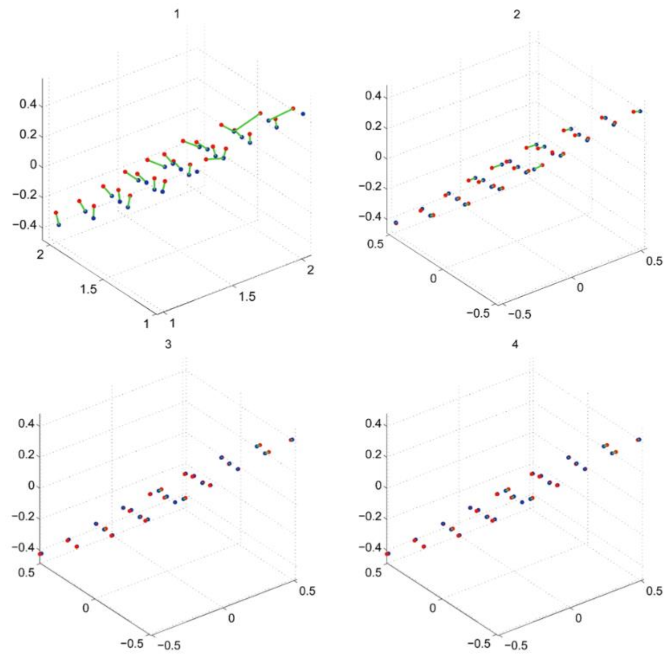

Figure 19 four iterations of the ICP steps (Baerentzen et al., 2012)

Implementation issues of the ICP algorithm
Baerentzen et al. (2012) discuss three implementation issues of the ICP algorithm. The first issue concerns the process of finding the closest vertex, which is done in step 1. The conventional methods, for example to traverse all the vertices in M_2 for all vertices in M_1, are relatively disadvantageous when ran for meshes that contain thousands of points. Therefore, it is recommended to use other spatial data structures, for example a kD-tree.

The second issue concerns that the closest points do not have to be unique in step 1. As a result, a vertex in M_1 can have more than one vertex in M_2 as its closest point. Therefore, the algorithm is considered to have non-symmetric outcomes. The differences should however be negligible when successfully carrying out the algorithm.

The last issue regards finding a proper rigid transformation, associated to step 3. A nonlinear optimization algorithm seems straightforward. There are however more direct methods to match point sets.

2.4.3 Method from Van Natijne et al. (2018)

Van Natijne et al. (2018) focusses specifically on linking LiDAR point clouds to PS-InSAR data. He describes the process of linkage based on five steps:

1. Create a common visualization of the PS-InSAR data and LiDAR point clouds. Add the visual aids of plane estimates and error ellipsoids to improve the interpretation of the scene geometry and the radar signal (Figure 20).
2. Find nearest neighbor linking with a Nearest Neighbor algorithm. Prior to the algorithm all points of both LiDAR and PS-InSAR have to be subject to the Whitening Transformation. The whitening transformation transforms the coordinate systems of the points so that the Euclidean metric represents distance not in meters but in σ, which represents the population standard deviation. As

a result, the errors of both datasets are now normally distributed allowing any Nearest Neighbor algorithm to be used. Due to the relatively small error of the LiDAR point cloud (AHN2) the LiDAR point cloud is considered as the ground truth in the Nearest Neighbor search (Figure 20)

3. Link PS-InSAR points to a single surface of a predefined selection of AHN points by fitting a single plane trough the points
4. When the planes identified in step 3 are non-flat, link the PS-InSAR points to multiple surfaces. Based on random sample consensus. In Figure 20 the multiple (two) surfaces are the vertical and horizontal one. The error ellipsoid of the PS-InSAR point intersects both surfaces. Both surfaces are therefore considered as a candidate surface.
5. Linking the PS-InSAR points to dihedral and trihedral geometries of the surface. The deformation signal (PS-InSAR point) should not be placed at the surfaces themselves, but at the intersection of the surfaces Figure 20.

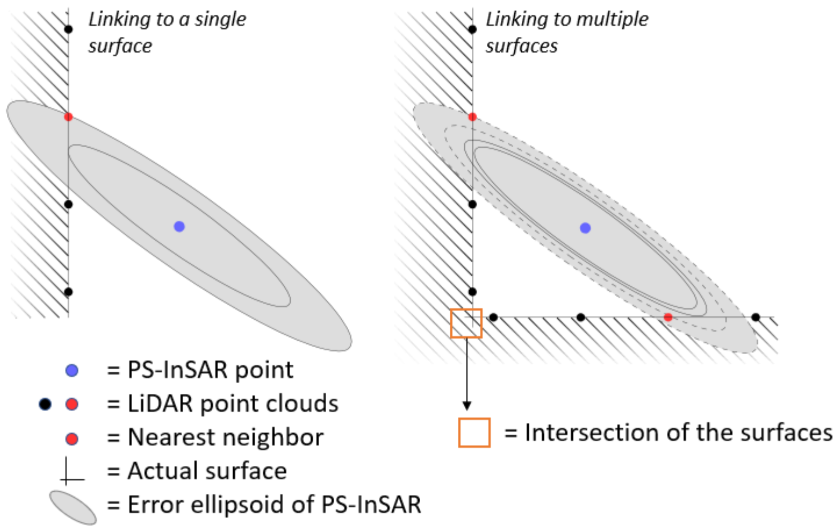

igure 20 Step 3 and 4 of Van Natijne et al. (2018) linking PS-InSAR to LiDAR point clouds (derived from Van Natijne et al., 2018)

Implementation issues of the method from Van Natijne et al. (2018)

Van Natijne et al. (2018) discusses a possible issue that might occur when using a nearest neighbor algorithm on point clouds: the distances on low density surfaces may be overestimated.

The method takes the geolocation error model as a constant for the entire area covered by the radar image and for the different types of scatterer. However, it is rather likely that this assumption is incorrect (Dheenathayalan, 2016 in van Natijne et al, (2018).

The quality of the determined point of intersection is not defined. Instead, there are two separate and independent metrics that define the quality of the intersection and the quality of the surface fit. Hence, a single error model is currently not implemented.

Main differences between the three techniques

The main difference that can be established is that the 3D-NDT technique does not have to find correspondence between features of points whereas the ICP and the method from Van Natijne et al. (2018) do have to find this, while this has been indicated as the part of many approaches that is most prone to errors (Magnusson, 2009).

A second difference is that both the method of Van Natijne et al. (2018) and IPC do not provide an error model for their results. As a result, it cannot be established whether the algorithm has been carried out successfully or not. As previously explained, the 3D-NDT technique uses a success factor to establish whether the algorithm was successful or not.

The 3D-NDT and ICP technique link the PS-InSAR points and their deformation signal to surfaces, whereas the method of Van Natijne et al. (2018) aims to link the PS-InSAR points and their deformation signal to the intersection of surfaces.

2.5 Spatio-temporal Visualization of Three-Dimensional Deformation Data for the Public

The previous chapter has discussed the methods that can be used to combine PS-InSAR and LiDAR point clouds into one visualization. This chapter will discuss design principles of three types of visualizations: visualizations for the public, spatio-temporal visualizations and three-dimensional visualizations, to get an understanding of how to design the combined visualization. The chapter will end with an explanation of why it is important in the process of visualization and design to constantly consider the path the final user of the map will take to derive information.

2.5.1 Designing a Visualization for the Public

Schoffetelen et al. (2015) studied how visualizations that reveal issues of public concern can best be designed to stimulate the public to interest and engage in participatory processes. Their study is aligned with the three roles of land subsidence communication, previously presented in Figure 3: (1) the study discusses what design principles should be integrated in a visualization (*general role: interface*), (2) to communicate the visualized data to the public (*presenting role: communication to public realm*), (3) to allow citizens to engage in participatory processes (*engagement role: engage in governance processes regarding adverse effects of land subsidence*). As a result of this alignment, the study of Schoffelen et al. (2015) can be seen as valuable contribution for the designing process of a visualization of deformation data for the public.

Central in the study of Schoffelen et al. (2015) are the two terms transparent and readable, which are both seen as significant components in making data public. In this perspective, transparency refers to visualizing the latent or driving forces behind the data in a way that allows or stimulates the expression of new perspectives, rather than visualizing the data as indisputable facts without any insights regarding the associated driving forces. In short, transparency refers to the ability to reveal complexity. Readability refers in this perspective to the ease to make sense of or comprehend a visual representation, or the ability to reduce the perceived complexity. One might perceive the definitions of transparency and readability as contradicting (reveal complexity versus reduce perceived complexity, respectively), they should therefore be balanced. One however needs to find a proper designing method that allows the integration of readability and transparency in a well-balanced way. Schoffelen et al. (2015) propose three aspects that allow to communicate data in a transparent and readable way:

1. *Attract users to engage with the visualization:* Users should first be attracted by the visualization to be able to engage with the data (Venturini, 2010 in Schoffelen et al., 2015)
2. *Encourage users to make sense of the dynamic back story of the data:* Chose between two design principles: either design to engage users for a longer period of time to allow the exploration of multiple perspectives by adding visual difficulties (Venturini, 2010 in Schoffelen et al., 2015), or design to aid users in identifying and understanding the different involved perspectives by reducing visual difficulties (Hullman et al., 2011 in Schoffelen et al., 2015).
3. *Enable users to reflect on interpretations:* Allow users to react and contest by providing them with knowledge of lesser-known perspectives of the data in relation to the common perspective(s). As

a result, users are enabled to relate different perspectives to each other, also referred to as an open space of contestation (DiSalvo, 2012 in Schoffelen et al., 2015)

Additionally, based on three different case studies, Schoffelen et al. (2015) articulated three recommendations relevant for successfully designing a transparent and readable visualization. The first one concerns staging interactions, with the use of for example a step-by-step guide to explore the visualization. The second recommendation relates to using location for contextualization (considering the visualized phenomenon in the situation in which it happens or exists). The last recommendation regards contextualizing via a medium (linkage with other sources the user is already familiar with), and allowing users to add their perspective concerning the visualized phenomenon by providing users with an access point for participation.

This section discussed aspects and recommendations for visualizing data for the public in a relative abstract way, as it was not specific for the application of this study (a spatio-temporal visualization of three-dimensional deformation data). The next two sections will discuss the design principles of three-dimensional and spatio-temporal visualizations respectively.

2.5.2 Three-dimensional Design Principles

Haeberling et al. (2008) defines a three-dimensional map as a perspective view visualized in a two-dimensional space, but perceived as a three-dimensional reality. Perspective views are often perceived as attractive due to their graphic expressiveness and graphic appearance (Hurni, 1995; Haeberling, 1999; Slocum et al., 2005 in Haeberling et al., 2008). Additionally, three-dimensional visualizations are less frequently applied than conventional two-dimensional maps, and are therefore more frequently fascinating viewers. The difference with conventional two-dimensional maps is that individual objects cannot all be positioned precisely within the image, and distances cannot be measured in three-dimensional maps.

Three main aspects that have to be considered in designing a three-dimensional map are the conceptual, technical and product aspects (Hake, 2002 in Haeberling et al., 2008). The conceptual aspect requires knowledge of the personal environment of the user (competence and skills, the use of application, and the circumstances of location and time), and must be taken into consideration during the design process. The technical aspect requires specific computer applications and digital input data. The last aspect, the product aspect, concerns decisive points regarding whether a user is willing to use the map or not: the availability (for example costs), usability and handling, thematic content and the design and visual appearance of the three-dimensional map.

Besides these three main aspects of the design process of a three-dimensional map, the workflow of designing a three-dimensional map can also been categorized into three main steps: modeling, symbolization and visualization (Terribilini, 2001 in Haeberlingen et al., 2008). Each step has associated design aspects (Table 4). Design aspects are groups of parameters that can influence the appearance or position of objects within a map.

Workflow step	Design aspect
Modelling	- Characteristics of geometric modelling
Symbolization	- The graphical appearance of the thematic content
Visualization	- Camera parameters related to the map model - Shading and lighting settings - Rendering parameters

Table 4 Design aspects associated to the workflow steps of designing a 3D map

The complete process of designing a three-dimensional map can be composed of the three main aspects that constantly have to be taken into consideration in the designing process, the three workflow steps (Terribilini, 2001 in Haeberlingen et al., 2008) and their associated design aspects (Figure 21). The complete workflow and the individual steps can be iterated when necessary.

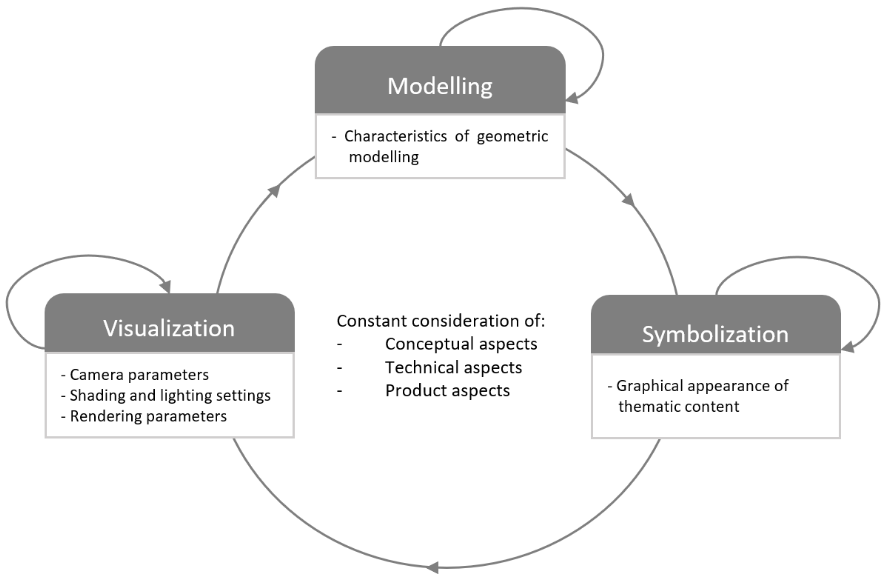

Figure 21 Workflow of designing a three-dimensional map

Haeberling et al. (2008) propose nineteen principles for designing three-dimensional maps, derived from interviews with specialists in three-dimensional cartography. Table 5 lists the design principles per workflow step.

Modelling	Symbolization	Visualization
Shapes and patterns of the objects must not look just as they do in reality	The appearance of point map objects must not be too dominant	The addition of slight haze improves depth perception in a perspective view
3D map symbols improve the perspective perception of a 3D map	Point map objects can be sized larger than linear or area map objects	Perspective can be perceived in a 3D map even with no haze effect
3D symbols for point map objects are well suited for image-like representations	The size of linear and point map objects must be chosen so that they do not cover too much of the terrain	A neutrally colored model background, even without sky structure, generally fits well with perspective views of 3D map models
3D symbols may consist of simple geometric shapes	The size of map objects must be defined so that they do not obscure each other too much	The lightning direction of a 3D map model must be mainly lateral or slightly from ahead
3D objects can have a natural, realistic appearance, but they do not have to be photo-realistic	The size of topographic map objects must be chosen so that they can be clearly identified in the foreground as well as in the background (or reversed)	To look at a 3D map model, an average inclination angle of about 45˚ is preferable
Structural patterns can be useful textures for area map objects		

Structural patterns for area map objects must not be designed to be too dense or too fine	The character of the terrain is emphasized when exaggerating the digital elevation model	
Structural patterns for area map objects must exhibit good color contrast to the terrain		

Table 5 Design principles for three-dimensional maps, categorized per process step

This section provided insights into the design principles and developing process of three-dimensional maps. The next section will discuss the basic design principles of developing a spatio-temporal visualization.

2.5.3 Spatio-temporal Design Principles

Spatio-temporal data is data that is temporal and includes references to geographic locations. An example of spatio-temporal data has been visualized in Figure 22: it illustrates how a certain attribute (Y-axis) varies in time (t and t+1) and space (X-axis). In this section it is assumed that users of spatio-temporal visualizations have three requirements: they want to compare time-series of different locations, they want to see the distribution of spatial events in space and time and they want to see the variation of all attributes in time and space. Questions that are associated to these user requirements are for example:

- *Compare time-series of different locations*: how does the temporal pattern of the deformation values from location A differ from location B?
- *See distribution of spatial events in space and time:* when and where does the land subside four or more millimeters over a time period of one year?
- *See variation of all attributes in time and space:* how do the different spatial patterns of land deformation differ in the time period 2015-2020 in the Netherlands?

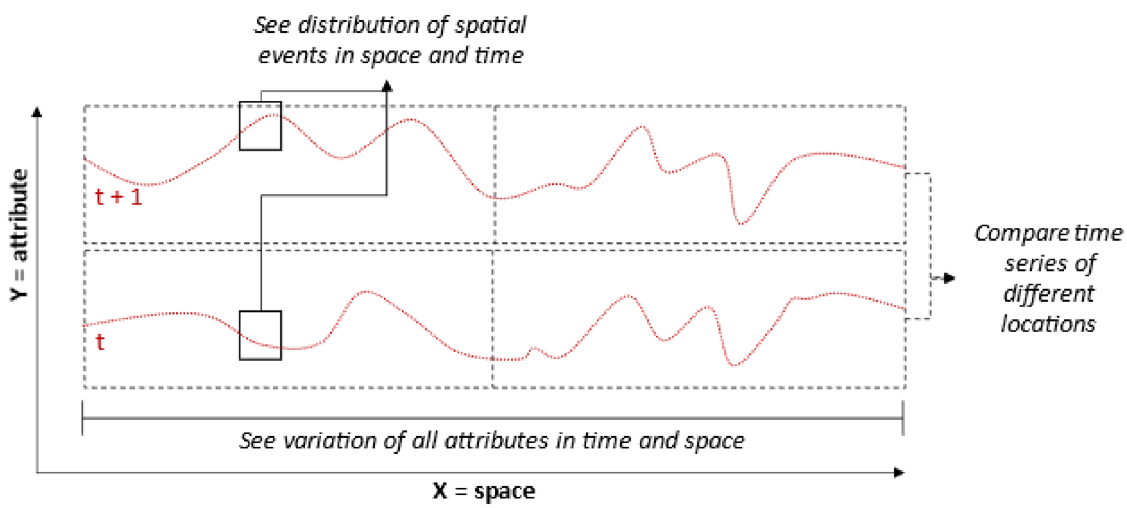

Figure 22 Spatio-temporal data and the assumed user requirements

Each user requirement can be realized by design principles. The remaining of this section will discuss these design principles per requirement.

Compare time-series of different locations

An important aspect of the visualization of time-series is to allow the ability to compare time-series of different locations. Andrienko et al. (2020) suggest two approaches to allow this comparison: (1) make use of separate displays for the time-series of the selected locations, and place these side by side to allow for comparison, or (2) make use of lines that represent time-series of different locations superposed in one display. For the latter technique, the time-series of the selected locations need to be temporary aligned.

Distribution of spatial events in space and time

Andrienko et al. (2020) describe the technique of visualizing spatio-temporal data in the space-time cube. An example of this cube has been visualized in Figure 23. The geographic space is represented by the horizontal plane, time is visualized on the vertical axis of the visualization (from bottom to top). The red dots in Figure 23 represent epidemic related messages, and are located in the cube according to their associated location and time. This technique allows the visualization of the spatio-temporal distribution of spatial events in one view.

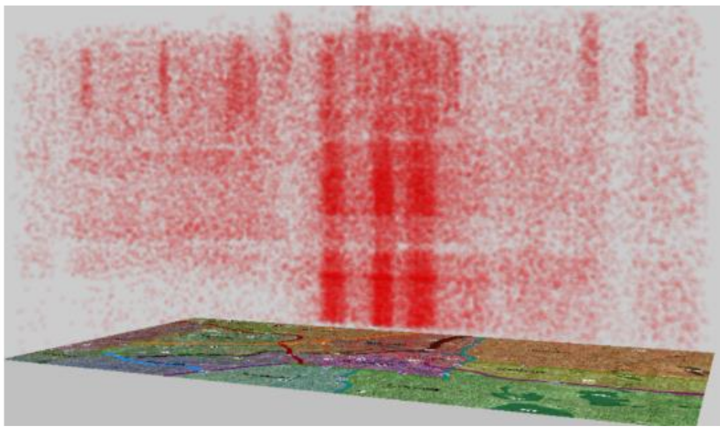

Figure 23 Example of a space-time cube visualization (Andrienko et al., 2020)

Variation of the attributes of the data in space and time

When visualizing time-series, the designer has to use a technique that allows the visualization of spatial variation of the attribute values that took place in different time steps. The most common approach with relatively large amounts of data is clustering (Andrienko et al. 2020). Clustering can be applied to both the spatial and temporal variation. They are however complementary, and will together provide insights of the spatio-temporal variation. An example of these two types of clustering has been visualized in Figure 24, the map represents the spatial clustering of the data (number of cars in London), and the two-dimensional graphs represent temporal clustering of the data. The visualization allows the user to see temporal patterns of the data in the two-dimensional charts and the distribution of these patterns in space can be seen in the map.

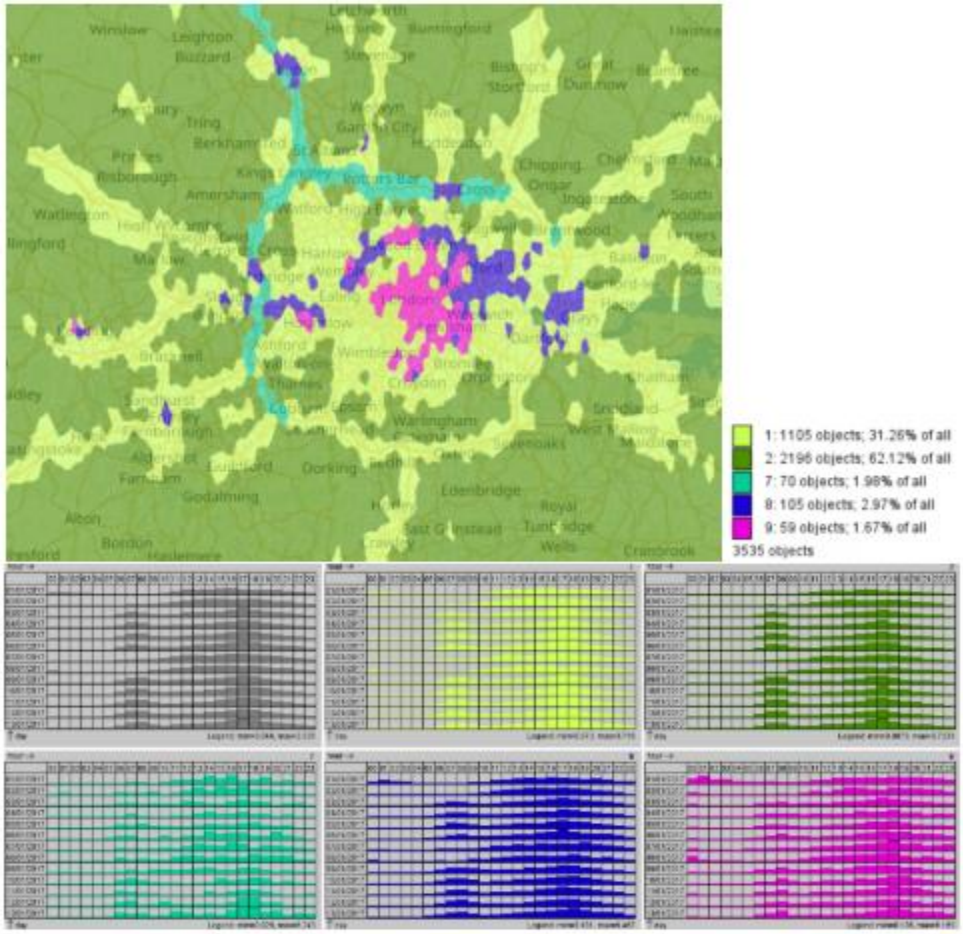

Figure 24 Spatial and temporal clustering (Andrienko et al., 2020)

The tesselation of the map in Figure 24 is not that of a regular grid. Andrienko et al. (2020) explain that discrete aggregation of data by a regular grid results in a distortion of the spatial distrubition patterns. To prevent this distortion, a data-driven space tesselation is suggested. A data-driven tesselation consist out of compartments that enclose spatial clusters of points. The advantage of a data-driven tesselation over a regular grid is that spatial patterns of distribution can be captured much better.

2.5.4 The Path of the Cartographer and the Path of the Map User

Van der Schans (2001) describes a framework that represents the dimensions of dynamic geodesy and cartography. In this framework, the existence of actions (handelingen), objects (objecten) and processes (processen) are central. The objects refer to things that exist in the real-world. Actions refer to an act that causes deliberate change of an object. Processes refer to autonomous change of an object, change that people cannot directly control. The framework describes how these three aspects exist in four different dimensions of dynamic geodesy and cartography: in the human environment, in thoughts, in forms of expression and in graphical representation. In the *human environment* the actions, objects and processes are the ones that exist in the real world. In *thoughts* the actions, objects and processes exist in our brains or in a computer as chemical or electrical patterns to describe a landscape. In *forms of expression* the actions, objects and processes exist as graphical means of expression and their associated perception properties to describe a landscape, this too exists in our brains or in a computer as chemical or electrical patterns. In *Graphical representations* the actions, objects and processes of a landscape are represented in one visual plane, for example a map.

Van der Schans (2001) refers to the two dimensions of *thoughts* and *forms of expression* as models: a landscape model and a visualization model, respectively. In these two models the actions, objects and processes can be stored in the mind or in a computer in various ways with different levels of detail of the semantic categories: attributes, time and geometry. Figure 25 provides an overview of the framework and possible relations within the framework of Van Der Schans (2001) that has been described. One might perceive this framework as rather philosophical, while in fact the framework can be of high value in the process of designing maps. When one designs a map, one wants to communicate a certain or several message with this map. However, to get to the dimension of a graphical representation (a map), the cartographer has to follow path A (Figure 25). The user who wants to derive information about the human environment dimension from the graphical representation has to follow path B (Figure 25). The mind of the cartographer is part of path A, while the mind of the user is part of path B. The cartographer cannot control the mind of the user. To prevent misinterpretation of the mind of the user, it is important to create a correct graphical representation. That is why the previous sections of this chapter have been committed to understanding the data, and their relevant associated graphical and design principles. To confirm that the user that follows path A derives the same actions, objects and processes from our human environment as the ones that have been presented by the cartographer, the outcomes of path A have to be tested and compared to the start of path B.

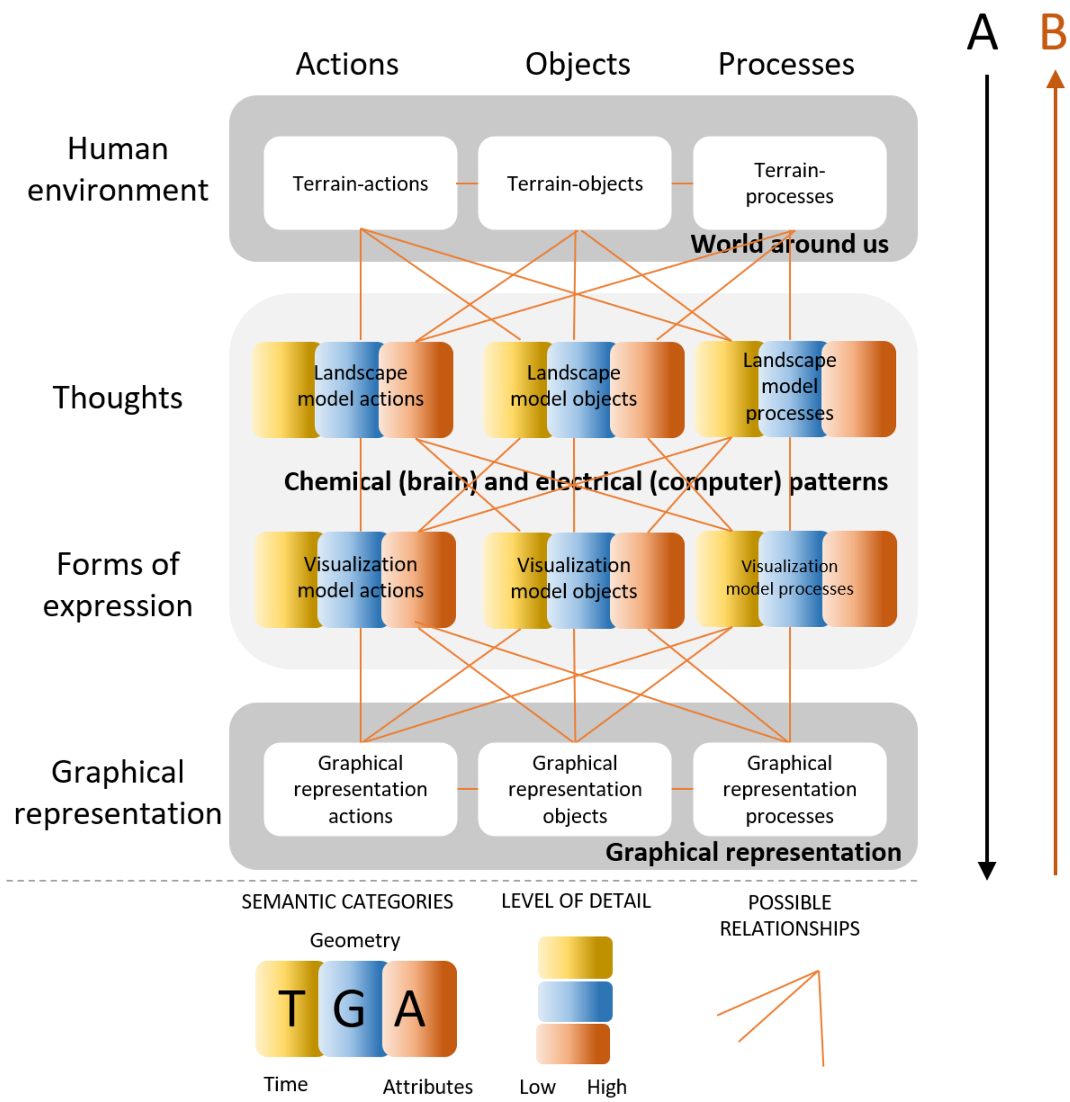

Figure 25 Framework of the dimensions of dynamic geodesy and cartography (based on Van der Schans, 2001)

3

Methodology

The objective of this research is to answer the question: t*o what extent can a spatio-temporal visualization of a combination of PS-InSAR deformation data with LiDAR point clouds improve the interpretability of the communication of land subsidence in the Netherlands?*

This research aims to answer this question by answering the following set of research questions:

1. To what extent is the PS-InSAR deformation data visualization, used for the current communication of land subsidence in the Netherlands, interpretable?
2. What aspects of PS-InSAR deformation data visualization can be improved by linking it to LiDAR point clouds?
3. To what extent can PS-InSAR data and LiDAR point cloud be combined into one spatio-temporal visualization?
4. Which design principles and graphical visualizations can be applied to the visualization to ensure interpretability?
5. To what extent is the spatio-temporal visualization of the combination of PS-InSAR and LiDAR point clouds interpretable?

3.1 Conceptual Model

The methodology of this research is aimed to develop and design a conceptual interface in which the necessary design principles and graphical visualizations are integrated, to allow an exploration of the time-series of PS-InSAR deformation data visualized in the form of three-dimensional point clouds. The associated process to realize the concept is a combination of a research and design process.

The design process integrated in this research is based on the research of Wolniak (2017). Wolniak (2017) writes about design thinking as a design process that adds value to a specific project through the creation of a visual identity. The focus in design thinking is on creating a design solution that positively communicates with the targeted user group, rather than only looking aesthetically different. The original design thinking process consist of five successive stages (Figure 26B):

1. *Empathize:* identification of the user needs
2. *Define*: translation of the user needs into specific goals for the design of the product
3. *Ideate:* evaluating and selecting concrete design ideas to be integrated into the design
4. *Prototype:* realize the design concept
5. *Test:* check the functioning of the designed concept

In the perspective of this research, the creation of a visual identity, as described by Wolniak (2017), concerns the conceptual interface. The five previously described successive stages will serve as a basis for the conceptual model in this research, however in a slightly adjusted manner: the five stages have been integrated into a research process, and have been made specific to this research (Figure 26B):

1. *Empathize:* analysis of to what extent the user needs are met with the current communication of land subsidence in the Netherlands, by investigating the interpretability of this communication from a users' perspective (related to sub-question 1)
2. *Define*: translation of how a combination of PS-InSAR deformation data with point clouds can improve the current land subsidence communication (related to sub-question 2)
3. *Ideate:* evaluating and selecting a technique to combine PS-InSAR deformation data with point clouds (related to sub-question 3), design principles and graphical visualizations (related to sub-question 4)
4. *Prototype:* realize the design concept
5. *Test:* check the functioning of the designed concept (related to sub-question 5)

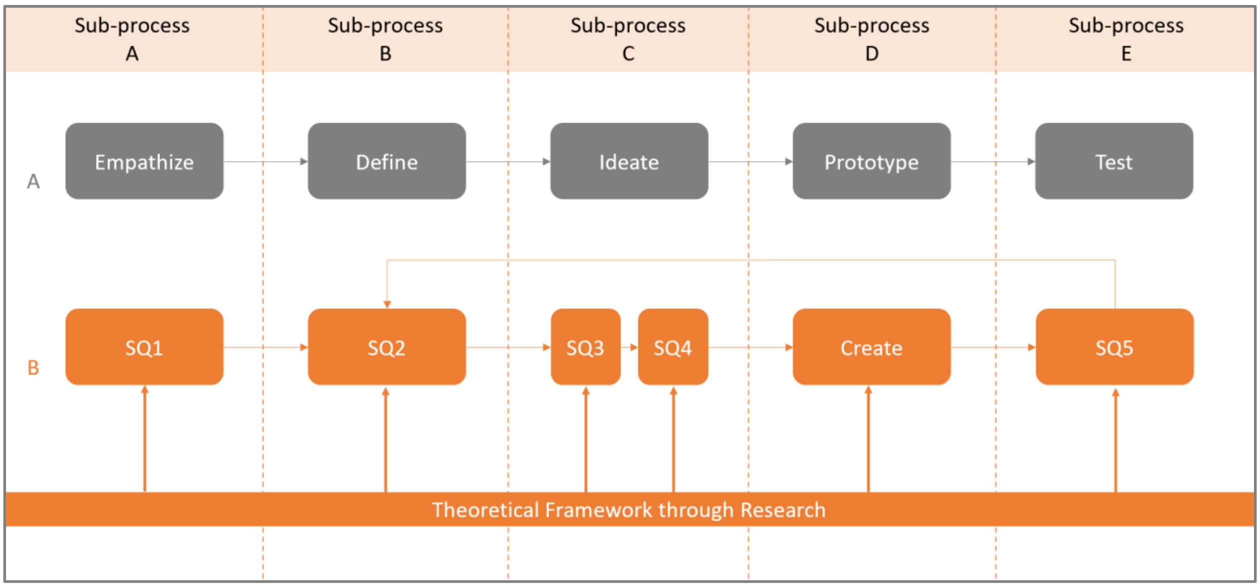

Figure 26 Overall Conceptual Model (based on Wolniak, 2017)

In Figure 26, the overall conceptual model of this research is illustrated. Figure 26A illustrates the original design thinking process, from which Figure 26B, the design process specific for this research, has been derived. Throughout the process of this research, a theoretical foundation (Chapter 2) for each sub-question is critical. The overall conceptual model of this research has not been divided by means of stages, as proposed by Wolniak (2017), but has been divided by means of sub-processes A, B, C, D and E. They are referred to as sub-processes, as each sub-process can be defined by its own methodology. This chapter will explain and illustrate the associated methodology for each of the sub-processes.

3.2 Analyzing the Interpretability of the Current Land Subsidence Communication (Sub-process A - empathize)

To understand the user requirements of a certain service, one first has to understand the needs of the users of that service. An analysis of those needs is useful, as users understand the actual use of the service. Additionally, users understand what ideas might be practical for improving the service (Welle Donker, 2020). In the perspective of this research, the service Welle Donker (2020) refers to concerns the land subsidence communication in the Netherlands. In an ideal scenario, the land communication should cover all the needs of its users, to allow an optimum interpretability of the visualized data. This ideal scenario is however not feasible in this perspective, as the needs of each individual user cannot be covered with just one service. As discussed in Section 2.1.1, the users of the current form of communication can be identified as the public and it can be rather hard to define the needs of the public as a user, as the public consist of unique individuals that can each have a different purpose of use for the data. Section 2.1.3 does however provide a framework with which the needs of the users of the land subsidence communication can be determined. The framework presented consists of three elements: (1) the overall goal of communicating land subsidence data to the public, (2) the three roles that the current form of communication has to fulfill to achieve its overall goal, and (3) the twelve different key components associated to these roles that need to be present in the current form of communication to achieve its roles. Based on this framework, one can state that the twelve key components are required to fulfill the overall goal of the current form of communication. As the goal is communication of land subsidence to the public, it is assumed that the twelve key components are equal to the needs of the public.

By looking at the user needs that are not yet covered by the current communication, potential improvements can be identified that can contribute to an increase of the interpretability of the communication of land subsidence. Therefore, in this sub-process, it will be analyzed to what extent the PS-InSAR deformation data visualization, used for the current communication of land subsidence in the Netherlands, is meeting the needs of its users, which will be an indication for the interpretability of the communication.

The methodology for sub-process A has been schematized in Figure 27. The first step is to identify the user needs. Step two is to look at the current form of communication through the perspective of the user needs. This way, the user needs that are already covered in the current communication can be determined, illustrated in the orange area. The orange area symbolizes the level of interpretability of the current form of communication. The third and last step concerns the identification of the grey area, which forms the basis of the other sub-processes: it contains the information for potential improvements to make the current land-subsidence communication more interpretable. The next section will discuss the role that LiDAR point clouds can play in realizing the potential improvements to increase the covered needs (orange), and hence increase the interpretability of the current communication.

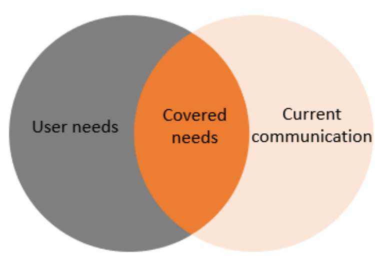

Figure 27 *Methodology of Sub-process A*

The three steps of sub-process A have been implemented in the theoretical framework Chapter 2: the user needs or the key components have been identified and defined in Section 2.1.3 (step 1), Section 2.1.4 looked at the current form of communication through the perspectives of these user needs or key components (step 2), and Section 2.1.4 provided the information for potential interpretability improvements in the form of recommendations (step 3). An overview of the results can be found in Section 4.1.

3.3 Using LiDAR Point Clouds to Improve PS-InSAR deformation data (Sub-process B - define)

To understand the role point clouds can play in increasing the interpretability of the current communication it is important to understand the two different methods so they can be compared. The methods behind the current communication and point clouds are PS-InSAR and LiDAR, respectively. Based on a literature study, the two methods' capabilities and functionalities to visualize deformation data have been compared (PS-InSAR: Section 2.2, and LiDAR: Section 2.3). The literature study will be used to analyze what the benefits are of adding the method of LiDAR to the PS-InSAR method in visualizing deformation data. To understand the added user-value of these benefits, it will be studied to what extent these benefits can cover the user needs that are not yet covered. The methodology has been visualized in Figure 28.

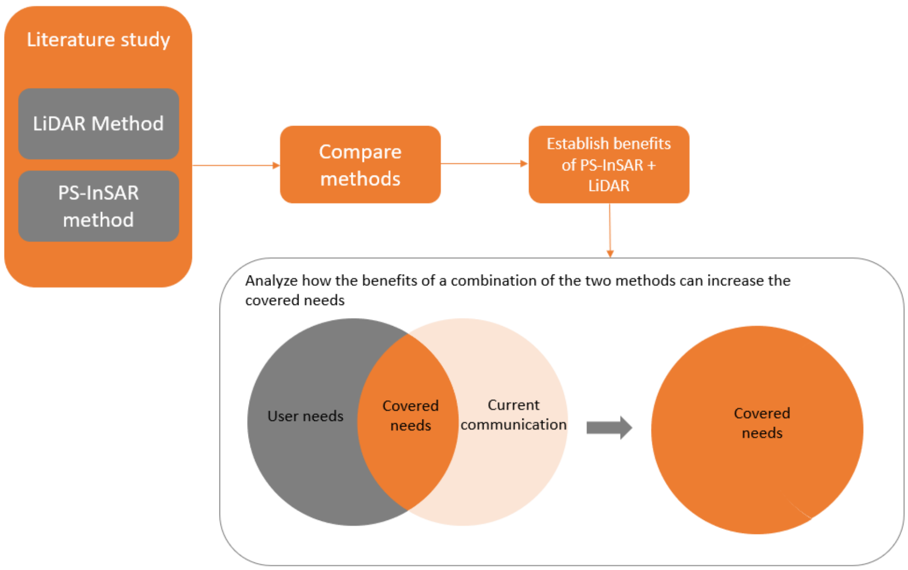

Figure 28 Methodology of Sub-process B

The results of sub-process B are illustrated in Section 4.1. In the next section, it will be analyzed how a combination of LiDAR point clouds and PS-InSAR deformation data can be realized.

3.4 Combining PS-InSAR deformation data with LiDAR Point clouds, and the Selection of necessary design principles and graphical visualizations (Sub-process C - ideate)

In this chapter it will be discussed how the LiDAR points and PS-InSAR points can be combined into one visualization, and how this visualization can best be represented and visualized.

3.4.1 Combining PS-InSAR Deformation Data with LiDAR Point Clouds

The three methods: 3D-NDT technique, ICP algorithm and the method from Van Natijne et al. (2018) have been discussed in Section 2.4. These three methods allow the combination of one point data set, to another point dataset, for example LiDAR and PS-InSAR points. When one wants to visualize the LiDAR points and PS-InSAR points in one view it is highly recommended to use a linking method, for two main reasons:

1. The absolute position (x, y & z) of PS-InSAR points is relatively imprecise, whereas the absolute position of LiDAR points is relatively precise. Using the LiDAR points as the ground truth for improving the absolute position of PS-InSAR points, which is what is being done in the previously described three methods, can therefore be justified.

2. Due to the imprecise absolute position of the PS-InSAR points, the displacement values cannot be assigned to the objects represented by point clouds. For example: due to the imprecise absolute position the PS-InSAR point will not be located at the wall of the building that it actually represents. Therefore, the derived deformation cannot be assigned to the wall of the building, which can lead to misinterpretations.

The method of Van Natijne et al. (2018) is assumed to result in the most accurate results, as this method has been specifically designed for combining PS-InSAR data with LiDAR data. The method takes for example the direction of the radar signal and the direction of flight of the radar system used for collecting the PS-InSAR data into account to limit errors (Van Natijne et al., 2018). This refutes the statement made in Section 2.4.3 *Main differences between the three techniques* that: finding correspondence between features of points (as done in ICP and the Method from Van Natijne et al. (2018)) is the part that is most prone to errors. Due to the consideration of the direction of the radar signal, and the direction of flight of the radar system this can be refuted for the Method of Van Natijne et al. (2018) but not for the ICP method, as the ICP method does not take these two factors into account. However, as also stated in Section 2.4.3, the 3D-NDT technique uses a success factor to establish whether the algorithm has been successfully carried out or not, whereas both the method from Van Natijne et al. (2018) and ICP do not. Adding a success factor to the method of Van Natijne et al. (2018) could improve the value of the results, as it adds valuable information to the data regarding the precision of the absolute position of the points.

Currently the last step 'linking the PS-InSAR points to the dihedral of trihedral geometries' has not been implemented in the research of Van Natijne et al. (2018). The results of the method (excluding the last step) will therefore be similar to Figure 29. The absence of this step might result in an ambiguous graphical representation, as not all PS-InSAR points can be linked to just one surface represented by LiDAR points but to two. Figure 20 *Linking to multiple surfaces* illustrates this by the error ellipsoid of PS-InSAR that intersects two surfaces.

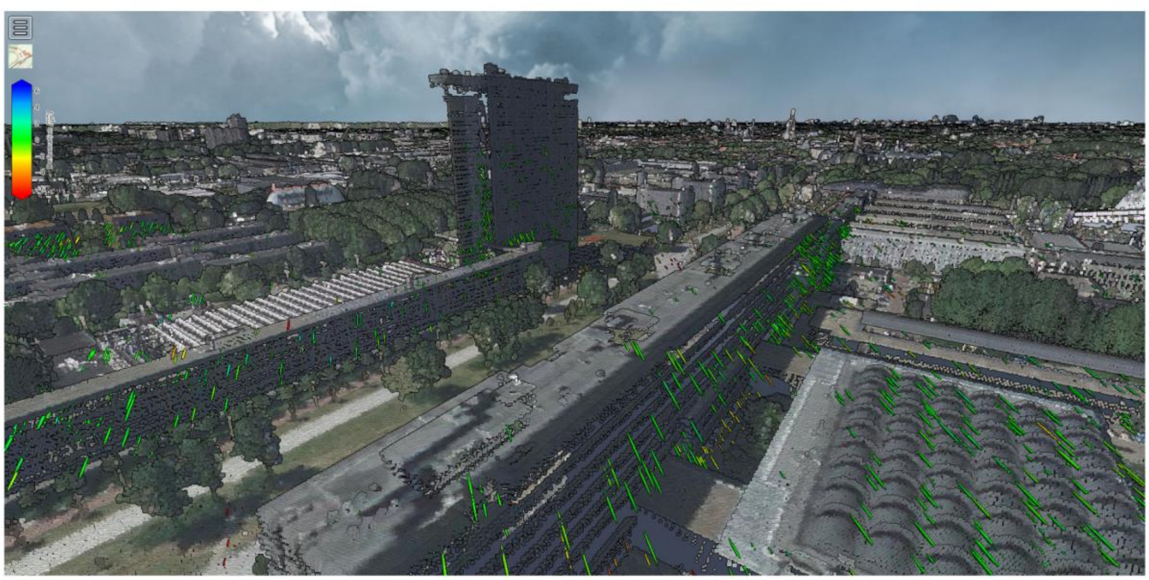

Figure 29 Results of method Van Natijne et al. (2018), where AHN3 is overlaid with the PS-InSAR trend estimates (shown as 1σ error ellipsoids around the expected position, colored by their deformation signal) (Van Natijne et al.,2018)

Figure 30 illustrates the change in the two-dimensional position of the PS-InSAR points as a result from the method of Van Natijne et al. (2018).

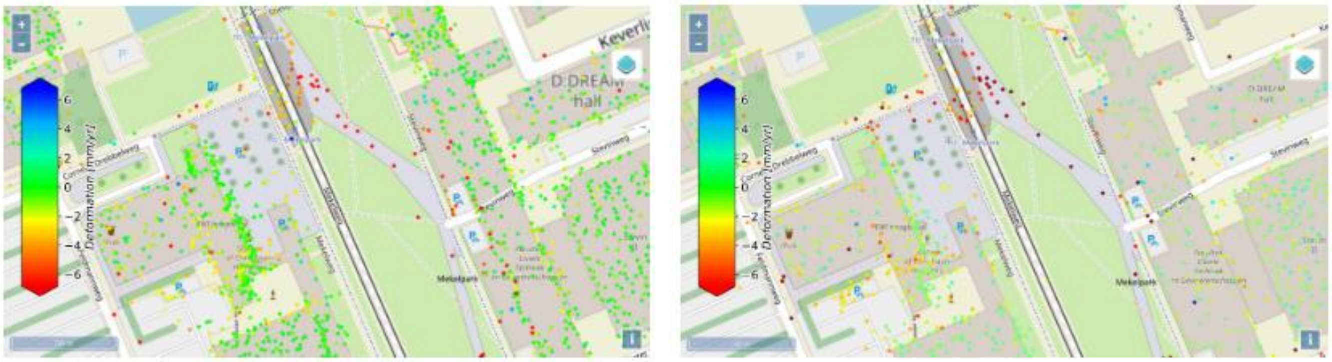

Figure 30 Improvement of the absolute 2D location of the PS-InSAR points due to the method of Van Natijne et al. (2018). Left: original situation. Right: after implementation (Van Natijne et al., 2018)

The method of Van Natijne et al. (2018) is however infeasible within the restraints of this research. Hence, the absolute position stored in the geometry (longitude, latitude and point height) of the PS-InSAR data will be used to visualize the PS-InSAR points. Using this alternative method allows the data to be visualized together with the LiDAR data in a three-dimensional way. To limit the effect of the imprecision of the absolute height (z) of the PS-InSAR points, the points will be visualized in both a two-dimensional and three-dimensional way. This alternative method will not include the improvement of the absolute positions resulting from the Method of Van Natijne et al. (2018) as shown in Figure 30 for the x and y, which means that it cannot be assumed that with this alternative method the PS-InSAR points are positioned at the correct real-world position.

The workflow for creating the visualization of PS-InSAR and LiDAR can be seen in Figure 31.

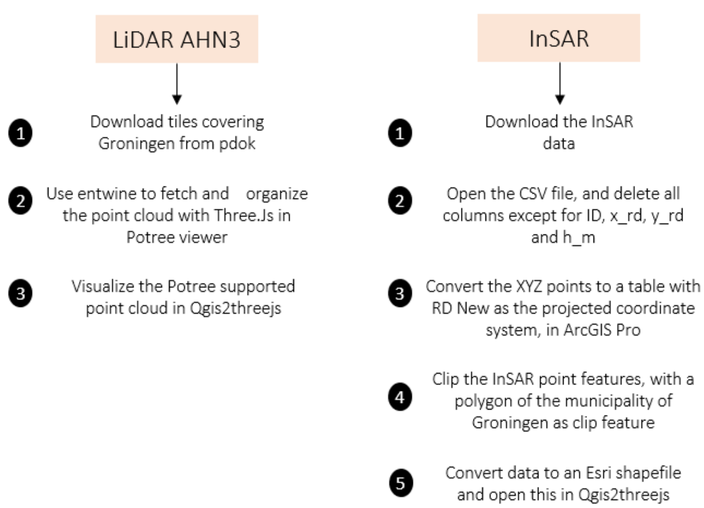

Figure 31 Workflow for visualizing AHN3 and PS-InSAR

It has been chosen to first visualize the two datasets in Qgis2threejs, as this allows a smooth navigation through the scene in which the data is represented. Similarly, in step 2 the majority of the columns of the PS-InSAR data has been removed to make it less computationally-intensive to navigate through the visualized data, and thus make it easier to compare the two datasets (in particular the location of the points) from different perspectives.

3.4.2 Selection of Design Principles for Representing Point Clouds

In Section 2.5.1 it has been explained that one of the recommendations to successfully design a transparent and readable visualization, location should be used for contextualization. It is therefore important that users of the conceptual interface will be able to derive the geometry of buildings from different perspectives, as this will allow users to recognize the spatial context of the data. A possible method to allow users to derive this geometry from different perspectives has been introduced by Poux (2020) in Section 2.3.2. Poux (2020) explains how point clouds can be transformed to three-dimensional models, which can either be a solid or a boundary representation. In the perspective of the to be realized conceptual interface, a solid representation would not add value as the volume of the buildings is irrelevant for the users to derive deformation data. Using a boundary representation might add value to the concept, as it would aid users in deriving and recognizing the shape of objects. However, when looking at the distribution of the LiDAR AHN3 points on objects (Figure 32), it becomes visible that in AHN3 the roofs are represented with a relatively large number of points, whereas the walls are represented with a relatively small number of points.

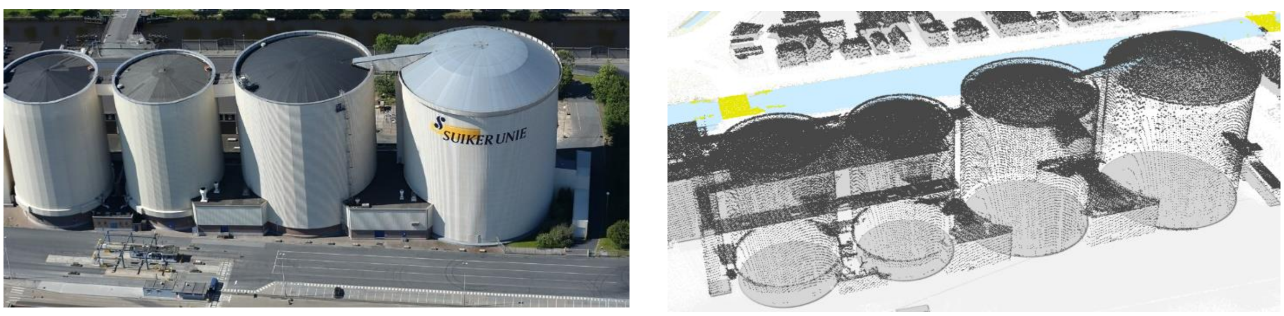

Figure 32 Left: image of Suiker Unie. Right: point cloud representation of Suiker Unie

The interpolation from the points representing the walls is therefore less likely to accurately represent the real-world shape of the walls. In the case of the example shown in Figure 32, the interpolation of the walls would consist of relatively large flat triangles approximating the real-world shape. Due to the planar triangles, the real-world shape of for example round objects cannot be exactly simulated (Figure 33).

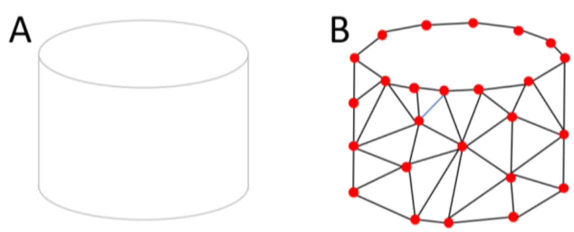

Figure 33 A: real-world object. B: Boundary representation of point cloud (simplification)

Next to the inability of a boundary representation to exactly simulate round objects, a second point of attention of using a boundary representation is that it is a form of expression of something that we expect to exist in the human environment. For example, in Figure 33 *(B)* the black lines connecting the LiDAR points are a prediction or expectation of the shape of the surface of the real-word object. From the perspective of the framework of the dimensions of dynamic geodesy and cartography (Van der Schans, 2001) (Figure 25), as explained in Section 2.5.4, one can say that the LiDAR points are landscape model objects of parts of the terrain-objects that exist in the human environment dimension. When one uses a boundary representation to represent the LiDAR points, an external source of objects is added to the 'forms of expression' dimension, namely: the predicted shape of the objects' surface (the black lines). This external source is added to the path of the cartographer (path A of Figure 25), and results in a boundary representation in the graphical representation dimension. The user (path B of Figure 25) derives information of the human environment from this graphical representation dimension. As described in Section 2.5.4 the actions, objects and processes from the human environment observed by the cartographer should be the same actions, objects and processes as derived by the user in the human environment dimension. There are two logical ways to deal with this:

1. The user should have in-depth knowledge of the method used for implementing the boundary representations, so they can filter the effect of the method
2. The cartographer does not implement the method for boundary representations

One can however advocate for a third way: the cartographer does implement the method of boundary representations, if usage of the map does not include derivation of information of specific parts of objects. This way, the external source of objects that is added to the 'forms of expression' dimension as previously explained, will not have an impact on the derived information. An example of this is a graphical representation in which users only derive information based on objects, such as: building A has been built in 1930, whereas building B has been built in 2011. The fact that the buildings are represented with a boundary representation, and therefore include a prediction of the surface of the buildings, does not have any effect on the derived information: the construction years are still the same. In the perspective of the to be created conceptual interface of this research, users should be able to link a certain displacement value to a certain part of an object. The difference here is that different parts of one building can have different derived displacement values. Whereas in the previous example, the whole building has an identical construction year. The third option can therefore be disregarded.

Similar to the third option, the first option can be disregarded as the users of the interface are defined as the public (Section 2.1.1), and are assumed to not have geospatial knowledge (Section 1.4), and hence no in-depth knowledge of the method used for implementing boundary representations. As option two is the only one remaining, the boundary representation method will not be implemented in the concept of this research. The result of this is that objects, such as buildings, will be represented with the use of points. The density of these points is not sufficient to make the objects look exactly like they do in reality, this can be due to for example a limited density of points representing a wall. The example has been illustrated in Figure 34, where the majority of points representing the walls is missing.

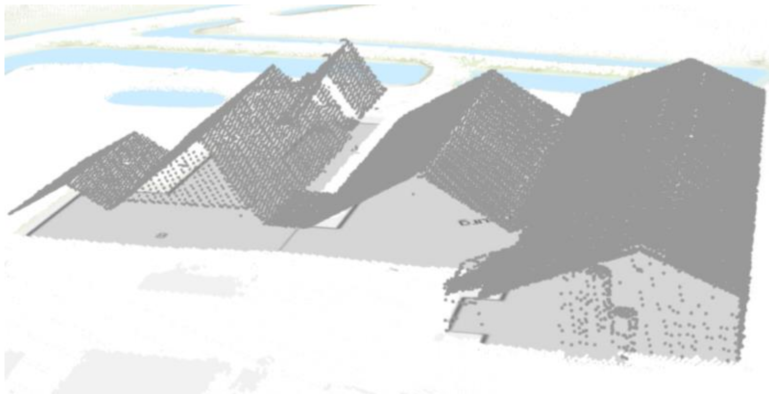

Figure 34 *The roof is represented with a relatively large number of points, whereas the walls are presented with a small number of points (LiDAR AHN3)*

Haeberling et al. (2008) underline that it does not have to be problematic to represent three-dimensional objects on a map different than how they look in reality by stating that: shapes and patterns of objects in three-dimensional maps must not look just as they do in reality (Section 2.5.2). Haeberling et al. (2008) also states that three-dimensional symbols for point map objects are well suited for image-like representations. Poux (2019) takes it to the next level and presents the SPCI (Section 2.3.3), which is a framework in which point clouds are represented in an intelligent environment that makes use of a semantic memory. The semantic memory allows users to extract or mine relevant information concerning a specific application domain (Poux, 2019). However, as indicated in Section 1.4, it is not within the scope of this research to take different purposes of use of the deformation data into consideration. Therefore, a specific application domain cannot be established. Without a specific application domain, it is not relevant to make use of a semantic segmentation. This is due to the fact that the desired semantic segmentations vary too much for each possible application domain. Four examples of application domains listed in Table 6 do already show that the desired semantic segmentations of only four applications varies significantly.

Application domain	Examples of desired semantics
Infrastructural management	Segmentation of the different types of roads
Organizations active in compensations for damage to buildings due to gas extraction	Segmentation of each individual wall of a building, categorized per floor
Coastal management	Segmentation of types of coastal reinforcement
Pipeline infrastructure management	Segmentation of soil type that is on top of the infrastructure

Table 6 *Examples of specific application domains of deformation data*

Although a semantic segmentation would add significant value to an interface that is being designed for one specific application domain, it is not feasible and realistic to use a semantic segmentation for a concept of which the specific application domain is not known but rather versatile. Therefore, the step from Heaberling et al. (2008): *image like representations of points*, to Poux (2019): *SPCI*, will not be implemented. Hence, only the image like representation of the point clouds will be used in the conceptual interface.

3.4.3 Selection of Graphical Visualizations and Design Principles for the Conceptual Interface

In sub-process A the user needs or key components of the users of the communication of land subsidence have been identified. In this perspective, the user needs refer to graphical visualizations or functionalities the users desire in the communication. To ensure user satisfaction, the key components will be integrated in the conceptual interface of this research. The conceptual interface will therefore provide users with: the functionality to use different administrative levels, the ability to configure layers, a selection tool, the functionality to draw boxes, the presence of visual graphs, the functionality to retrieve data in different formats, additional functionalities (for example pop-up legends, a locator map, printing and downloading facilities), the functionality to compare maps, metadata, a search function, and the ability to view dynamic time-series and the presence of a geoportal that can be accessed without any restrictions such as a language barrier.

In Section 2.5 various types of graphical visualizations for public, three-dimensional and spatio-temporal data have been discussed. The remaining part of this section will have the same structure, and will discuss the graphical visualizations that will be integrated in the conceptual interface of this research.

Public

The aim of the conceptual interface is to communicate deformation data to the public in a readable and transparent way. To realize this aim, the concept will fulfill two requirements that have been derived from the study of Schoffelen et al. (2015): attract users to engage with the visualization and encourage users to make sense of the dynamic back story of the data. Schoffelen et al. (2015) did however provide three aspects that allow to communicate data in a transparent and readable way. The aspect 'enabling users to reflect on interpretations' will not be integrated in the concept of this study, as this requires the provision of lesser-known perspectives of the data, which are in the perspective of land deformation the different causes of land deformation. However, as discussed in Section 1.4, this research will not discuss the causes of land subsidence. The next two paragraphs will discuss how the remaining two requirements will be integrated in the conceptual interface.

Attract users to engage with the visualization: It can be rather hard to define when a visualization can be labelled as attractive for users to stimulate engagement, as not all users have the same definition of attractive. In communicating deformation data to the public, it is assumed that users are attracted to engage with the visualization when: the interface is understandable, users understand the (spatial) context, and when users have the opportunity to participate in the concerned topic. These three assumptions are in line with the three recommendations proposed by Schoffelen et al. (2015), to successfully design a transparent and readable visualization: add a step-by-step guide for the visualization (u*nderstandable interface),* use location for contextualization, and contextualization with other resources (*understandable (spatial) context)* and provide an access point of participation *(the opportunity to participate in the concerned topic*). The three assumptions and their corresponding recommendations of Schoffelen et al. (2015) are translated into the following concrete features:

- *Understandable interface*: in Section 2.1.5 the interface of the BDK2.0 has been thoroughly analyzed. The recommended category of change 'add metadata' in Table 2 provides recommended changes for BDK2.0 to make its interface more understandable, and will be integrated in the conceptual interface:
    - An instruction of how to use the interface
    - An explanation of how to interpret the graphical visualizations (charts and tables)
    - An explanation of areas that have no cell value or measure points
    - Information of the used coordinate system and projection
    - Information of the update frequency of the data

  An explanation of the two different versions of Midden, Oost and West, and how to deal with the contradicting results will not be added, while this has been recommended in Section 2.1.5. This explanation does not add any value to the interface, as the research area Groningen is fully covered by the Oost layer. Hence, the Midden and West layer will not be present in the concept.

- *Understandable (spatial) context*: a spatial context in the conceptual interface will be provided by means of the point cloud LiDAR data, resulting in a three-dimensional digital world in which users can recognize buildings by their color, shape, orientation, and location. Next to that, as people move through the real world via infrastructural networks, it is assumed that users can make more sense of the spatial context when the streets are vividly visible, as these are recognizable features.

Participate in the concerned topic: in the interface there will be a link to a forum where people can share their thoughts.

Encourage users to make sense of the dynamic backstory: Schoffelen et al (2015) stated that there has to be made decisions regarding the design principles of a visualization: either focus on engaging users for a longer period by means of visual difficulties, or focus on aiding users in identifying and understanding different perspectives by reducing visual difficulties. The aim of the conceptual interface is not to engage users for a certain time, but its goal is to communicate a message to the user, a message that can be perceived differently from various perspectives, which is in line with the latter. Therefore, the visual difficulties present in the interface will be limited. By making the interface interactive, the users are able to explore the data from different perspectives (for example scale, location and time). Additionally, users will be given the option to view the deformation data in the perspective of events (which will be further explained in Section 3.4.3 *spatio-temporal*), allowing them to view only selected events such as the locations that have faced a displacement of more than 3 millimeters per year. This way, it is relatively easy for users to compare the data from different perspectives, creating a relatively non-complex visualization structure.

Three-dimensional

Before realizing any three-dimensional features in the interface, three aspects as discussed by Haeberling et al. (2008) will be considered: conceptual, technical and product aspects.

The conceptual aspect concerns knowledge of the personal environment of the user, such as its competences and skills, purpose of use of the application and the circumstances of location and time during the usage of the three-dimensional visualization. As explained in Section 2.1.1, the users of the prototype are the public. As the public cannot be defined by one set of skills and competences, and discrimination within the user group is not desired, it is assumed that the users do not have any skills and competences in geo-science, but do know how to use a computer. This way, discrimination is prevented, as there is not a certain level of knowledge required for using the three-dimensional visualization. Additionally, it is assumed that the users do know how to use a computer, as 91 percent of the Dutch population owned a computer in 2017 (CBS, 2018). It will however not be considered what the purpose of use is of the user, as defining different purposes of use are not within the scope of this research (Section 1.4). The interface will be accessible when one has access to internet, making it suitable for infield use. The time to render the visualization can however increase due to a relatively bad internet connection.

The technical aspect concerns the specific computer applications and the digital input data. The interface will use open data: Base map Topo RD (ESRI, 2012), elevation 3D (RD) (Esri, 2018), AHN3 (PDOK, 2020), PS-InSAR (Bodemdalingskaart, 2020), subsurface properties data (PDOK, 2020), administrative units (PDOK, 2021) and aerial images (PDOK, 2020). To process and analyze the data, a computer with 500 gigabytes of free space, with a Solid-State Disk (SSD) of 500 gigabytes will be used. This allows to store large datasets and various types of software (ArcGIS Pro and FME) necessary for processing the data.

The product aspects concern decisive points regarding whether a user is willing to use the map or not: the availability (for example costs), usability and handling, thematic content and the design and visual appearance of the three-dimensional map. The interface will be available for free, and will be host online, allowing users to view the data without having to download anything.

As explained in the previous section regarding public data, the interface will be made understandable by the integration of five concrete features. When the users understand the interface, the interface becomes relatively easy to use and handle. The thematic content is land deformation, which is a relevant topic in the Netherlands, the level of relevance is however not homogeneous distributed across the Netherlands: some regions have relatively high displacement rates. In a region with high displacement rates citizens have to deal more with the adverse effects of land subsidence, making them more likely to be interested in the thematic topic of land deformation. The visual appearance is considered to be attractive to engage users in the visualization as it will offer an understandable interface and an understandable (spatial) context, and it will allow users to participate in the concerned topic.

To design a three-dimensional map that users are willing to use, certain design principles have to be taken into account during the steps of modelling, symbolizing and visualizing the data (Figure 21), as proposed by Terribilini (2001) in Haeberlingen et al. (2008). During these three steps, the conceptual, technical and product aspects will constantly be considered. For example: is this understandable without any geo-spatial knowledge (conceptual), is this realistic with the available data (technical) or is this an easy-to-use feature (product). In each of the individual steps of the workflow several design principles derived from the study of Haeberling et al. (2008) will be taken into account, however when one of the principles will not be taken into account an explanation on why it is unsuitable is provided:

- Modelling: The shape, patterns and appearance of the objects will not look exactly as they do in reality. To increase the perspective perception of the interface, only three-dimensional map symbols with simple geometric shapes will be used. The buildings will have a good color contrasts to the terrain.
- Symbolization: The terrain of the map will not be exaggerated to emphasize it, as this might have an effect on the interpretation of land subsidence data. The symbols will however not be made slightly transparent, as the relatively small density of points already prevent obscurance.
- Visualization: The sky of the interface will have a neutral color, and the lightning direction will be lateral.

Spatio-temporal

In Section 2.5.3 it has been discussed how one can represent spatio-temporal data. Central in that section is the research of Andrienko et al. (2020), and three assumptions regarding desires of users of spatio-temporal visualizations: users want to be able to see the distribution of spatial events in space and time, compare time-series of different locations, and see variation of all attributes in time and space. One of the requirements of the conceptual interface of this study is that the end-user must be able to answer questions related to these three assumptions. The three requirements will therefore be integrated in the interface to mitigate users in answering these questions and to prevent misinterpretations. However, as explained in Section 2.5.4, whether the users derive the right answers from the graphical representation has to be tested, as one can simply not assume that when using a certain set of design principles all users are able to derive the right answers.

To allow users to compare time-series of different locations, the interface will make use of line graphs that represent time-series of different locations, superposed in one display, with on the X-axis time, and on the Y-axis the displacement. Andrienko et al. (2020) does propose a second method that makes use of separate displays that can be placed side by side. This is however considered to be inconvenient, as the size of a computer display is only limited and placing several displays side by side can be rather chaotic.

The space-time cube as discussed by Andrienko et al. (2020) will be integrated in the interface to enable users to see the distribution of spatial events in space and time. The horizontal plane in the cube will represent the study area of Groningen and the dots will represent a defined event (for example a displacement rate of four or more millimeters per year). The dots will be placed according to their associated location and time. This way, users can easily gain insights in the spatial and temporal distribution of a certain event.

Spatial and temporal clustering has been defined by Adrienko (2020) as a convenient method to aid users in exploring temporal and spatial variation of all attributes of the concerned data. The spatial clustering is represented by a data driven tessellation, and the temporal clustering by graphs. The map and the graphs become integrated with the use of unique colors associated to the same pattern.

The results of Sub-process C can be found in Section 4.3. The next section will explain how the combined visualization of deformation data LiDAR point clouds, and the identified design principles and graphical visualizations can be merged into one interface.

3.5 Implementing the Conceptual Interface (Sub-process D - prototype)

In Section 3.4 the design principles and graphical visualizations to be implemented in the conceptual interface have been discussed. This section will build on Section 3.4 by explaining the implementation process of the design principles and graphical visualizations. This section will start with an explanation of how the PS-InSAR data is prepared before it can be visualized. Subsequently, the process of visualizing both the PS-InSAR data and the LiDAR point clouds is explained. The section ends with an explanation of the construction of the conceptual interface.

3.5.1 Preparation of the PS-InSAR data

The PS-InSAR data is structured by rows that each represent a unique measurement point, the columns represent the properties of the measurement points. The properties that are relevant for this study are: the unique identification (pnt_id), the latitude (pnt_lat), the longitude (pnt_lon), the height (pnt_height), geoidal separation (pnt_geoid), the linear displacement value in meters per year (pnt_linear) and all the displacement measurements ordered by collection date (d_20150119 up to and including d_20191031).

To reduce the processing time of preparing the PS-InSAR data, a geographic subset representing the study area will first be selected before making any adjustments to the data. Based on the latitude and longitude of each point, a two-dimensional point feature class is derived from the PS-InSAR data.

The coordinate system of the feature class is set to ETRS89, as the geometry of the points is stored in the European Terrestrial Reference System 1989. ETRS98 is the standard coordinate system for Europe, with relatively small station velocities (Marel, 2014). To define how the data should be projected on the local scale of Groningen, the latitude and longitude of the data is transformed to the projected coordinate system Rijkdriehoekscoördinaten (RD_new). This is done with the Amersfoort_To_ETRS_1989 (WKID=1751) geographic transformation. This transformation has an accuracy of 0.6 meters (ESRI, 2019).

The official reference system for heights in the Netherlands is NAP (Normaal Amserdams Peil). The aim is therefore to set NAP as the vertical coordinate system of the PS-InSAR points. The NAP height of the points is calculated by subtracting the geoidal separation (pnt_geoid) from the point height (pnt_height). This way the orthometric height of the concerned point remains, the orthometric heights are visualized at an absolute height. This is visualized in Figure 35.

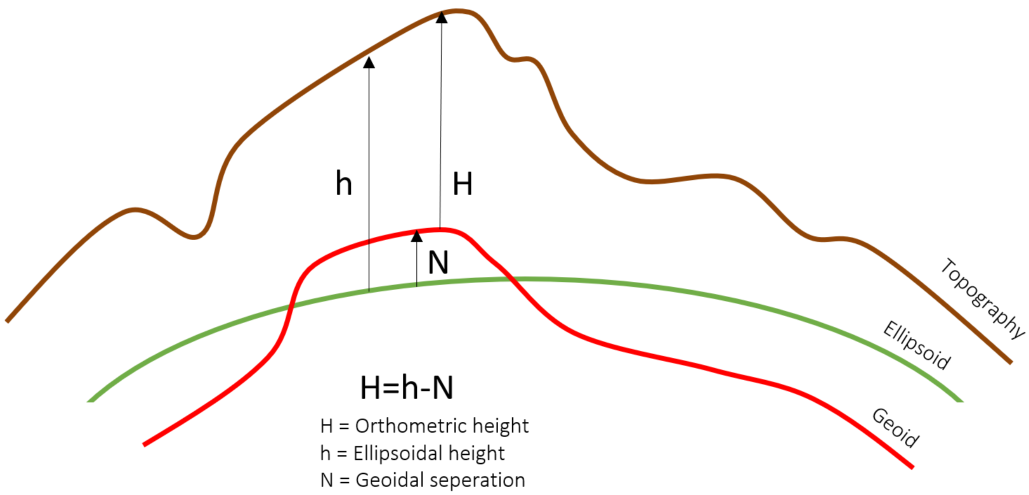

Figure 35 Orthometric, ellipsoidal and geoidal height

The PS-InSAR points are now stored in a point feature class, and a new feature class that only represents the point features in the study area (Groningen) is created. A polygon, with the same projected coordinate system RD_new, that represents the shape of the municipality of Groningen is used as a clip feature. The output contains only the PS-InSAR feature points that fall within the clip feature.

Currently, the PS-InSAR dataset only stores the average linear displacement values in meters per year for each point. In Section 3.4.3 it is stated that to ensure user satisfaction, the users will be provided with the ability to view dynamic time-series of the data. The average linear displacement value in meters per year does represent the time-series of each point, it does however not provide any insight into the dynamic behavior of the time-series of each point. The linear displacement values will therefore also be calculated in meters per individual year (2015, 2016, 2017, 2018 and 2019). These displacement values can be determined by calculating for each point the slope of the trendline from the scatterplot where the displacement values (y) are plotted against time (x), where time is defined for only one year. However, currently the columns' names that represent the time are stored as strings, with unequal intervals (6, 12 or 24 days), while only numeric fields can be used as an input for a scatterplot. Therefore, the date fields are converted to serial numbers. A sample of this conversion can be found in Figure 36.

Date field
d_20150119
d_20150224
d_20150320
d_20150401
d_20150413
d_20150425

Serial number
42023
42047
42059
42083
42095
42107

***Figure 36** Conversion of date field to serial number*

For each measure point (each row) five scatterplots are created, one for each year (Figure 37). The value (represented in red) of the slope of the trendline of each of these scatterplots is then multiplied by 365 and 1000. First by 365, as the current slope represents the increase or decrease in meter per serial number, and one serial number represent one day. The multiplication by 1000 is done because the displacement values are stored in the order of meters. Whereas the order of millimeters is desired. To allow for comparison, the pnt_linear field is also multiplied by 1000.

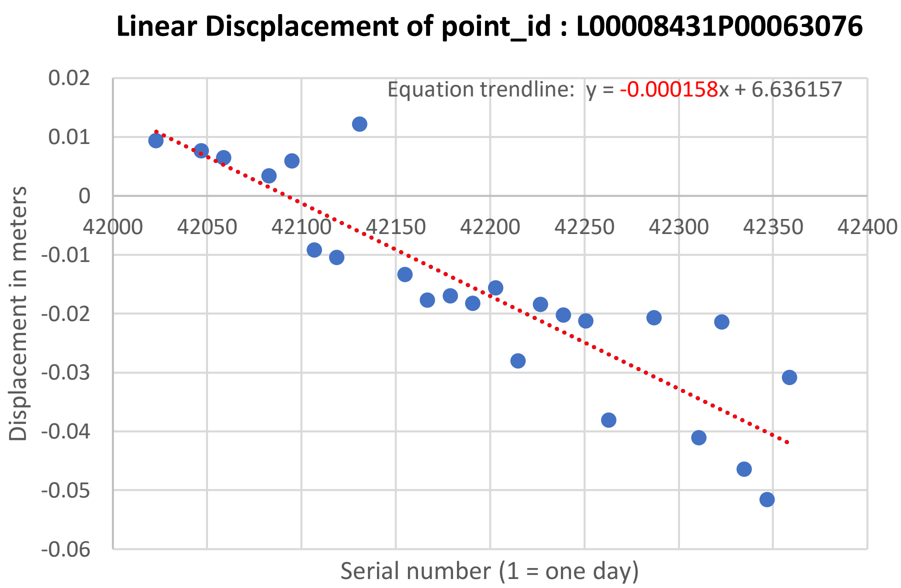

Figure 37 Scatterplot of point L00008431P00063076, with trendline and slope value (meters per year) in red

The PS-InSAR data is now ready to be visualized, which will be explained in the next section.

3.5.2 Visualizing the Data

The data input for the conceptual interface consists of five feature layers derived from the PS-InSAR data, and one LAS (laser) layer derived from the LiDAR data. This section will discuss the visualization method used of each layer. Layer 1, 3, 4.1, 4.2 and 5 have been visualized for a sample area within Groningen.

Layer 1: PS-InSAR in three dimensions

The attributes of the clipped feature layer (Section 3.5.1), covering the municipality of Groningen, and the newly calculated displacement trends will be used to create a three-dimensional layer of the PS-InSAR points. The aim of this layer is to provide users with information regarding the measure points and their associated average displacement value in meter per year. Therefore, the field containing these values will serve as an input for the symbology of this layer. The average displacement values can be classified as quantitative, as it is a numerical expression, and as relative ratio, as it has an absolute zero (no displacement) and because the values represent trends. According to Bertin's theory on visual variables (Feringa, 2019) the proper visual variable that should be used to represent relative ratio data is value, represented by graduated colors (Appendix A). Using graduated colors comes with the important decisions regarding classification that have to be made: which method to use, how many classes to use, and how to define the class boundaries in the legend (Knippers, 2019). A graphic array of the data can aid in deciding on the proper classification method. In Figure 38 the possible graphic arrays and their corresponding classification methods are illustrated.

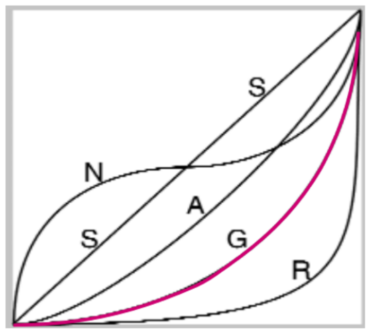

S (straight line): equal/defined interval or quantiles
N (Normal) : standard deviation
A,G & R : progressive increase: arithmetic (A), geometric (G) and reciprocal classification method (R)
Alternative : natural breaks

Figure 38 Graphic arrays of data, and their corresponding classification methods (Based on Knippers, 2019)

At first sight, when analyzing the graphic array of the average displacement values in millimeters per year (Figure 39A), one might decide to use the natural breaks classification method as the graph does not match one of the theoretical curves in Figure 38. However, when looking at the histogram (Figure 40), which displays the distribution of the data across the average displacement values, it becomes visible that there are six clusters: three left and three right from the mean. The values that are excluded from these clusters, and thus from the normal distribution, can typically be considered as outliers. When excluding these outliers from the graphic array, the new graphic array (Figure 39b) does match the theoretical curve of the standard deviation classification method.

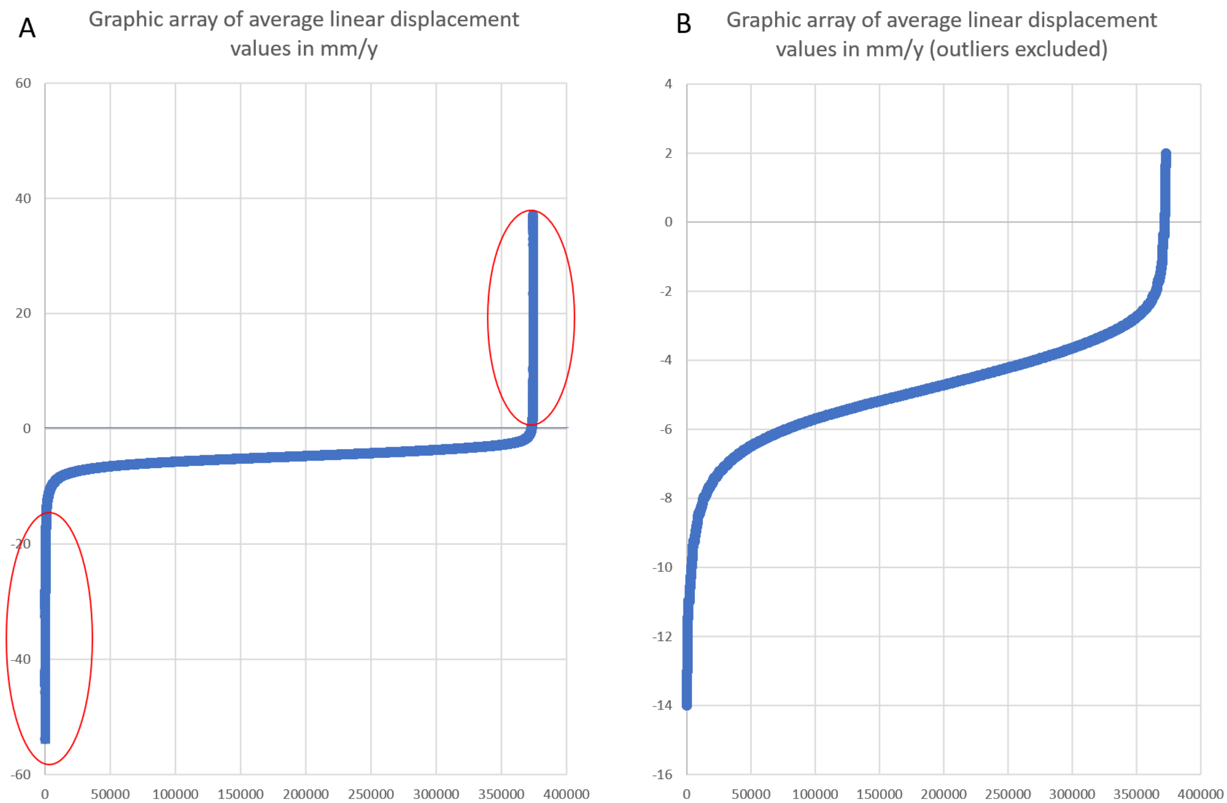

Figure 39 A. Graphical array of linear displacement values in mm/y B, with outliers in red. Graphical array of linear displacement values in mm/y excluding outliers

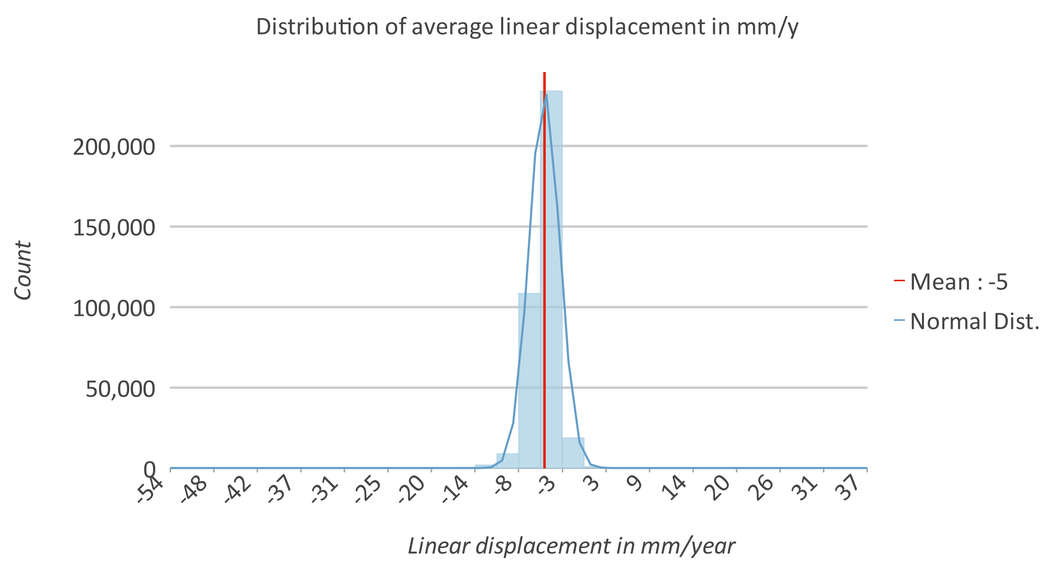

Figure 40 Distribution of the average displacement values

The normally distributed shape of the histogram underlines the suitability of the standard deviation classification method. In the standard deviation method, the class widths are defined using standard deviations from the mean of the graphic array, which is -5. It has previously been explained that the values outside the normal distribution can typically be considered as outliers, they can be derived from the histogram and are the values less than -14 or more than 3. Feringa (2019) suggests to use open classes for outliers. When implementing this suggestion of Feringa (2019) the upper value of the lowest class should be -14, and the lower value of the highest class should be 3. This way you create two open classes: a class containing all values lower than or equal to -14, and a class containing all values higher than or equal to 3. Feringa (2019) states that it is common to use 5-9 number of classes. With an increase in the number of classes, the ability for users of the map to recognize spatial differences also increases. It is however not desired to focus solely on recognizing spatial differences, as the layer is also designed to allow users to recognize spatial patterns. To balance these two desires, the number of classes that is used to visualize the displacement data is 8. The resulting classes of using 8 classes, with the two previously described open classes and the standard deviation classification method on the displacement data are shown in Figure 41.

Color	Upper value	Label
	≤ 38.0	More than 3
	≤ 3.0	0 up to and including 3
	≤ 0.0	-2 up to and including 0
	≤ -2.0	-4 up to and including -2
	≤ -4.0	-6 up to and including -4
	≤ -6.0	-8 up to and including -6
	≤ -8.0	-14 up to and including -8
	≤ -14	Less than, or equal to -14

Figure 41 Classes and their associated colors of the PS-InSAR data, based on the standard deviation method

The colors associated to the classified PS-InSAR data have also been illustrated In Figure 41. The colors are based on a purple to orange color ramp. Lavery (2019) classifies this color ramp as an above and below color ramp, which can be particularly useful in providing an anchor point. In the perspective of the PS-InSAR data, a displacement value of zero represents the anchor point. Classes above the anchor point are represented in a different color than classes below the anchor point. This way, it becomes more convenient for the users of the map to see the difference between locations where the ground subsides, and where the ground rises. Lavery (2019) suggests to deemphasize values close to the anchoring point. The two classes adjacent to zero have therefore both been given a neutral color, similar to the light grey color that will be used for the base map. The colors purple and orange have been chosen as these colors are rather neutral, and cannot be translated into 'bad' or 'good', which is for example the case for green (good) and red (bad). This is deliberately done, as both the rise and subsidence of the ground can have devastating adverse effects, and as explained in Section 1.4 the aim of this conceptual interface is not to point out the effects of the land subsidence, but only to communicate the displacement values. Spheres are used to represent the measure points, and they are projected in the color that is associated to the class the displacement value of the point falls in. A sphere is a simple geometric shape which is typically being used to represent three-dimensional data (Haeberling et al., (2008). The size of the symbols has been set to real-world units: three meters. A size of three meters has been chosen to prevent overlap of symbols. The final visualization of layer 1 can be found in Figure 42.

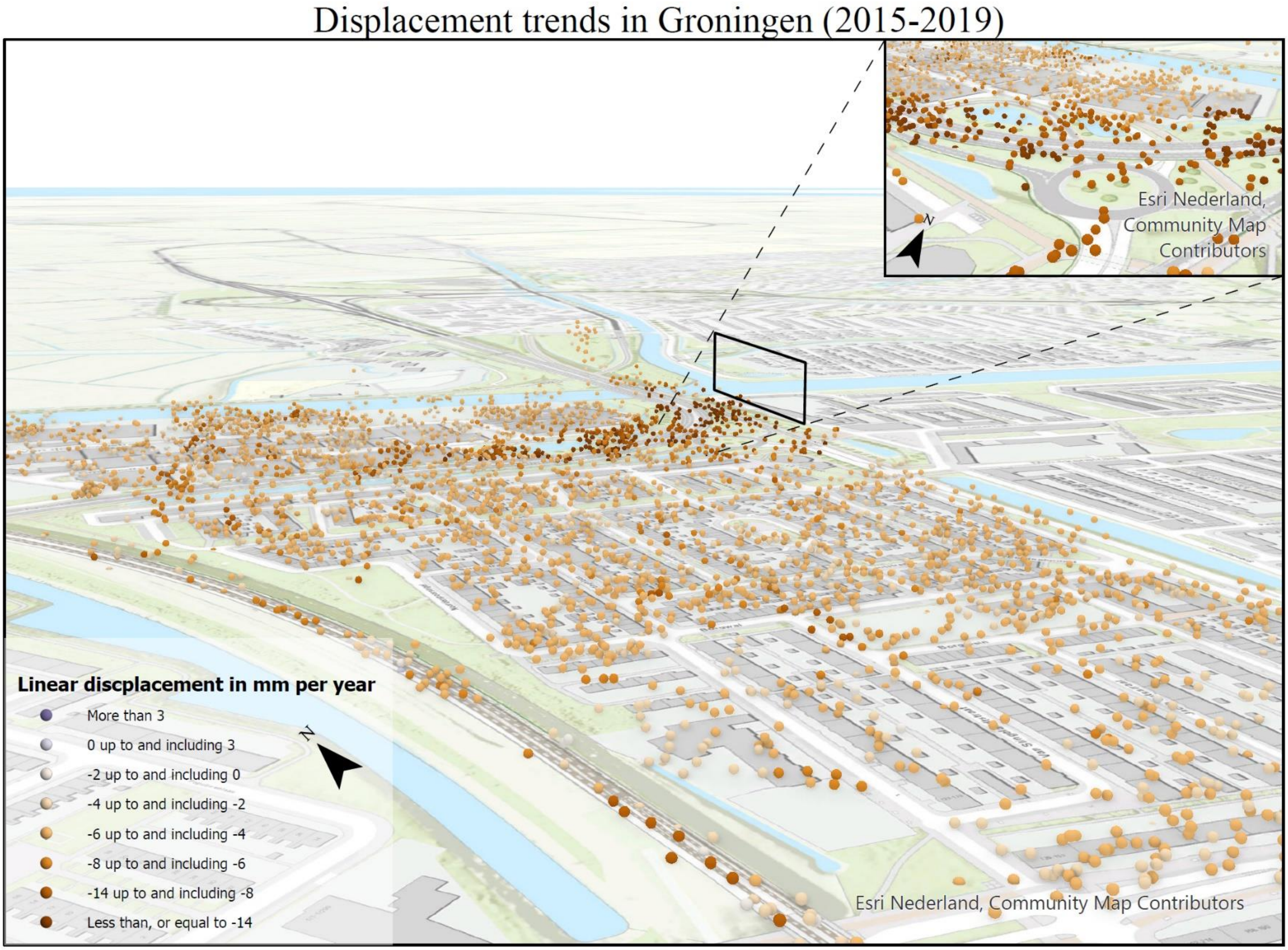

Figure 42 PS-InSAR visualized in three dimensions (layer 1)

Layer 2: PS-InSAR in two dimensions

In Section 3.4.1, it has been explained that to limit the effect of the imprecision of the absolute height (z) of the PS-InSAR points, the points will both be visualized in a three-dimensional and two-dimensional way. The second layer will therefore exist of the PS-InSAR points in two dimensions. The same input used for layer 1 is used to create layer 2, only now the height properties of the points are neglected resulting in a point feature layer derived from the longitude and latitude from the PS-InSAR points. The exact same transformation, classification and visualization methods as used for creating layer 1 are used to create layer 2. However, as layer 2 is two-dimensional, two-dimensional points instead of spheres will be used to represent the measure points. The final visualization of layer 2 can be found in Figure 43.

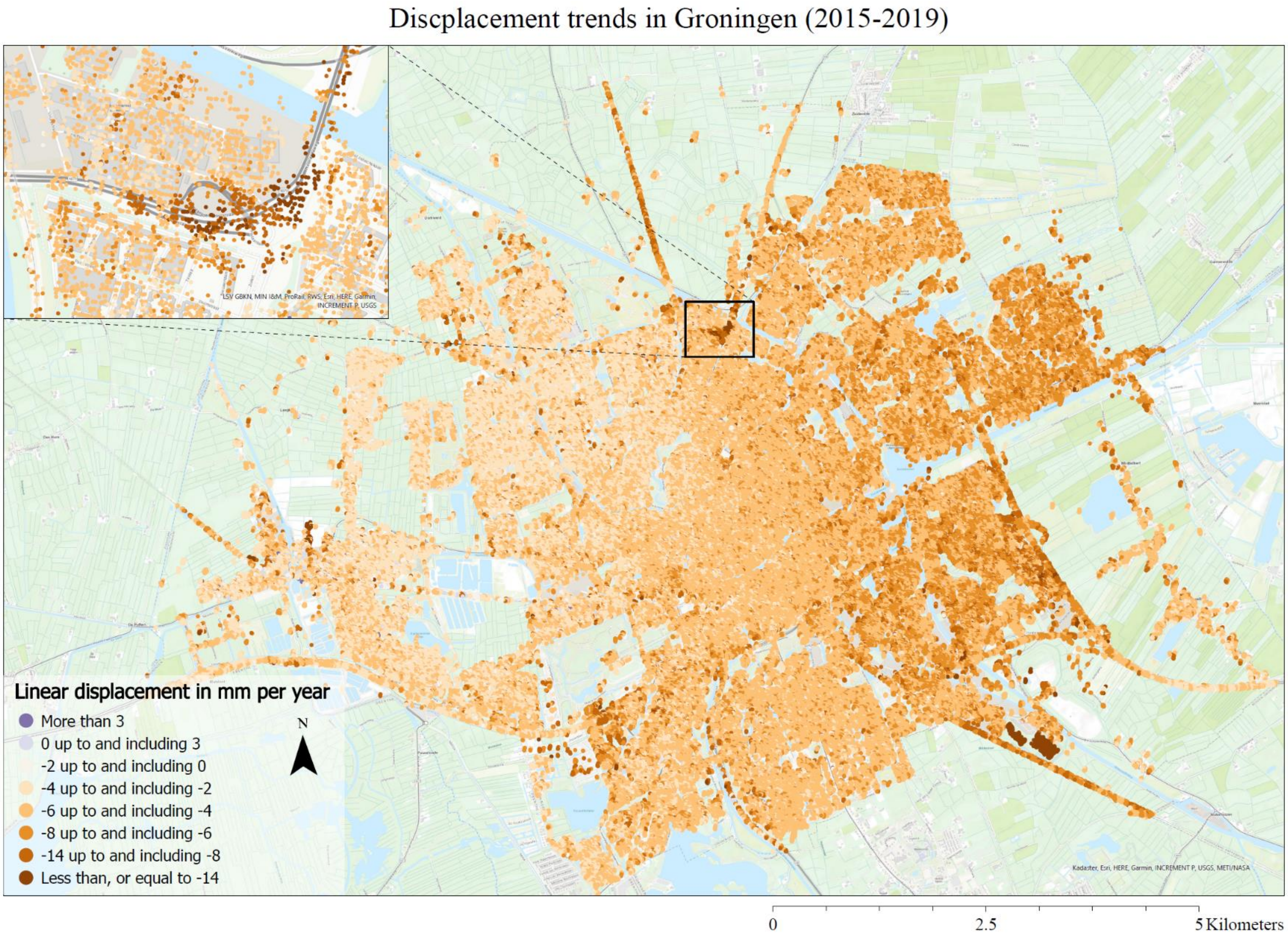

Figure 43 PS-InSAR visualized in two dimensions (layer 2)

Layer 3: Spatial and temporal clustering of the PS-InSAR data

To allow users to see variation of all attributes in time and in space, Andrienko et al. (2020) suggests the method of spatial and temporal clustering (Section 2.5.3). The purpose of the third layer is to allow users to see the variation of displacement in time and space. For the spatial clustering a data driven tessellation is used rather than a regular grid, as a regular grid results in distortion of the spatial distribution patterns (Andrienko et al., 2020). The spatial driven tessellations are derived from two methods: Thiessen polygons and aggregated points. Thiessen polygons divide the area covered by the PS-InSAR points into proximal zones. Each zone represents an area where any location within the zone is closer to its associated PS-InSAR point than to any other PS-InSAR point (Esri, 2020). The process has been illustrated in Figure 44.

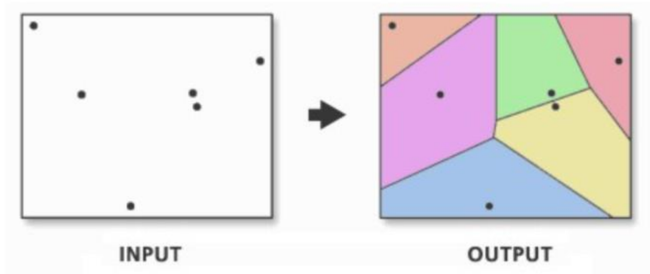

Figure 44 Input and output of Thiessen polygons

A characterizing feature of PS-InSAR data is that the measure points are not homogeneously distributed across the study area, resulting in rather large Thiessen polygons associated to just one measure point at locations where points are sparse. Similar to the discussion in Section 3.4.2, regarding whether to use a boundary representation for point clouds or not, it is not desired to give a certain attribute (external source) to a location of which the value of the attribute in the human environment is not known, as this can lead to misinterpretations by the user of the map. To exclude areas that are not located within a twenty-meter radius of a PS-InSAR point, the method of aggregating points is used. This method creates polygon features around clusters of proximate PS-InSAR point features. An aggregation distance of twenty meters is used, which implies that clusters are created with points that are within a twenty-meter radius from each other. The output polygon features are used to clip the Thiessen polygons, resulting in polygons that are associated to just one measure point, and the exclusion of areas that do not contain any measurement points. The process from Thiessen polygons and aggregated points to clipped Thiessen polygons is illustrated in Figure 45.

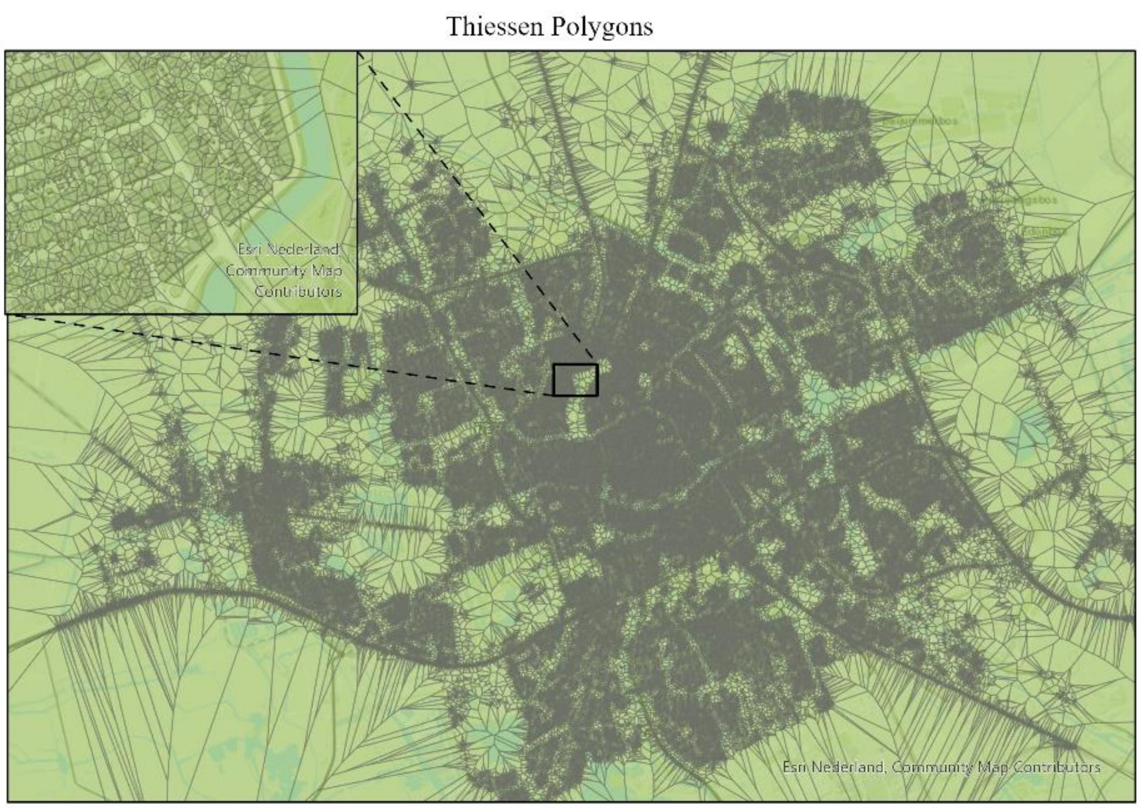

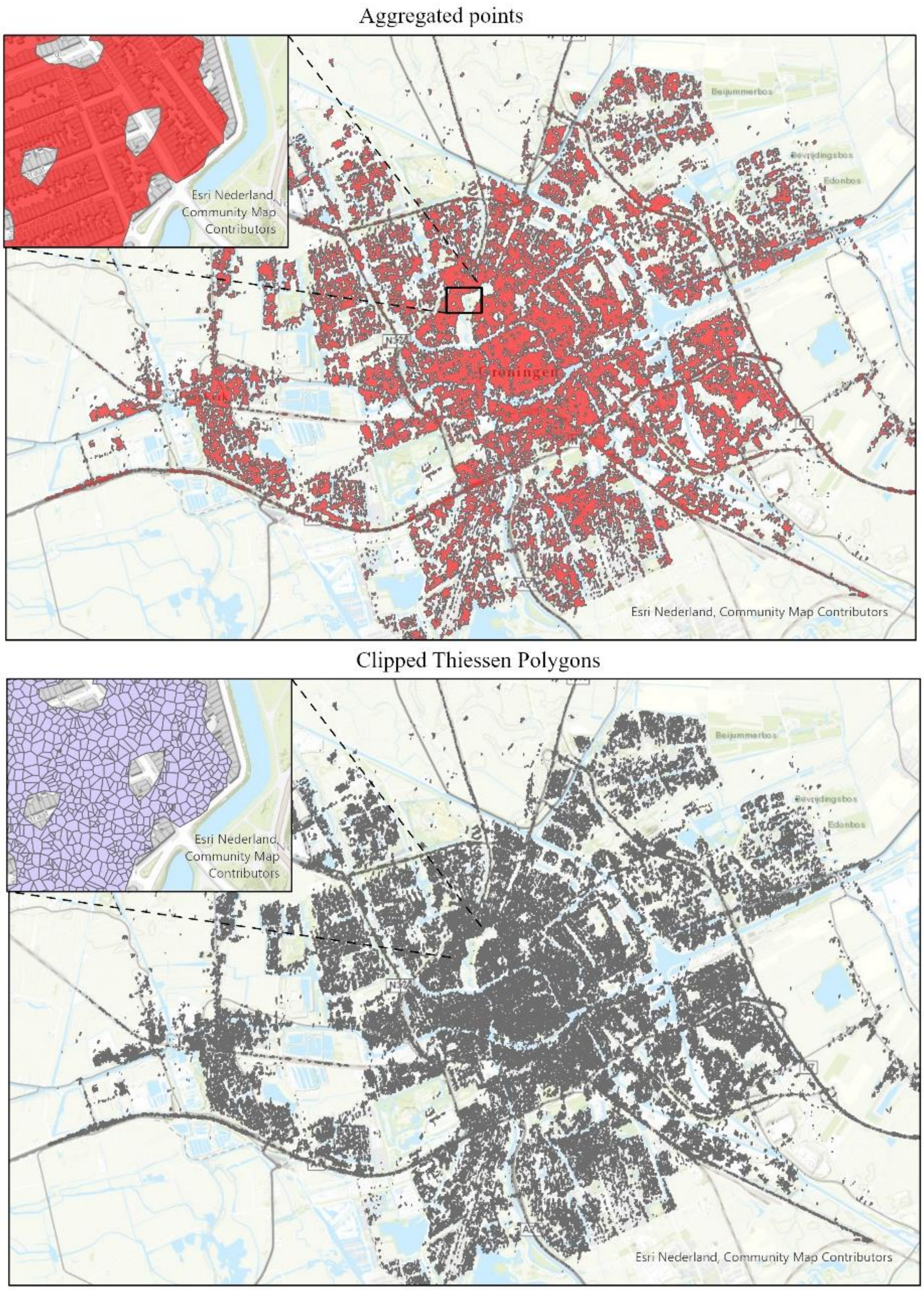

Figure 45 From Thiessen polygons and aggregated points to clipped Thiessen polygons

Each zone or tile is given a color based on the associated points' class in which the linear displacement value of the measure point falls (Figure 41). To create a merging effect of matching classes, no outline color for the Thiessen polygons is used. This way, the map effect similar to Figure 24 is being simulated.

For the temporal clustering, the average linear regression formulas associated to the previously defined classes (Figure 41) are used. The average linear regression formula of a class is the average of the linear regression formulas of the measure points that fall within the concerned class. The average linear regression formulas are shown in a graph below the map project in the same colors as the classes on the map, allowing users to see the variation of displacement values in both space and time. The final visualization of layer 3 can be found in Figure 46.

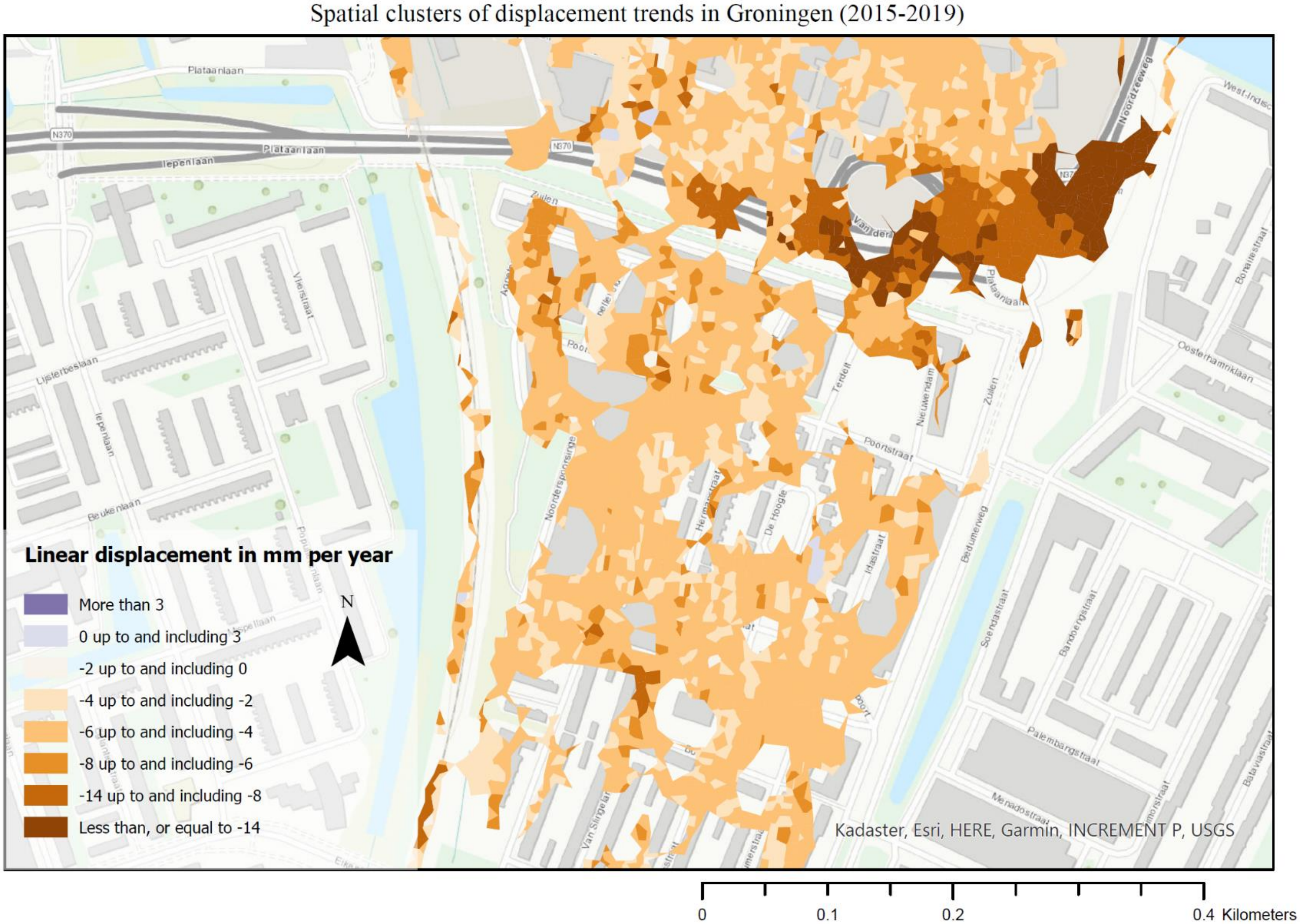

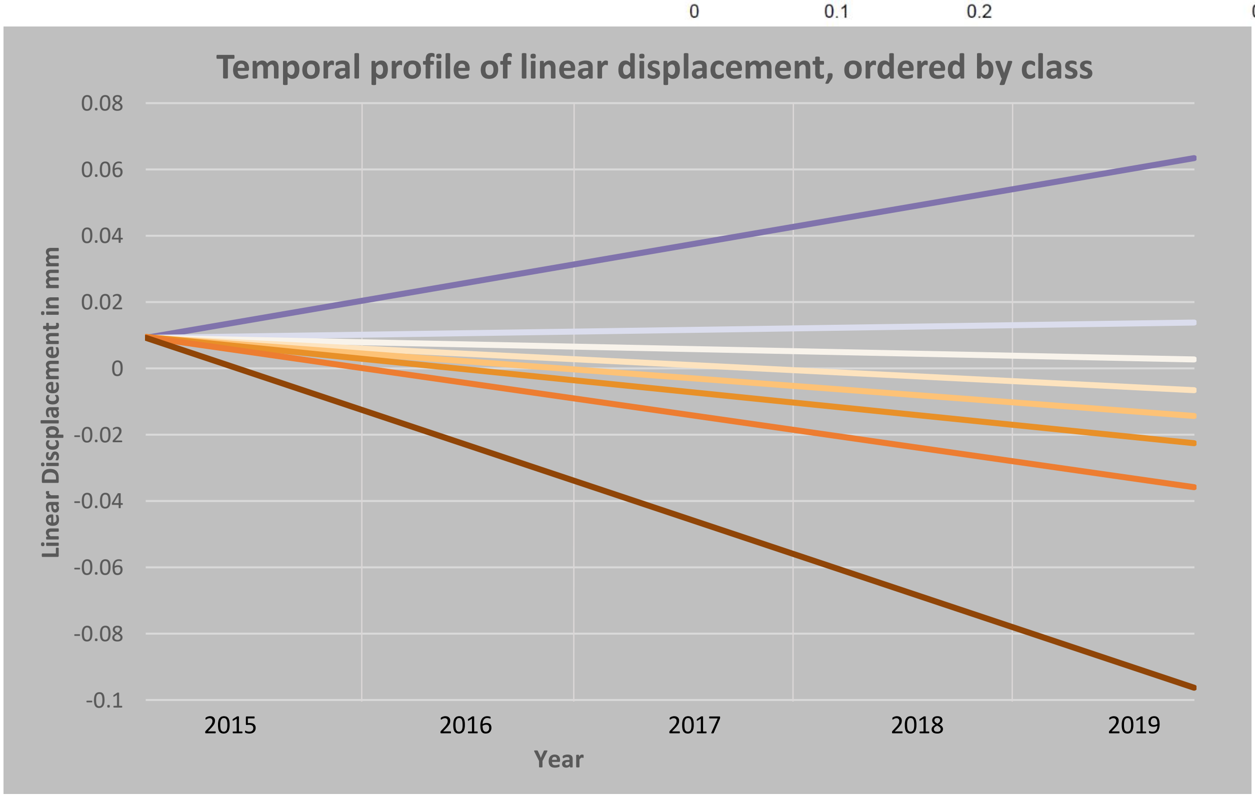

Figure 46 Spatial and temporal clustering of the PS-InSAR data (layer 3)

Layer 4.1 and 4.2: Time-series of the PS-InSAR data

Layer 4.1: Dynamic time-series of the PS-InSAR data
The aim of layer 4.1 is to allow users to see the distribution of spatial events in space and time (Section 2.5.3) and to see dynamic time-series. The linear displacement values that have been calculated for the individual years 2015, 2016, 2017, 2018 and 2019 are used to visualize layer 4.1. Similar to the method as suggested by Andrienko et al. (2020) to visualize the distribution of spatial events in space and time in Section 2.5.3, a space-time cube (Figure 23) will be used for this layer. In this space time cube, the study area is represented by the horizontal axis, and the years by the vertical axis. A certain class of displacement is considered as an event. The difference with the method of Andrienko et al. (2020) is however that the space time cube of layer 4.1 has an additional purpose: to view the dynamic behavior of the time-series. This implies that the space time cube must have the ability to view all events of each year and location at the same time. This is done by placing three-dimensional cylinders on top of each other. Each cylinder represents a year, the cylinder on the ground represents 2015, and the highest cylinder represents 2019. By projecting a color that is associated to the event of the cylinder, a space time cube representing dynamic time-series of the PS-InSAR data is created. Similar to the spheres used for Layer 1, the cylinders used for layer 4.1 are simple geometric shapes, and are therefore in line with the research of Haeberling et al. (2008). To make the space-time cube comparable with layer 1, 2 and 3 the same classifications and colors have been used to represent the displacement trends. The size of the symbols has been set to real-world units: one meter. A size of one meter has been chosen to minimize overlap of symbols. The height of the cylinders is set to relative to the ground, which means that when ground elevation is turned on, the cylinders will be located on top of this elevation. The final visualization of layer 4.1 can be found in Figure 47.

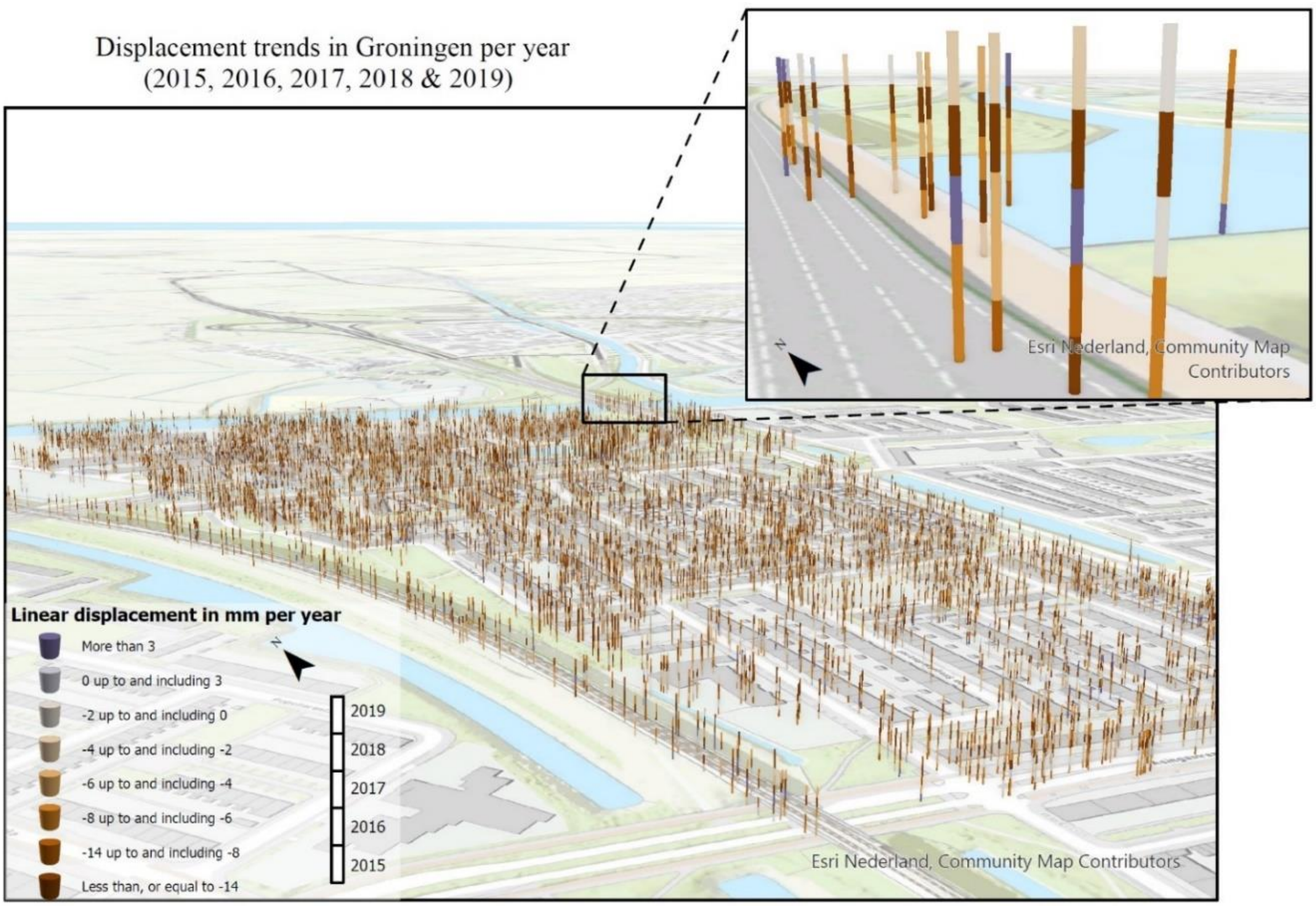

Figure 47 Space-time cube of the PS-InSAR data (layer 4)

Layer 4.2: Spatial patterns within time-series of PS-InSAR data

The aim of layer 4.2 is to allow users to explore spatial patterns within the time-series of the displacement values. This layer uses the same clipped Thiessen polygons as used for layer 3. Similar to layer 3, the zones are given a color based on their associated points' class in which the linear displacement of the measurement falls. The difference is however that layer 3 was created with the average values for the period 2015 to 2019, whereas layer 4.2 exists of five sub-layers, each representing an individual year 2015, 2016, 2017, 2018 or 2019. The final visualization of layer 4.2 can be found in Figure 48.

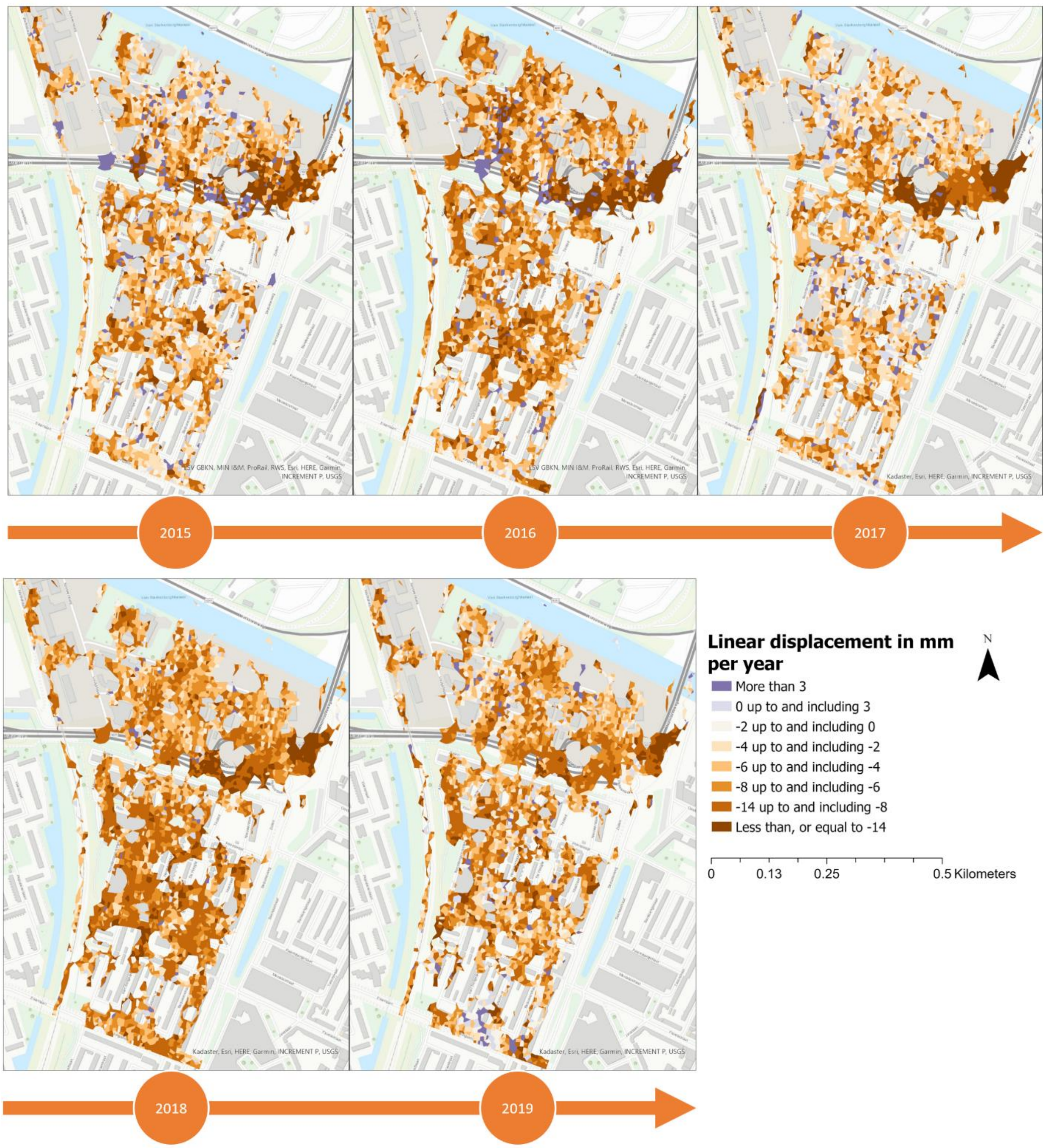

Figure 48 Spatial patterns within time series of PS-InSAR data

Layer 5: Clipped and colorized LiDAR point clouds

The fifth layer concerns the AHN3 point cloud layer. As explained in Section 3.4.2, the point clouds will be presented according to the suggestion of Haeberling et al. (2008), in an image like way. The aerial image with the RGB color codes of the Netherlands of 2019 (PDOK, 2020) is used as an input for the image like representation of the point clouds. To ensure consistency between the aerial image and the AHN3 point cloud the aerial image of 2019 is used. It is assumed that the aerial image of 2019 will provide the highest consistency, as the LiDAR data of the municipality of Groningen has also been collected in the year 2019 (PDOK, 2020). Each point of the point cloud will receive the RGB value of the raster image pixel that has the same location. The building and ground points of the point cloud are clipped to the extent of Groningen. Points representing water and vegetation have been excluded as both water and trees are typically not consistent over time, but rather season dependent. To measure displacement of a measure point, the point should be located at a stable or coherent location (Section 2.2.1). Due to the previously described inconsistency of water and vegetation, they are not suitable for measuring displacement with PS-InSAR. Therefore, no measure points will be located at either vegetation or water. Additionally, excluding trees from the point cloud will limit the obscurity of building and ground points and their associated PS-InSAR points, making it more convenient for users to link the measure points to their associated ground or building points.

Haeberling et al. (2008) stated that the lightning direction of a three-dimensional view must be mainly lateral or slightly from ahead (Section 2.5.2). The illumination altitude has therefore been set to 45 degrees, with an azimuth of 90 degrees. This implies that the sun or light source is located in the east, with an angle of 45 degrees above the horizon. The contrast is set to 30, where 0 means highest amount of shading applied to the surface, and 100 the lowest amount. In addition, Heaberling et al. (2008) explains that structural patterns of three-dimensional map objects must not be designed too dense or too fine. However, as illustrated in Figure 34, particularly walls of buildings are represented with a rather limited number of points. A denser point pattern would be desirable, this would however require an additional LiDAR data set. Preferable form a TLS or VLS, which is located at a convenient angle and location for the collection of points representing walls. It is however not within the scope of this research to combine multiple LiDAR datasets that have been collected with different systems: the focus is on AHN3 (Section 1.4). To limit the effect of the limited number of points at certain locations, the points are given a larger size than the conventional point size of a point cloud. This is also in line with the suggestion of Heaberling et al. (2008): to size point map objects larger than linear map objects. In addition, the points of the point cloud will not be vertically exaggerated, as this will only result in an increase of fine point patterns of map objects. At last, Heaberling et al. (2008) described how structural patterns of map objects must be represented with a good color contrast to the terrain. To ensure this good color contrast, the users will have the option to use a base map different than the aerial image of the study area, as the aerial image is projected on the point clouds. The final visualization of layer 5 can be found in Figure 49.

AHN3 colored by aerial image (Groningen, 2019)

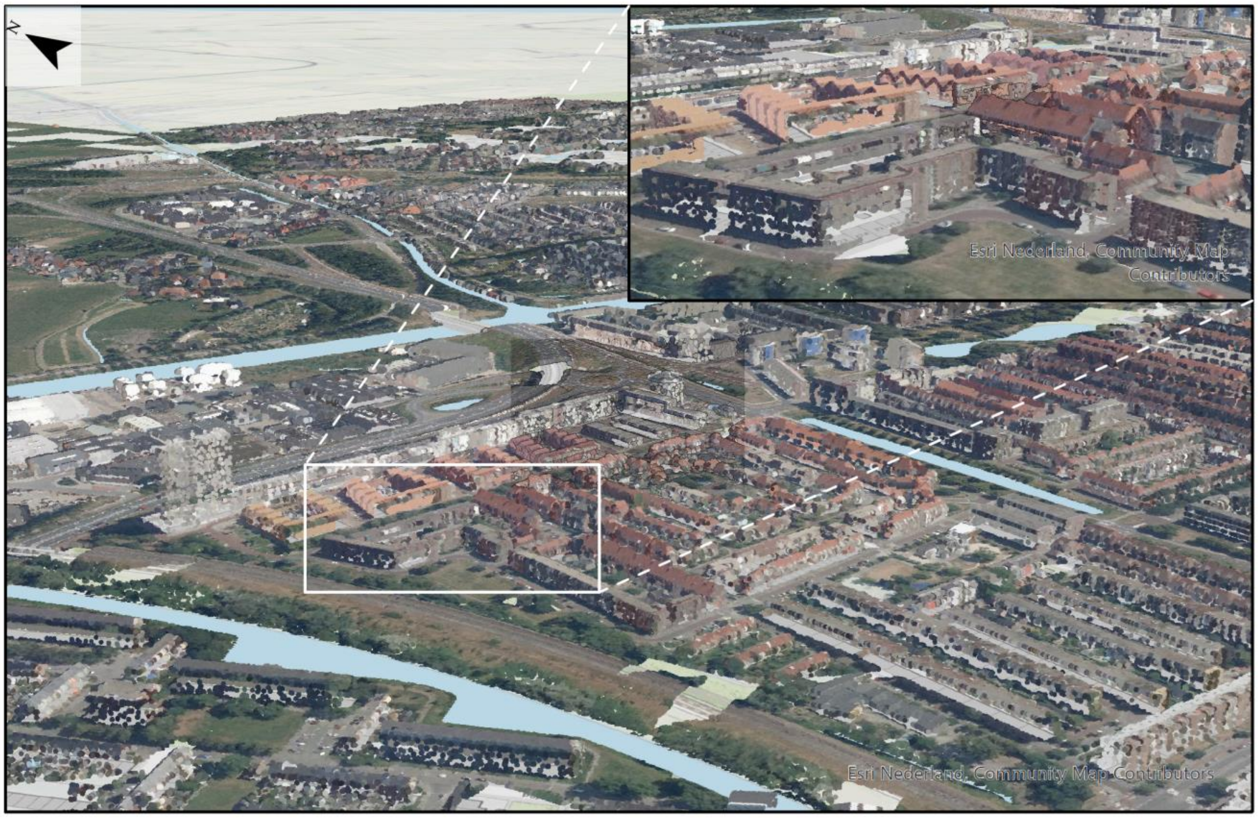

Figure 49 Colorized AHN3 (layer 5)

Additional layers

As explained in Section 3.4.3 *attract users to engage with the visualization*, one of the goals of the conceptual interface is to attract users to engage with it. An understandable spatial context can contribute to the level of attraction of the interface. As stated in Section 3.4.3, an understandable spatial context will be created with the LiDAR point clouds and with infrastructural network features. In Section 3.4.2 it has already been explained how the LiDAR point clouds will be integrated. The integration of infrastructural networks will be done with the Topo RD base map (ESRI, 2012). This base map represents boundaries, cities, water, parks, roads and buildings. The topo RD base map also ensures a good color contrast of the LiDAR point clouds to the terrain, which is in line with the design principle stated by Haberling et al. (2008) in Section 2.5.2: structural patterns for area map objects must exhibit good color contrast to the terrain. However, using a base map with a color contrast to the LiDAR point clouds can also result in large visual differences (Figure 50A) on places where the LiDAR points are sparse. Therefore, users will also be able to choose a second base map: the aerial image of 2019, which will limit the visual difference of places where the LiDAR points are sparse (Figure 50B).

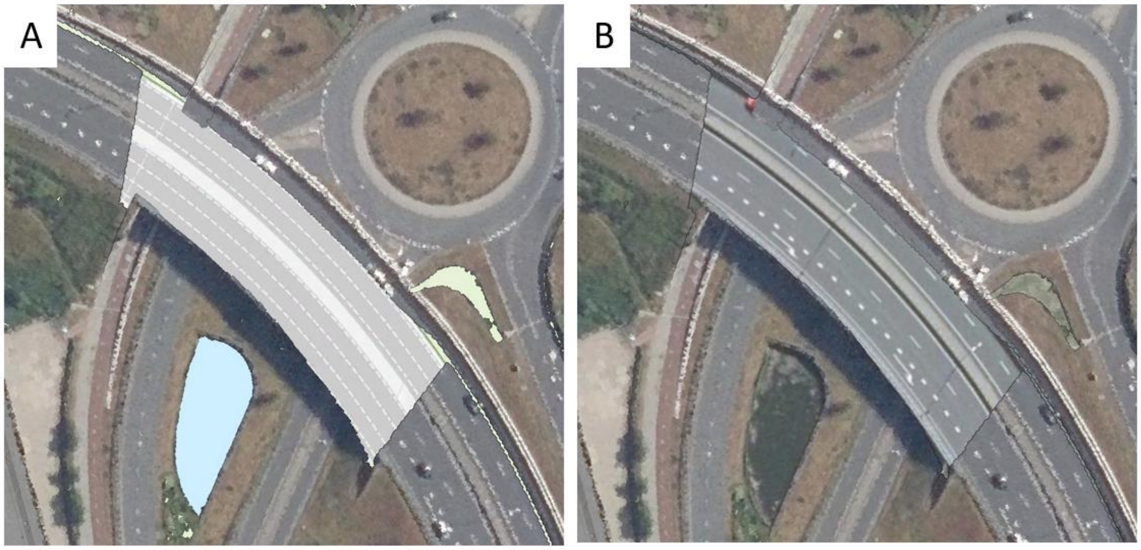

Figure 50 A: LiDAR point clouds with topo RD, the visual difference between the color of the basemap and the color of the LiDAR point clouds is relatively large. B: LiDAR point clouds with arieal image of 2019, the color difference is relatively small

As stated in Section 3.4.3 the users of the conceptual interface will be encouraged to make sense of the dynamic backstory of the data. However, as explained in Section 1.4 it is not within the scope of this research to identify the causes of land subsidence. To give the users some more background information like subsurface properties, the user is encouraged to find possible causes of the land subsidence patterns. Therefore, an additional layer illustrating subsurface properties (Figure 51) will be integrated in the prototype. The legend of the subsurface layer is rather long and is not considered to be relevant for the content of this section, however when interested please refer to Appendix B. Additionally, in Section 3.4.3 it has been explained that the functionality to use different administrative levels will contribute to user satisfaction. Therefore, three additional maps illustrating the boundaries of provinces, municipalities, and water authorities (Figure 51) will be integrated in the conceptual interface. The elevation surface of the interface is set to the elevation 3D (RD), which is derived from AHN3 (ESRI, 2018).

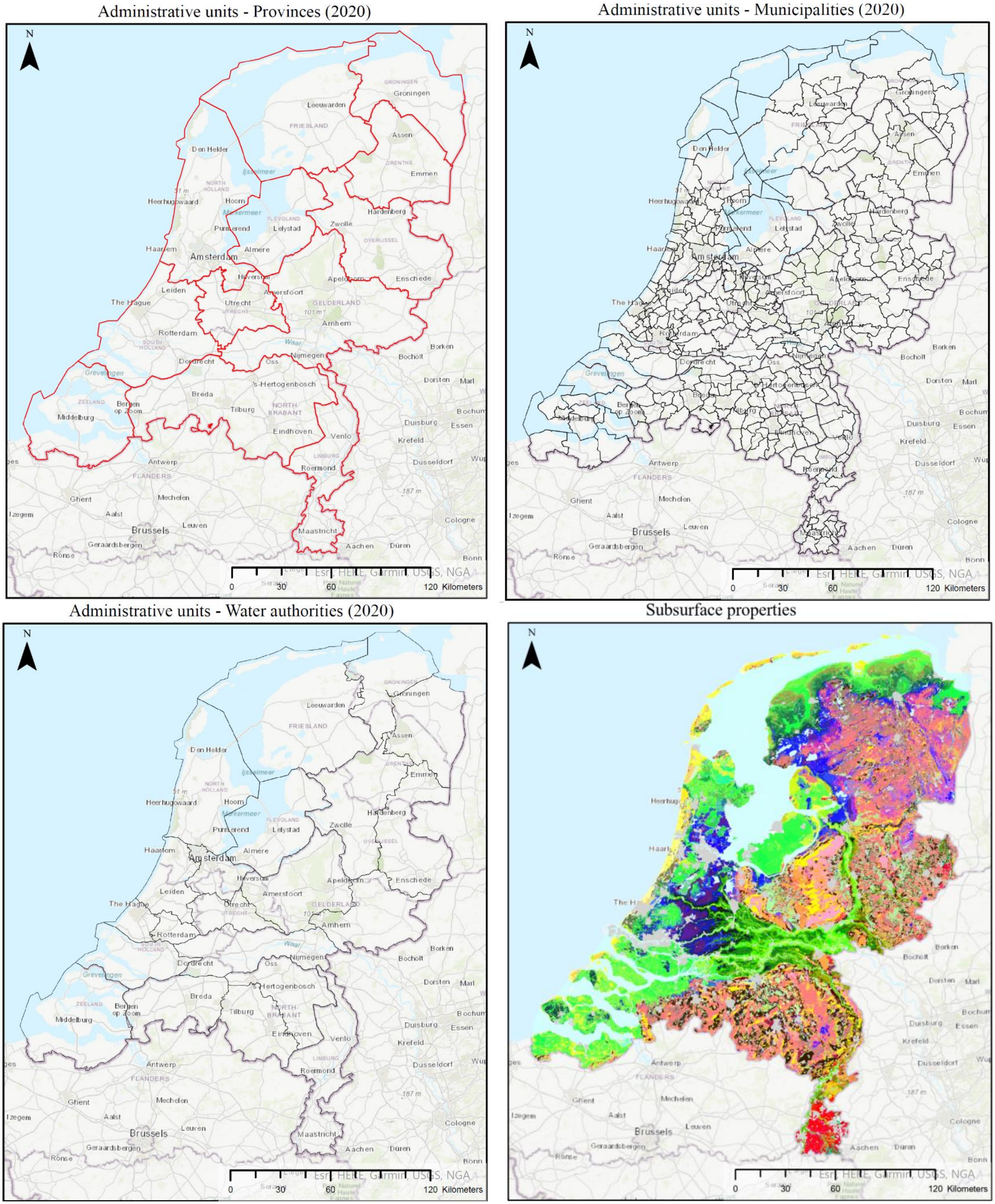

Figure 51 The administrative units, and the subsurface properties layers

3.5.4 Testing the Concept

To allow a comparison of the test results of BDK2.0 with the test results of the conceptual interface, the same assessment format as used in Sub-process A will be used to test the conceptual interface. In this framework it is analyzed to what extent the user needs are covered. The level of coverage is then used as an indication for the level of interpretability.

In the testing phase of the concept the objective of this research has to be kept in mind: to investigate to what extent a combination of PS-InSAR deformation data with LiDAR point clouds in a spatio-temporal visualization can support the communication of land subsidence by improving the interpretability of deformation data. From this objective the two components of the conceptual interface, that will be used for the communication of land subsidence, can be derived: spatio-temporal and the combination of LiDAR point clouds with PS-InSAR points. These two aspects of the conceptual interface need therefore to be evaluated. The evaluation of the spatio-temporal aspect is however already integrated in the assessment format, as one of the users' needs from the perspective of the presenting role of land subsidence communication is the ability to view time-series. The combination of LiDAR point clouds with PS-InSAR points is however not integrated in the assessment format from Sub-process A. Visualizations of PS-InSAR points with and without LiDAR point clouds will be compared to determine the effect of combining PS-InSAR points with LiDAR point clouds. The results of the testing phase can be found in Section 4.5.

4

Results

In this chapter the results of this study will be described. The results will be ordered according to the five phases of the conceptual model: empathize, define, ideate, prototype and test.

4.1 Analyzing the Interpretability of the Current Land Subsidence Communication (Sub-process A - empathize)

This sub-process consists of three steps: (1) identification of the needs of users of land subsidence communication, (2) assessing the current form of communication through the perspective of these needs, and (3) the identification of potential recommendations that can improve the interpretability of the current form of communication. The results of step one and three will be discussed in this section. To prevent redundancy, the findings of step two will not be discussed, as the results of step three are recommendations based on the results of step two.

The user needs can be defined based on the three different roles of the land subsidence communication: the general role, presenting role and the engagement role. All three different roles come with a certain set of desired components, without these components the communication cannot fulfill its associated role. The three different roles contribute to the overall goal of the communication: communicating land subsidence to the public. Without these roles, the land subsidence cannot be communicated to the public. The public is however assumed to have a desire for this communication as (1) it increases the effectiveness and implementations of large-area measures regarding the adverse effects of land subsidence which is useful as land subsidence is a process occurring at a large-area level, (2) it can aid public authorities in making better decisions and develop more informed measures and policies, and (3) it stimulates innovation, and aids society in dealing with subsidence. Following this argumentation (the users (public) have a desire for the communication, and the communication cannot exist without fulfilling the three roles, and the three roles cannot exist without their key components), the key components can be defined as user needs. The user needs can therefore be defined as: the functionality to use different administrative levels, the ability to configure layers, a selection tool, the functionality to draw boxes, the presence of visual graphs, the functionality to retrieve data in different formats, additional functionalities (for example pop-up legends, a locator map, printing and downloading facilities), the functionality to compare maps, the ability to view dynamic time-series and the presence of a geoportal, metadata and a search function.

To assess the interpretability of the PS-InSAR deformation data visualization, used for the current communication of land subsidence in the Netherlands, the visualization has been critically analyzed. This analysis has been done from the perspective of the previously described key components, or user needs. First the resulting strong points of the visualizations will be discussed, followed by the resulting limitations:

The PS-InSAR deformation data visualization is relatively good accessible, as both BDK1.0 and BDK2.0 can be accessed without any restrictions. The platform ‘Het Gebruikersforum’ allows user to share specific interpretations, making it easier for other users to understand the visualization. The pan and zoom, and text-based search function allows users to explore the data in a convenient way. Users are able to select points, and view the displacement over time from this point in detail. Additionally, users are able to turn layers on and off, and to change their order and transparency, allowing users to change the view of the map which makes the data easier to explore. Next to that, the users can view the data on a map, and temporal data of the measure points, municipalities and water authorities can be viewed in a chart and table. These different formats allow the users to explore the data as the they desire, and to explore patterns that are less obvious in the other format.

The PS-InSAR deformation data visualization lacks however a significant level of metadata, the explanation on how to use the interface is for example relatively limited, making it relatively hard for users to retrieve the desired information from the visualization. The interface is also partly in English and partly in Dutch, what might create a language barrier for certain users. Despite the pan and zoom and text-based search function, users of the visualization cannot use select a certain administrative level or object, or select a user defined area (by drawing a box), making it harder for users to view the data of a certain location. In addition, the land subsidence layers are classified with the use of a continuous color ramp without labels, preventing users to assign a specific value to different patterns of color on the map. Next to that, the layers ‘grondsoortenkaart’ and ‘aardgasvelden’ do not have a legend, making it impossible for users to derive information from it.

The results from the study suggest that the current PS-InSAR deformation data visualization is relatively interpretable, but an increase in the user friendliness of the interface, an improvement of the accessibility, additional metadata, and an enhancement of the visualization of the data will make the visualization significantly more interpretable.

4.2 Using LiDAR Point Clouds to Improve PS-InSAR Deformation Data (Sub-process B - define)

Point cloud visualizations have various advantages. When combining PS-InSAR data with LiDAR point clouds, these advantages will be linked to the PS-InSAR data. This study has found six aspects of PS-InSAR deformation data visualization that can be improved by linking it to LiDAR point clouds:

1. Point cloud visualizations have a significant added value for applications in which the end user can gain insights of the visualized phenomenon with the use of interactive, explorative, visualization methods and techniques
2. Point cloud visualization can evolve along time, allowing users to derive trends in temporal changes of the visualized data
3. The three-dimensional nature of point cloud visualization allows users to recognize the human environment and its objects
4. With point clouds, specific parts of deformation data can be linked to parts of the infrastructure, which can caid in early warning and maintenance management
5. (Regional) trends and errors in the radar processing can be mitigated and detected
6. Differential deformation trends can now be assessed, as signals can now be attached to the geometry of a building

To understand the added user-value of these benefits, it is essential to know how these benefits can cover the needs (table 7 *user needs*) that are not yet covered. The first point concerns an overall benefit for the interactive, explorative and visualization aspects of an application. As all the user needs concern a need for a functionality that is related to (one of) these three aspects, it can be said that a point cloud visualization can overall have a positive influence on all the identified user needs. The second point, allowing users to derive temporal trends, covers the need of users to view dynamic time-series of the data. Point three, four, five and six do not cover one of the user needs, but they are external benefits that result from the combination of PS-InSAR with point clouds.

4.3 Combining PS-InSAR deformation data with LiDAR Point clouds, and the Selection of Necessary Design Principles and Graphical Visualizations (Sub-process C - ideate)

Sub-process C has been divided into two sub-topics: the combination of PS-InSAR deformation data with LiDAR point clouds, and the selection of design principles and graphical visualizations. The results of Sub-process C will therefore have the same structure.

4.3.1 Combining PS-InSAR with LiDAR Point Clouds

In Section 2.2.3 it has been explained that the precision of the absolute position of PS-InSAR points (x, y & z) is relatively low. This imprecision in absolute position might be an obstacle when one wants to combine the PS-InSAR points with an external geo-data source as for example LiDAR point clouds. This is due to the fact that the absolute position (x, y & z) of PS-InSAR points is relatively imprecise, whereas the absolute position of LiDAR points is relatively precise. As a result, the displacement values cannot be assigned to the correct (parts of) the objects that are represented by the LiDAR data. Section 2.4 discussed three methods that aim to combine feature points to point clouds, where the point clouds configure as the ground truth: the 3D-NDT technique, the ICP algorithm and the method of Van Natijne et al. (2018). The Method of Van Natijne et al. (2018) has been assumed to lead to the most accurate results, due to two main reasons:

1. The method has been specifically designed for the combination of PS-InSAR points and AHN3 LiDAR point clouds
2. The method takes parameters associated to the radar system of the PS-InSAR points into account: the direction of the radar signal and the direction of the flight

This method was however not feasible within the constraints of this research. The absolute position of the PS-InSAR points have therefore not been adjusted, instead the geometry stored in the longitude, latitude and height fields has been used for the absolute position for the PS-InSAR points. The effect of not using the method of Van Natijne et al. (2018) will be discussed in Section 5.2.

4.3.2 The selection of Design Principles and Graphical Visualizations

Design principles and graphical visualization can increase the interpretability of the visualization of PS-InSAR with LiDAR. In Sub-process C the design principles and graphical visualizations that can contribute to the interpretability of the visualization of PS-InSAR and LiDAR have been explained. The resulting principles and graphical visualizations will be discussed in this section. First, the selection of design principles and graphical visualizations for representing point clouds will be presented. Subsequently, the selection of design principles and graphical visualizations based on the user needs, communicating data to the public, communicating three-dimensional data and communicating spatio-temporal data will be presented.

The literature study presented in Section 2.5.1 indicated that location should be used for contextualization when one wants to successfully design a transparent and readable visualization. In the perspective of point clouds this implies that spatial context should be derivable from the point clouds. This might however be rather difficult with AHN3, as the point density of the point clouds is not homogeneously distributed in space: horizontal faces are predominantly represented with a high point density, whereas vertical faces are predominantly represented with a low point density. The study of Poux (2019) (Section 2.3.2) does however provide the method of three-dimensional models to also derive spatial context from objects that have faces that are represented with a relatively low point density. These models either consist of solids or boundaries. The three-dimensional model that makes use of solids is however irrelevant in the perspective of communicating land subsidence, as the volume of objects is not relevant in the communication of land subsidence. Similarly, the boundary representation is considered to be irrelevant for the communication of land subsidence, which is due to two reasons:

1. A boundary representation consists of planar triangles, which makes it impossible for a boundary representation to correctly represent round features of objects
2. When looking from the perspective of the dimensions of dynamic geodesy and cartography (Van der Schans, 2001) (Section 2.5.4) one can state that with a boundary representation an external data source is being added to the graphical representation of the data, namely: a prediction of the shape of objects. One does not know if the predicted shapes do indeed exist in the human environment, while the predicted shape are presented to the user. As explained in Section 3.4.2, it is not desired to present predictions of shapes of objects to users of the land subsidence communication because of two reasons:
    1. The users of the land subsidence communication are assumed to not have any in depth knowledge of the boundary representation method, and do therefore not understand the presence of predictions
    2. Eventually, users of the communication should be able to link the PS-InSAR points to specific parts of objects that are represented with point clouds. To prevent misinterpretations, these specific parts of objects must not consist of predictions

The three-dimensional models discussed by Poux (2019) are therefore both considered to be irrelevant for the communication of land subsidence. The value that three-dimensional models can add to point clouds should however not be neglected. If the aim of land subsidence communication would for example be to link PS-InSAR points to objects, instead of parts of objects, it would be of significant value to convert the point clouds to a boundary representation to increase spatial contextualization.

Since the solution of Poux (2019) has not been implemented, the problem of low point densities of vertical faces remains to exist in the AHN3 point cloud. Haeberling et al. (2008) (Section 2.5.2) do however state that three-dimensional objects on maps must not look exactly as they do in reality. Therefore, it is not assumed to be problematic to have vertical faces represented with a relatively low point density. Three-dimensional point features are however well suited for image like representations.

The current land subsidence communication is designed for the public, rather than for a specific purpose. The SPCI method as introduced by Poux (2020) (Section 2.3.3) is considered to be irrelevant for land subsidence communication, due the lack of a specific purpose. However, similar to the three-dimensional models as suggested by Poux (2020), the ability of SPCI to add value to point clouds should not be neglected. Would the land subsidence communication have been designed for a specific purpose of use, then the implementation of SPCI would add significant value to this communication.

The design principles and graphical visualizations that have been derived from the user needs, and literature regarding communicating data to the public, communicating three-dimensional data and communication spatio-temporal data are illustrated in Table 7, and are organized by category.

Table 7 Design principles and graphical visualizations

User needs	Public	Three-dimensional	*Spatio-temporal*
Functionality to use different administrative levels	Step-by-step guide of the interface	Shape, patterns and appearances of objects do not have to look exactly as they do in reality	Line graphs that represent different parts of the time-series, superposed in one display
The functionality to configure layers	Explanation of how to interpret the graphical visualizations	Simple geometric shapes for map symbols to increase perspective perception	A data layer representing the spatial and temporal clustering of the data
Selection tool	Explanation of areas that have no cell value or measure point	Good color contrasts of buildings to the terrain	A layer representing the data in a space time cube
Functionality to draw boxes	Information of the used coordinate system and projection	No exaggeration of the terrain	
Visual graphs	Information of the update frequency of the data	Slightly transparent buildings, to limit obscurance	
Functionality to retrieve the data in different formats	Spatial contextualization by using 3D building geometries and 2D infrastructural networks	A neutral sky color, and lateral lightning direction	
Pop-up legends	Platform for communication	Image like representation of point clouds	
Locator map	Interactive interface	Structural patterns to represent map objects, but the patterns must not be too dense or too fine	
Printing and downloading functionality		Represent objects that are represented by point clouds so that they can be identified on the foreground and background	
Functionality to compare maps		Do not use a too dominant size of map objects, but define them so that they do not obscure each other	
View dynamic time-series			
Metadata			
Search functionality			

4.4 Realizing the Conceptual Interface (Sub-process D - prototype)

A representation of the concept of the interface can be found in Figure 52. All functionalities of the map are explained in the interface. When the user clicks on the question mark, the user is being forwarded to the explanation of the functionalities of the tools. The left explanation panel can be minimized by clicking on the minus symbol. Similarly, when multiple layers with different classifications are selected, the user can maximize the legend panel to view the different legends. When one of the land subsidence layers is visualized simultaneously with the time-series layer, the chart panel (where currently the chart 'linear displacement of selected features' is being displayed) will be divided into two parts, one part for the 'linear displacement of selected features' chart and one for the 'temporal profile of linear displacement, ordered by class' chart (Figure 46). The concept (Figure 52) has been made based on the design principles and graphical visualizations that have been derived in Sup-process C from the user needs, and literature regarding communicating data to the public, communicating three-dimensional data and communicating spatio-temporal data, and from the testing phase (Sub-process E). The features in the conceptual interface that are a result from Sub-process E are outlined in red and numbered with their associated number, the number are explained in Section 4.5.

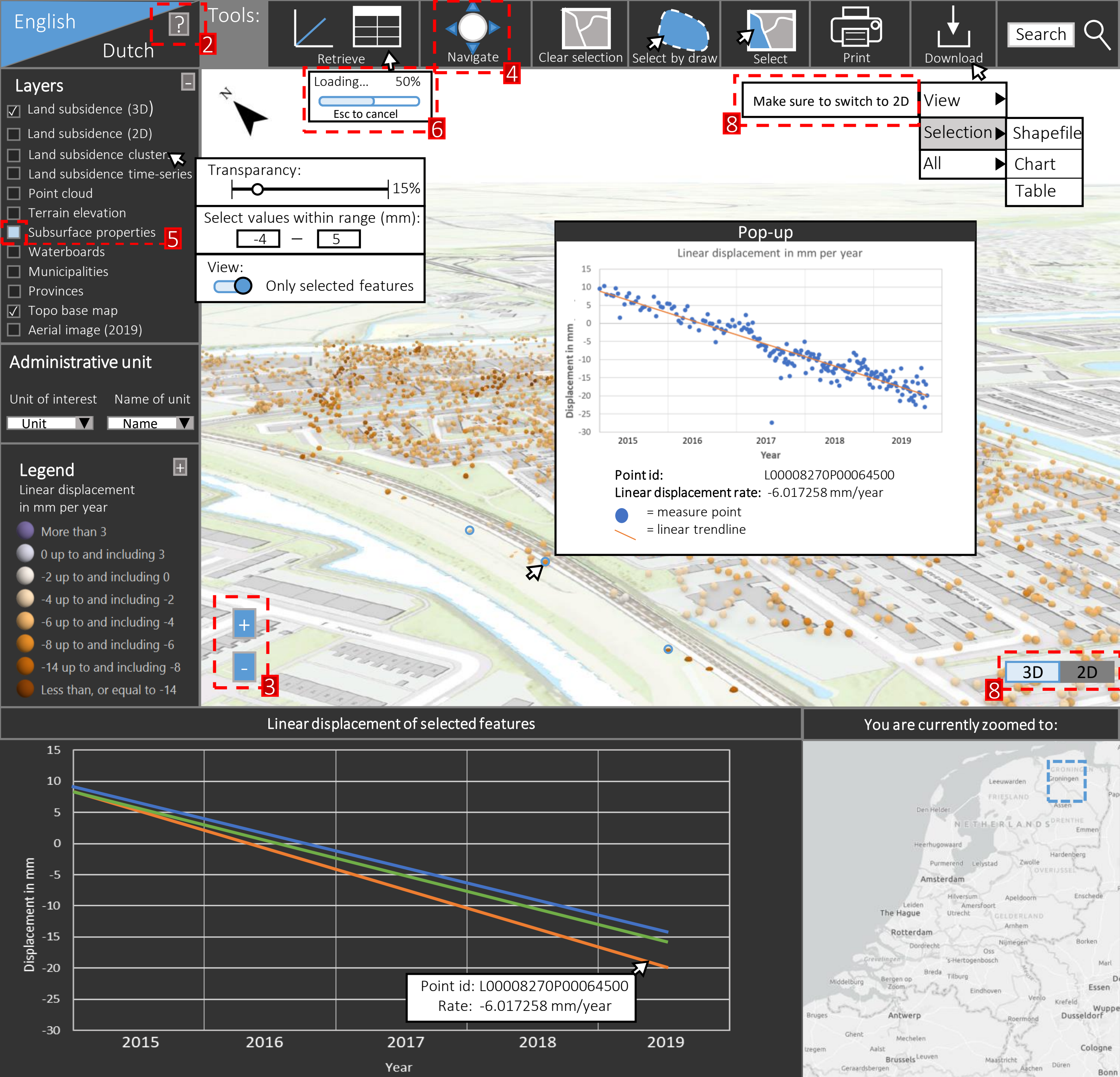

This interface is developed for indicative purposes. No rights can be derived

There is not a fixed update frequency of the data
Last updated: February 2020

How to use this map?

Explanation of available layers

Map navigation

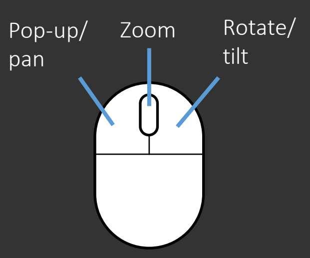

All layers are projected in the RD new horizontal coordinate system, with NAP as the vertical coordinate system. To overlay different layers, the transparency of each layer can be adjusted with a slider by right-clicking the layer in the legend. Next to that, layers can be dragged to change the order of overlay. Specific features of the land subsidence layers can be selected by specifying a range of displacement values. This can also be done by right clicking the layer, and results in a selection of only the points that have a displacement value that fall within that range. In addition, for each layer there is the option to visualize all data or just the selected features.

By clicking on the box in front of a layer the box will turn blue, which means that the layer is loading. When the checkmark appears in the box, then the concerned layer has fully loaded.

Land subsidence (2D and 3D): illustrate the average displacement in mm per year (from 2015 to 2019) of the position of the associated measure point. The measure points are located at objects that are coherent through time, and at non-horizontal surfaces. Non-coherent objects are too unstable to get precise displacement values, and horizontal surfaces prevent backscattering of the signal used for measuring displacement values.

Land subsidence clusters: illustrates the average displacement in mm per year of the position of the associated cluster for six different time periods: 2015, 2016, 2017, 2018, 2019 and the average of 2015-2019. An animation time line allows you to play the animation and see the change through time, but also allows you to pause on a desired layer. Areas located outside a 20-meter range of a measure point are not given any value, hence the blank areas. The temporal behavior of the clusters of 2015-2019 is shown in the associated chart (will be displayed below the map after selection).

Land subsidence time-series: illustrates the average displacement in mm per year for each year (2015,2016, 2017, 2018 and 2019). Each year is being displayed with the use of a cylinder, and all the years together are chronologically stacked, with 2015 at the bottom, and 2019 at the top. As the colors of the cylinders represent a certain range of displacement, the values of the cylinders must be interpreted individually and must only be used to compare the dynamics within 2015-2019 of a certain position (they can for example not be subtracted or added together).

Point cloud: shows the real-world in three dimensions, with the use of points. The points have been collected with the use of airborne systems, which cannot view all objects from all angles. As a result, walls of buildings might be represented with only a limited number of points.

Terrain elevation: illustrates the terrain of the Netherlands

Subsurface properties: illustrates the components of the subsurface of the Netherlands, based on the top 1.50 meter of the subsurface.

Waterboards: illustrates the waterboard boundaries

Municipalities: illustrates the municipality boundaries

Provinces: illustrates the province boundaries

Topo basemap: topography Nederland

Explanation of administrative units

Select the unit you are interested in in the 'unit of interest' drop down box. You can choose from: provinces, municipalities and waterboards. In the 'name of unit' drop down box, select the name of the province, municipality or waterboard you want to zoom to.

Explanation of pop-up

When clicking on a point or cylinder of one of the land subsidence layers (2D, 3D or time-series) a pop-up chart appears. The chart shows the measurement values of the associated measurements of the point over time. The linear trendline of these measurements represents the average displacement in mm per year (from 2015 to 2019) of the point.

Explanation of linear displacement of selected features chart

With the selection tool multiple land subsidence points or cylinders from the land subsidence layers (2D, 3D or time-series) can be selected. To compare the trendlines of the pop-up charts, the trendlines of the selected points will be visualized in this chart. When hovering over the lines, a pop-up appears containing the information on the id and linear displacement rate of the point.

Toolbar

: allows you to search a specific adress, with suggestions based on what you entered. After selection the view of the map will be zoomed to the selected adress

Select

: allows you to select measure points, cyllinders ,provinces, waterboards and municipalities by clicking on them

Select by draw

: allows you to select measure points,provinces, waterboards and municipalities by drawing a polygon. Only features that completely fall within the polygon will be selected

Figure 52 Conceptual interface

4.5 Testing the Concept (Sub-process E - test)

In this section the assessment format used for Sub-Process A is used to evaluate the conceptual interface. Subsequently, the results from the assessment format will be used to determine what features have not directly been integrated in the conceptual interface, but would result in an added value for the concept. At last, the PS-InSAR visualizations with and without LiDAR point clouds are evaluated to determine the effect of a combined visualization of PS-InSAR with LiDAR point clouds. The assessment formats to assess the coverage of the user needs are shown in Table 8 A - C.

Table 8 Assessment format

Engagement role	
Geoportal	- Currently the interface is a concept, and therefore not accessible. The intention is however to publish the concept via a website, that can be accessed without any restrictions - In the concept there is a link to a communication platform, on which users can share the patterns they have found - Users can choose to either view the interface in Dutch or English
Metadata	- The charts in the pop-ups are explained - The chart that superposes the linear displacement trendlines of the selected points or cylinders is explained - All tools of the interface are explained below the interface - The content of the layers available in the interface is explained, as well as the used horizontal and vertical coordinate system - It is explained why measure points of the land subsidence layers are predominantly located at objects - It is explained how users can navigate on the map - It is explained how users can select different administrative units - For the land subsidence cluster layer, there is an explanation on why there are cells with no values - There is information on the update frequency of the map - There is no marker that can be placed by the user. Instead, the interface allows users to select one or multiple features that will be outlined in blue - There is an option to get more information on the technical background of the land subsidence data - All tools are explained with the use of a question mark that is linked to the information concerning the functionality of the concerned tool, which means that the icons used are not self-explanatory - Each panel in the interface contains a question mark that is linked to the information concerning the associated functionality, resulting in six question marks. The use of six question marks might result in the interface being less visually attractive for its users
Search function	- There is a search bar, with which one can search an address - Users can pan and zoom in and out - There is not a specific button in the interface which users can use to zoom in and out - Users can use the drop-down boxes in the administrative unit panel as an alternative for the text search bar

7a Engagement role: assessment of key components (based on Hu & Li, 2017)

General role	
Administrative levels	- Users can select the administrative level they want to view the data for
Selection tool	- Measure points, cylinders (from the time-series layer), water authorities, provinces and municipalities can be selected - It is not clear for users how to switch from the selection tool back to the map navigation
Drawing boxes	- An area of interest can be defined by drawing a polygon on the map
Visual graphs	- There is an explanation concerning the charts after selecting a measure point

Layer configuration	- Layers can be turned off and on, and layers can be dragged to change their order of overlay - It takes a relatively long time to visualize large datasets such as LiDAR point clouds and PS-InSAR data. One of the consequences is that when a user selects a certain layer, and the box in front of the layer gets checked, it might take some time before the data is actually visualized. Users that are not familiar with rendering processes might not understand why a layer is not directly being visualized

7b General role: assessment of key components (based on Van Elzakker et al., 2003)

Presenting role	
Retrieve in different formats	- Users can view the data on a map - The displacement data of the selected measure points can be viewed in a table - Temporal data of measure points and cylinders of the time-series layer can be viewed in a graph - A relatively large number of selected measure points might result in a relatively long waiting time for retrieving the selected data in a graph or table format
Pop-up legends, locator map, printing and downloading facilities	- The values of the color ramps of all layers are static. Meaning that the user is not able to change the minimum and maximum value linked to the color ramp of the land subsidence layers. A dynamic color ramp would make it easier for users to make visually discriminations - When multiple layers are selected, the legend panel can be extended - The panel on the left side of the map can be minimized - There is a print functionality - It is possible to download data in three different formats: table, charts and shapefiles - For the download tool there is an option to download the measure points that fall within the current map view. This might however be rather difficult when using a 3D view, as due to the perspective the user might select undesired measure points - The tables and charts are also downloadable - There is a locator map
Compare maps	- Maps can be compared with the use of an overlay function, maps can however not be visualized simultaneously without an overlay - Layers can be made transparent - Visual graphs can be visualized simultaneously, and can thus be compared
Time-series	- When selecting a certain measure point one can see the time-series of deformation of that location of 2015-2019 in the form of a graph, where displacement measures have been plotted against time - The layer 'land subsidence time-series' (layer 4.1) illustrates the dynamic behavior within the time-series of displacement by showing the average displacement value of each individual year. One could however state that the level of temporal detail (a year) is still limited.

7c Presenting role: assessment of key components of BDK2.0 (based on Van Elzakker et al., 2003)

There can be nine features derived from the assessment format that have not directly been integrated in the conceptual interface but will increase the level of coverage of the user needs:

1. *Concerning the metadata*: icons in the interface should not need an explanation, but should be self-explanatory. This will however not be integrated in the conceptual model, as the scope of this research does not include a study regarding icons that can be used in an interface. The issue of the lack of self-explanatory icons will be further discussed in Section 5.3.4.
2. *Concerning the metadata:* to increase the visual attractiveness of the interface there should be only one question mark that refers to the explanation of all tools, instead of six.
3. *Concerning the search function:* to aid users in navigating through the scene there should be two buttons that allow users to either zoom in or out on the map.
4. *Concerning the selection tool:* to make it clear for users how to switch from using their mouse for selecting features to navigating through the scene there should be a navigation tool that can be selected by the user.
5. *Concerning the layer configuration:* to help users understand that it might take a relatively long time for certain layers to fully load on the map, *a* layer list with checkboxes for each layer that turns blue when the user selects the layer, and where a check mark appears when the concerned layer

is actually rendered should be used. This way, users will know when a layer is loading, preventing the users to assume that a certain layer cannot be loaded.

6. *Concerning the retrieve in different formats:* to make it clear for users that it might take a relative long time to retrieve a chart or table for a relatively large amount of selected measure points, a loading bar should be used once the user uses the retrieve tool. This bar should show the process of the retrieval, and should allow users to cancel the retrieve tool. This loading bar should also be applied to the download tool.
7. *Concerning the legends:* A dynamic color ramp would make it easier for users to make visually discriminations. This will however not be integrated in the conceptual model due to time constraints, but will be further discussed in Section 5.3.4.
8. *Concerning the downloading facility:* to prevent users to download undesired data with the tool to download the measure points that fall within a certain view, users should only be able to use this tool on a two-dimensional view, and not from a three-dimensional perspective. This can be done by adding a switch button that allows users to view the data in either two or three dimensions. It should however be explained that the measure points within a certain view can only be downloaded when the view is switched to two dimensions.
9. *Concerning the time-series:* one could state that the level of temporal detail (a year) of layer 4.1 is still limited. Time-steps of one month are however not desired, which will be discussed in Section 5.3.4.

As shown in Figure 26, the test outcomes of Sub-process E will be used as an input for Sub-process D, in which the interface is created. The previously discussed features 2 to 6 and 8 will be integrated in the conceptual interface. The new features that resulted from this testing phase are outlined in red in the conceptual interface, and are marked with their associated feature number (Figure 52).

To assess the effect of a combined visualization of PS-InSAR Point with LiDAR point clouds, a Ps-InSAR visualization with and without LiDAR point clouds will be compared. Both visualizations represent the same area. The first visualization is shown in Figure 53. This figure illustrates that from the visualization with LiDAR point clouds (Figure 53A) height can be derived, whereas height cannot be derived from the visualization without LiDAR point clouds (Figure 53B). The added value of the LiDAR point clouds (Figure 53A) is that differences in height can now be linked to the PS-InSAR points, resulting in the insight that the higher areas (in the white frames) have higher displacement values than the lower areas (black frames). This insight cannot be derived from Figure 53B.

The second visualization is shown in Figure 54. This figure illustrates that from a visualization without LiDAR point clouds (Figure 54B) the PS-InSAR point in the white frame can be linked to the wall of the building. It can however not be determined at what part of the wall the PS-InSAR point is positioned, whereas this can be determined from the LiDAR point cloud visualization (Figure 54A).

The third visualization (Figure 55) illustrates the same as the second visualization: in Figure 55A the PS-InSAR point in the white frame can be linked to a specific part of the object, whereas in Figure 55B this cannot.

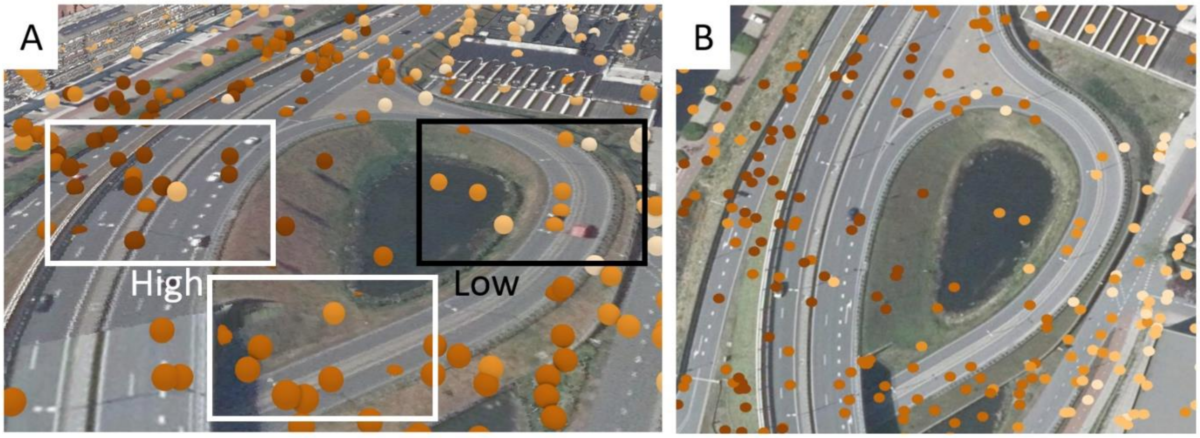

Figure 53 A: three-dimensional PS-InSAR with point clouds. B: two-dimensional PS-InSAR point without point clouds. White frames represent higher areas, black frames lower areas.

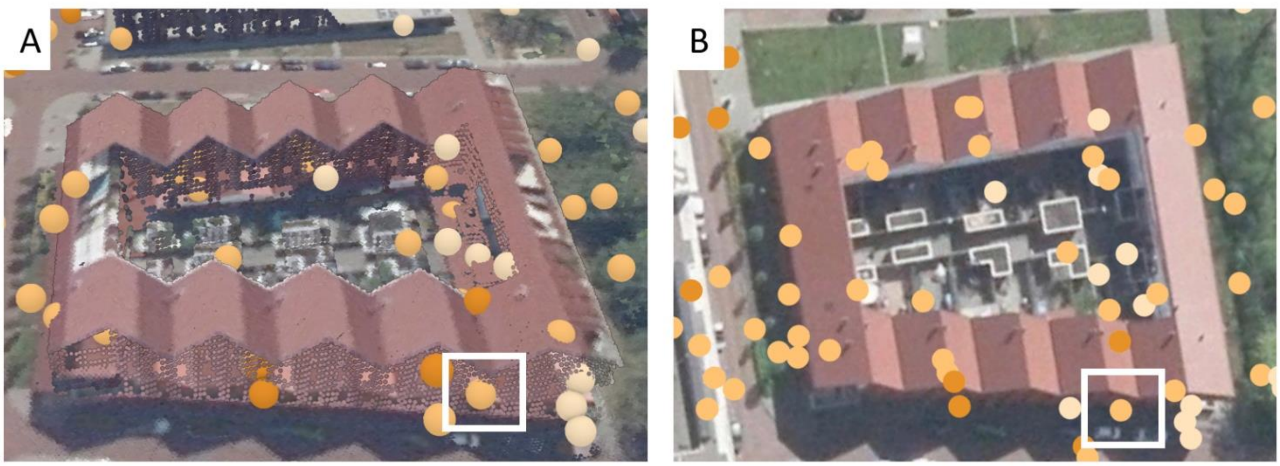

Figure 54 A: three-dimensional PS-InSAR with point clouds. B: two-dimensional PS-InSAR point without point clouds. White frames represent higher areas, black frames lower areas

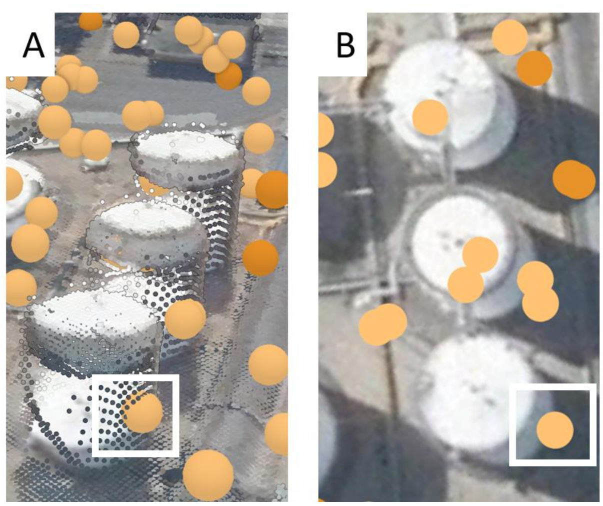

Figure 55 A: three-dimensional PS-InSAR with point clouds. B: two-dimensional PS-InSAR point without point clouds. White frames represent higher areas, black frames lower areas

5

Discussion & Research Directions

5.1 AHN3 LiDAR Point Clouds

In Section 3.4.2 it has been described that in AHN3 certain parts of buildings, for example walls, are represented with a limited number of points. This is due to the fact that AHN3 has been collected with an ALS, which predominantly collects LiDAR data from above with a limited angle. As a result, horizontal faces, such as roofs, are represented with a relatively large number of points, whereas vertical faces, such as walls, are represented with a relatively small number of points. An increase in point density on vertical faces would however increase the level of detail of the geometry of buildings. An increase in point density can be accomplished by combining the AHN3 data set with a LiDAR dataset collected with a different LiDAR system, for example VLS or TLS. Combining point clouds gathered by different systems reduces the errors of a point cloud representation (Section 2.3.4). However, as explained in Section 1.4, it is not within the scope of this research to combine AHN3 with other LiDAR datasets. The consequence of this is however that not all vertical faces are well represented in the concept of this research, making it harder for users to link PS-InSAR points to vertical faces. This can have a relatively large impact on the interpretability of the PS-InSAR points, as due to the backscattering properties of objects radar signals are predominantly located at non-horizontal surfaces (Section 2.2.1). Using point clouds collected by different LiDAR systems for land subsidence communication might be interesting for future research.

A second point of discussion is that in this research, only a concept for the municipality of Groningen has been implemented. For this concept only the AHN3 tiles covering Groningen have been used, which is already a considerate amount of data: 60 gigabytes. Considering that the Netherlands covers approximately 41.543 square kilometers, which is almost 210 times larger than the municipality of Groningen (which is approximately 198 square kilometers), an AHN3 dataset covering the whole of the Netherlands would exist of nearly 1260 gigabytes. Implementing the concept of this study on a national scale would therefore require hard- and software that is able to deal with this amount of data. The software used in this research is currently not considered as convenient for 1260 gigabytes, as for example ArcGIS Pro seized to work when running an operation with 60 gigabytes of AHN3 point clouds. As a result, one could question whether an implementation of the concept on a national scale is realistic. This point of discussion is related to the abilities of existing software to work with point clouds, and the desired LoD. However, the abilities of software to work with point clouds is still evolving. QGIS has for example announced that they are currently working on adding point cloud support to QGIS (North Road, 2020). The question whether an implementation of the concept of this research on a national scale is achievable depends on the development of for example software, algorithms and data structures. To what extent these developments will be able to deal with LiDAR data is currently still uncertain. However, to gain insights in the current capabilities of point cloud support software, van Oosterom et al. (2015) investigated and benchmarked various point cloud data management systems, and compared the results of this in their research. In their study they tested Oracle, PostgreSQL, MonetDB, and LAStools.

In this research the used design principles for visualizing point clouds do not include the concept LoD. Zhang et al. (2020) discuss the concept continuous level-of-detail (cLoD), which can aid in realizing good interactive visualizations of point clouds. As the conceptual interface of this research concerns an interactive visualization of point clouds, the aspect cLoD is considered to be valuable in the perspective of this thesis. With cLoD an interactive visualization of point clouds with proper resource consumption and relatively good visual quality can be realized by removing points that are unnecessary without changing the point density. In addition, the cLoD method considers the camera orientation, position, and distance from the camera to the point clouds. An integration of the cLoD method in future research is considered to be of significant value in the perspective of this research, and is therefore recommended as a future research direction.

5.2 Ps-InSAR Data

It has been explained in Section 3.4.1 that the absolute position (x, y & z) of the PS-InSAR points is relatively imprecise, which can lead to misinterpretation of the data when visualized with LiDAR point clouds. The described method of Van Natijne et al. (2018) allows an improvement of the absolute positions of the PS-InSAR points with the use of error ellipsoids. This method is however not implemented in the concept of this study, as the method is infeasible within the restraints of this research. The alternative method used is using the geometry attributes longitude, latitude and point height, stored in the raw PS-InSAR data, for the absolute position. However, to limit the effect of the imprecision of the absolute height (z) of the PS-InSAR points, the points have been visualized in both a two-dimensional (layer 2) and three-dimensional way (layer 1). However, as also explained in Section 3.4.1, it cannot be assumed that with this alternative method the PS-InSAR points are located at the correct real-world objects, or at the correct ground point. The imprecision of the PS-InSAR points results in that the maximum potential of the role of point clouds (to increase the interpretability of PS-InSAR data) cannot be utilized: the users are now able to derive the human environment and objects from the AHN3 point cloud, but they are still not able to link a certain point of PS-InSAR to a specific (part of an) object. One could question the decision to use the geometry stored in the PS-InSAR data, instead of using one of the alternative methods: the 3D-NDT technique or the ICP-algorithm, which might be feasible within the constraints of this research. However, the literature study indicated that the method of van Natijne et al. (2018) will lead to the most precise results, as it has been specifically designed for PS-InSAR data and takes for example the direction of the radar signal and the direction of flight of the radar system used for collecting the PS-InSAR data into account to limit errors (Van Natijne et al., 2018). The implementation of either the 3D-NDT technique or the ICP-algorithm will not lead to the desired results, and would thus only be an additional unnecessary step in the realization of the concept. Instead, it has been chosen to use the geometry of the absolute position that is already stored in the PS-InSAR points. It is however important that the user of the conceptual interface is informed about the fact that the current concept cannot be used for specific projects or policy making processes, due to the imprecision of the absolute position of the PS-InSAR points. The Implementation of the method of van Natijne et al. (2018) in the conceptual interface is a recommendation for future research.

There are three points of discussion of PS-InSAR that one working with PS-InSAR data should be familiar with: the assumptions made regarding horizontal displacement, phase ambiguity and the selection of PS-InSAR measure points.

First, the PS-InSAR displacement values represent vertical displacement of the measure points. In order to assign a vertical displacement value, an independent assumption had to be made in the horizontal displacement of the concerned measure point (Section 2.2.3). However, Hanssen states in SkyGeo (2020) that it is possible that a wrong assumption regarding horizontal displacement has been made, resulting in the exclusion of horizontal displacement of certain measure points in the PS-InSAR data, whereas the horizontal displacement does exist in the real-world.

Second, as explained in Section 2.2.3 the displacement of PS-InSAR measure points have been calculated with the use of phases. To resolve the 2π -ambiguities in the phase observations certain assumptions have been made. One of the risks of using assumptions is that one might overlook a wave cycle (0-2π). To minimize imprecise displacement values, the values have been compared to expected displacement values that have been calculated with machine learning. A wave cycle that has been overlooked can be recognized when the PS-InSAR displacement values differ significantly from the expected displacement values (SkyGeo, 2020).

In the conceptual interface the PS-InSAR points of 2015 to 2019 have been used. Using this relatively long time period has an impact on the number of measure points present in the PS-InSAR data set. This is due to the fact that only stable or coherent measure points are suitable for measuring displacement. Measure points located at for example areas in which a certain type of construction takes place, for example infrastructure, are not considered stable due to excavation or elevation. When using the dataset that covers 2015 to 2019 it implies that when construction took place at a certain measure point in 2018, the measured displacement in 2015 to 2017 is also excluded from the PS-InSAR dataset. A solution would be to use datasets for each individual year. This was however not possible, as the PS-InSAR data is only published in the format 2015 to 2019. As a result, the concept of this research does not have any measure points located at locations where construction took place in 2015, 2016, 2017, 2018 or 2019 (SkyGeo, 2020).

4.3 Methodological Approach Taken

The discussion points for each of the individual sub-processes will be discussed in this section.

4.3.1 Sub-process A – empathize

Section 3.2 described that user needs can be valuable in the process of improving a certain service (Welle Donker, 2020). The ideal scenario in the perspective of the land subsidence communication would be to cover all the needs of its users, to ensure an optimum interpretability of communication. This ideal scenario is however not feasible in this perspective, as the needs of each individual that is part of the public cannot be covered with just one service. As a result, a form of land subsidence communication that covers the needs of all its users is not realistic. In the method used in Sub-process A (Section 3.2), the assumption has been made that the twelve key components discussed in Section 2.1.3 are equal to the needs of the user of the communication: the public. The fact that these key components contribute to the overall goal of the land subsidence communication (Figure 3) increases the reliability of this assumption. It does however have to be acknowledged that these key components do not cover the needs for all individuals in the user group, as the user can have less or additional desires.

4.3.2 Sub-process B – define

The identified aspects of PS-InSAR deformation data that can be improved by Linking to LiDAR point clouds have been derived from the studies from Verbree and Van Oosterom (2015), Javaheri et al. (2019). Azari et al. (2012), Van Natjine et al. (2018) and Ackere et al. (2017) as described in Section 2.1.6. Azari et al. (2012) stated that point cloud visualization can evolve along time, allowing users to derive trends in temporal changes in the data. However, this would require either an extra attribute storing the temporal change for each point of the point cloud, or a second point cloud with a different date of collection. Both options would result in an increase in the size of the point cloud data set in terms of storage. Consequences might be an increase in running time of operations, a decrease in smooth rendering of the data and a need for more storage space. These are aspects one should constantly consider when using point clouds to visualize temporal change in data, such as deformation.

A second point of discussion of the literature used as input for Sub-process B is that of Van Natijne et al. (2018). Van Natijne et al. (2018) state that with point clouds (1) specific parts of deformation data can be linked to parts of the infrastructure, which can caid in early warning and maintenance management, (2) (Regional) trends and errors in the radar processing can be mitigated and detected and (3) differential deformation trends can be assessed, as signals can be attached to the geometry of a building. When one aims to link PS-InSAR to LiDAR point clouds, one should know that these aspects are however only assumed to exist when the absolute positions of the PS-InSAR measure points are improved with the method of or a similar method to Van Natijne et al. (2018).

4.3.3 Sub-process C – ideate

In Section 3.4.3 the selection of graphical visualizations and design principles of the conceptual interface has been discussed. The graphical visualization and principles selected for visualizing data for the public are predominantly based on the study of Schoffelen et al. (2015). This study is however focused on visualizations in general, and not specifically on geographic visualizations. The study was however still considered to be valuable in the perspective of this research, as the main goal of both visualizations in general and cartographic visualizations are to make things or data public through visualization.

Similar to the selection of graphical visualizations and design principles for visualizing data for the public, the selection for visualizing three-dimensional data is predominantly based on the study of Haeberling et al. (2008). The visual variables, as discussed by Haeberling et al. (2008), are intended primarily for static map legends and images. The conceptual interface of this research is however interactive. Haeberling et al. (2008) is still considered to be valuable for the concept, as the interactive interface does make use of static visual variables. The color, shape or brightness of symbols in the concept are for example static, and not dynamic.

5.3.4 Sub-process D – prototype

The PS-InSAR layers of the conceptual interface (layer 1, 2, 3 & 4) have all been visualized with the use of static color scales. This implies that at all scales or zoom levels the scale of the color bar does not change. Currently, the concept has only been developed for the municipality of Groningen, where the variation in displacement values is relatively low. However, when extending the concept to other parts of the Netherlands, or when an increase in visual discrimination is desired, a color re-scaling can be used. A rescale of color implies a change in the value range of the color scale. Due to the relatively low variation in displacement values in Groningen, the effect of using a static color scale is rather limited. However, the use of a dynamic color bar would make it easier for users to make visually discriminations. Therefore, the inclusion of a dynamic bar is an interesting integration for future research.

In this research, the PS-InSAR points have been transformed from ETRS 89 to RD new with the Amersfoort_To_ETRS_1989 (WKID=1751) geographic transformation (Section 3.5.1). However, the RDNAPTRANS transformation procedure has specifically been designed to transform from ETRS 89 to RD New, and is suggested to use when transforming data from RD New to ETRS 89, or the other way around (Marel, 2014). This transformation is only supported by a few number geographic information systems, and makes use of a seven-parameter transformation, a map projection, a conventional correction grid for the x and y coordinates in RD new, and a quasi-geoid for the conversion of the heights. The difference between the used transformation (Amersfoort_To_ETRS_1989) and RDNAPTRANS procedure is the level of precision: Amersfoort_To_ETRS_1989 has a precision of 0.6 meters, whereas RDNAPTRANS has a precision of one to a few centimeters (Marel, 2014). To make the absolute position of the PS-InSAR points of the conceptual interface more precise, the RDNAPTRANS procedure is recommended for a continuation of this research.

As explained in Section 3.4.3 the PS-InSAR data, of which the time-series originally covers the time period from 2015-2019, has been broken down into time steps of individual years for layer 3. One could however question whether a time-step interval of a year is the proper way. Andrienko et al. (2020) states that the chance to perform temporal abstraction, allowing users to observe higher scale patterns, decreases when time-series are long. Andrienko et al. (2020) therefore suggest to use data transformation methods that can reduce details and produce higher level constructs. A time step of one year seems to be in line with this suggestion of Andrienko et al. (2020), as the details of the data are reduced by excluding details of variation of the data within a year. It should however be noted that the collection frequency of PS-InSAR differs per year: 2015 has 24 dates of collection, 2016 has 29, 2017 has 47, 2018 has 58 and 2019 has 48. So, when one does decide to increase detail of the PS-InSAR time-series by using smaller time steps, such as months, the resulting displacement trends per month would be questionable as they would have been derived from only two (2015) to five (2018) dates of collection. As a result, it is not desirable to increase the detail of the time-series of PS-InSAR, which is in line with Andrienko et al. (2020).

A rather minor point of discussion is the fact that to calculate the displacement trends of the individual years the slope of the linear regression formula, which is expressed in days, has been multiplied by 365. The year 2016 is however a leap year, with 366 days instead of 365. It has been chosen to neglect the fact that 2016 is a leap year, to make the displacement trends per year easier to compare.

A point of discussion for the point cloud layer is its illumination. Haeberling et al. (2008) suggested to use a mainly lateral lightning direction for three-dimensional maps. As explained in Section 3.5.2, the settings of layer 5 have been set to simulate a lateral lightning direction. The effects of this will however be limited, as the layer does not exist of solid shapes but of points, which will have none to a limited shadow effect.

A discussion point of the conceptual interface is that the pop-ups of the land subsidence layers, the link to the discussion platform, and the link to the technical background information have not been developed in this research. The pop-ups are still a concept, its integration is however recommended for future research. Additionally, the links to both the discussion platform and the technical background information have not been developed in this study, as they do not fall within the scope of this research. Similarly, both links should be included in continuation of this research.

Unlike the current communication of land subsidence, the conceptual interface does not include layers on shallow and deep land subsidence. This is due to the fact that it is not within the scope of this research to include causes of land subsidence (Section 1.4).

Another point of discussion for the interface is that the icons used in the interface are not self-explanatory: they are now being explained with the use of a question mark that is linked to the information of the tools. This might result in the conceptual interface being less attractive for the users. It is however important that the interface is considered to be attractive for its users to engage with it (Schoffelen et al., 2015). A suggestion for future research is therefore: how to increase the level of self-explanation of the interface.

Currently the only layer that aids users in making sense of the dynamic backstory of the displacement values is the layer representing subsurface properties. As explained in Section 1.4, it is not within the scope of this research to take causes of land subsidence into account. The study of Schoffeling et al. (2015) does however show that information regarding the dynamic back story of the data adds value to communicating data to the public. Adding more information regarding the background of displacement data is therefore assumed to be valuable for future research.

5.3.5 Sub-process E - test

The conceptual interface has been tested with a framework based on the assumed needs of users of land subsidence communication. As explained in Section 1.4, it is not within the scope of this research to extensively test the concept. It is however assumed that to test the interface with the actual end users (instead of assumptions of their needs) would provide more accurate test results. Testing the concept with actual users would therefore be valuable for future research.

6

Conclusion

In this chapter the research objective and research questions will be revisited. First, it will be discussed to what extent the research objective has been achieved. Second, an answer on each of the sub-questions will be formulated based on the results, keeping the points of discussion (Chapter 5) in mind.

6.1 Research Objective

As stated in Section 1.3: the objective of this research is to investigate to what extent a combination of PS-InSAR deformation data with LiDAR point clouds in a spatio-temporal visualization can support the communication of land subsidence by improving the interpretability of deformation data.

In this research a conceptual interface that combined spatio-temporal PS-InSAR data with LiDAR point clouds has been designed and tested. The conceptual interface has been designed based on a selection of design principles and graphical visualizations. The design principles and graphical visualizations have been selected with the use of a user needs analysis, and literature regarding communicating data to the public, communicating three-dimensional data, and communicating spatio-temporal data. The users of land subsidence communication have been defined as the public, and their needs were assumed to be equal to the key components of the three roles of land subsidence communication: its general role, presenting role and engagement role. To ensure improvement of the conceptual interface relative to the current land subsidence communication, it has been assessed to what extent the current communication covers the needs of its users, and what improvements can be made to increase this coverage. These improvements have been integrated in the conceptual interface of this research. Hence, this research aimed to explore and design a spatio-temporal visualization of both PS-InSAR and point cloud data, to eventually improve the current form of land subsidence communication. The objective of this research is therefore achieved.

6.2 Sub-questions

1. *To what extent is the PS-InSAR deformation data visualization, used for the current communication of land subsidence in the Netherlands, interpretable?*

The current PS-InSAR deformation data visualization is relatively interpretable, but an increase in the user friendliness of the interface, an improvement of the accessibility, additional metadata, and an enhancement of the visualization of the data will make the visualization significantly more interpretable.

2. *What aspects of PS-InSAR deformation data visualization can be improved by linking it to LiDAR point clouds?*

From a user perspective, the improved aspects that result from linking LiDAR to PS-InSAR can be categorized into three classes: (1) an overall improvement of the level of coverage of the user needs, (2) an improvement of the need of users to view dynamic time-series, and (3) external benefits that are not directly related to the assumed user needs:

(1) The overall improvement of the coverage of the user needs results from significant added value of point cloud visualization to applications in which the end user can gain insights of the visualized phenomenon with the use of interactive, explorative and visualization methods and techniques.

(2) The improvement of the coverage of the need of users to view dynamic time series is due to the fact that point cloud visualizations can evolve along time, allowing users to derive trends in temporal changes of the visualized data.

(3) The external benefits are improvements that exclusively result from the combination of PS-InSAR with LiDAR. These external benefits are that [1] with point clouds, specific parts of deformation data can be linked to parts of the infrastructure, which can caid in early warning and maintenance management, that [2] (Regional) trends and errors in the radar processing can be mitigated and detected, and that [3] differential deformation trends can now be assessed, as signals can now be attached to the geometry of a building

3. *To what extent can PS-InSAR data and LiDAR point cloud be combined into one spatio-temporal visualization?*

It is not desired to combine PS-InSAR points and LiDAR point clouds into one visualization without a linking method. This is due to the fact that (1) the absolute position (x, y & z) of PS-InSAR points is relatively imprecise, whereas the absolute position of LiDAR points is relatively precise, and (2) that the displacement values cannot be assigned to objects represented by point clouds because of the imprecise absolute location of PS-InSAR points. The method of Van Natijne et al. (2018) is assumed to lead to the most accurate linking results as this method has specifically been designed for combining LiDAR with PS-InSAR, and because it is the only method that takes the radar signal and direction of flight of the radar system used to collect the PS-InSAR points into account. The method of Van Natijne et al. (2018) is however not complete yet, as the final step to link the PS-InSAR points to the dihedral of trihedral geometries is not yet implemented in the method. The absence of this step might result in an ambiguous graphical representation, as not all PS-InSAR points can be linked to just one surface represented by LiDAR points but to two surfaces. In addition, the method is knowledge and time intensive.

4. *Which design principles and graphical visualizations can be applied to the visualization to ensure interpretability?*

The design principles and graphical visualizations that ensure an interpretable visualization of the PS-InSAR points and LiDAR point clouds can be categorized into four perspectives: (1) needs of users of land subsidence communication, (2) communicating data to the public, (3) communicating three-dimensional data and (4) communicating spatio-temporal data.

(1) The suggested design principles and graphical visualizations from the user needs perspective are: the functionality to use different administrative levels, the functionality to configure layers, a selection tool, the functionality to draw boxes, visual graphs, the functionality to retrieve the data in different formats, pop-up legends, a locator map, a printing an downloading functionality, the functionality to compare maps, the functionality to view dynamic time-series, metadata, a search functionality and online accessibility without any restrictions.

(2) From the perspective of communicating data to the public, the suggested design principles and graphical visualizations associated to this perspective are: a step-by-step guide of the interface, an explanation of how to interpret the graphical visualizations, an explanation of areas that have no cell value or measure points, information of the used coordinate system and projection, spatial contextualization by using three-dimensional building geometries and two-dimensional infrastructural networks, and an interactive interface.

(3) The suggested design principles and graphical visualizations from the perspective of communicating three-dimensional data are: shape, patterns and appearances of objects do not have to look like exactly as they do in reality, the use of simple geometric shapes for map symbols to increase perception, good color contrast of buildings to the terrain, no exaggerated elevation, slightly transparent buildings to limit obscurance, a neutral sky color, a lateral lightning direction, image like representation of point clouds, structural patterns to represent map objects (patterns must not be too dense or too fine), represent objects that are represented by point clouds in such a way hat they can be identified on the foreground and background, and define the size of objects so that they do not obscure each other.
(4) From the perspective of communicating spatio-temporal data, the suggested design principles and graphical visualizations are: line graphs that represent parts of time-series superposed in one display, a data layer representing the spatial and temporal clustering of the data, and a layer representing the data in a space time cube.

5. *To what extent is the spatio-temporal visualization of the combination of PS-InSAR and LiDAR point clouds interpretable?*

The conceptual interface has been designed from the perspective of the user needs. As a result, the conceptual interface covers the user needs relatively good. The spatio-temporal aspect of the visualization allows users to both discover for each measure point the average displacement values for the individual years 2015, 2016, 2017, 2018 and 2019, and to discover the spatio-temporal patterns that can be derived from the spatial clusters for the individual years 2015, 2016, 2017, 2018 and 2019. Based on a comparison of a two-dimensional PS-InSAR visualization with a three-dimensional PS-InSAR visualization combined with LiDAR point clouds, it can be established that:
(1) The combined three-dimensional visualization of PS-InSAR points with LiDAR point clouds allows users to link a certain displacement pattern to differences in height. This link cannot be made in the two-dimensional visualization of PS-InSAR, as heights cannot be derived from this visualization.
(2) The combined three-dimensional visualization allows users to link a measure point to a specific part of an object. This is not possible with the two-dimensional visualization, as the height of a measure point relative to an object cannot be determined.
From a user needs perspective, a spatio-temporal perspective and the 'combining PS-InSAR points with AHN3 Lidar point clouds' perspective the visualization is perceived as relatively good interpretable.

6.3 Central Question

T*o what extent can a spatio-temporal visualization of a combination of PS-InSAR deformation data with LiDAR point clouds improve the interpretability of the communication of land subsidence in the Netherlands?*

First, whether a spatio-temporal visualization of a combination of PS-InSAR deformation is feasible depends on two factors: the availability of the required data, and the availability of resources required for linking PS-InSAR points to LiDAR point clouds with the method of Van Natijne et al. (2018). The data used for the conceptual interface of this research is all open, and therefore freely available. The method of Van Natijne et al. (2018) is assumed to be feasible when the resources time, and knowledge of the method are sufficiently accessible.

Second, from the perspective of the framework of the dimensions of dynamic geodesy and cartography (Van der Schans, 2001) it can be stated that the aim of the cartographer is to make a graphical representation of the actions, objects and processes of the human environment in such a way that users of the graphical representation derive the same actions, objects and processes of the human environment as collected by the cartographer. In the case of PS-InSAR data: the LiDAR point clouds allow users to derive the exact location of where the measure point is collected, and hence users derive the properties at the same location as the collected properties from the human environment.

Third, the spatio-temporal aspect of the visualization allows users to explore the dynamics and spatial patterns within the displacement time-series. The combined visualization of PS-InSAR points with LiDAR point clouds results in an overall improvement of the level of coverage of the user needs, a specific improvement of the coverage of the need of users to view dynamic time-series, and three external benefits that result from the fact that PS-InSAR points can now be attached to specific parts of objects:

(1) With point clouds, specific parts of deformation data can be linked to parts of the infrastructure, which can aid in early warning and maintenance management
(2) (Regional) trends and errors in the radar processing can be mitigated and detected
(3) Differential deformation trends can be assessed, as signals can be attached to the geometry of a building

Finally, it can be stated that when the resources, time and knowledge of the method of Van Natijne et al. (2018) are available, a spatio-temporal visualization of a combination of PS-InSAR deformation data with LiDAR point clouds can be implemented. This visualization can (1) allow users to derive the same deformation properties as the properties that are present in the human environment, (2) increase the level of coverage of the user needs of the users of land subsidence communication, (3) allow users to explore the spatial patterns and dynamics within the time-series of the displacement trends, which increases the level of coverage of the need of users to view dynamic time-series, (4) and allow users to attach a PS-InSAR displacement value to a specific part of an object. The answer to the central research question is:

Adding the spatio-temporal aspect and LiDAR point cloud aspect to a PS-InSAR visualization resulted in the previously described four advantages. These four advantages have a positive effect on how the visualization of land subsidence is interpreted by the users of land subsidence communication in the Netherlands. It can therefore be stated that the two aspects add a significant level of interpretability to the communication of land subsidence in the Netherlands.

7

Bibliography

Ackere, S. van, Glas, H., Beullens, J., Deruyter, G., De Wulf, A., & De Maeyer, P. (2016). Development of a three-dimensional dynamic flood Web GIS visualisation tool. *Flood Risk Management and Response*, *106*.

Andrienko, N., Andrienko, G., Fuchs, G., Slingsby, A., Turkay, C. & Wrobel. S. (2020). *Visual Analytics for Data Scientists*. Switzerland: Springer.

ArcGIS Hub (2019). *Dataset: Watershapsgrenzen*. Retrieved on February 8, 2021, from https://hub.arcgis.com/datasets/7adde9c6ad2d454780a725af3c42f3f2_0.

Azari, H., Cheng, I. & Basu, A. (2012). A time-series three-dimensional hierarchy for real-time dynamic point cloud interaction. SIGGRAPH Asia 2012 Technical Briefs.

Bærentzen, J. A., Gravesen, J., Anton, F., & Aanæs, H. (2012). 3D surface registration via iterative closest point (ICP). In *Guide to Computational Geometry Processing* (pp. 263-275). Springer, London.

Bodemdalingskaart (2020). Download gegevens bodembeweging. Retrieved on January 5, 2021, from https://bodemdalingskaart.nl/nl/download-kaartlagen/.

CBS (2018). *ICT-gebruik huishoudens.* Retrieved November 30, 2020, from https://longreads.cbs.nl/ict-kennis-en-economie-2018/ict-gebruik-huishoudens/#:~:text=Computers%20zijn%20niet%20meer%20weg,van%20de%20huishoudens%20een%20tablet

Chen, Z. (2016). *The Application of Airborne Lidar Data in the Modelling of 3D Urban Landscape Ecology*. Cambridge Scholars Publishing.

Clevers, J.G.P.W. (2017). Chapter 1. What is Sensing? In: Remote Sensing reader (Ed. J.G.P.W. Clevers), Wageningen University

Clevers, J.G.P.W. (2017) Chapter 4. Microwave Remote Sensing In: Remote Sensing reader (Ed. J.G.P.W. Clevers), Wageningen University

De Rechtspraak (2019). *Uitspraken.* Retrieved September 16, 2020, from https://linkeddata.overheid.nl/front/portal/document-viewer?ext-id=ECLI:NL:RBDHA:2019:3623.

DiBiase, D. (1990), Visualisation in the Earth sciences. *Earth and Mineral Sciences, Bulletin of the College of Earth and Mineral Sciences, The Pennsylvania State University 59*, 2, 13-18.

Donker, F. W., & Loenen, B. van (2016). Sustainable business models for public sector open data providers. *JeDEM-eJournal of eDemocracy and Open Government*, *8*(1), 28-61.

Earth Esa (2020). *Radar course 2.* Retrieved on October 19, 2020 from https://Earth.esa.int/web/guest/missions/esa-operational-eo-missions/ers/instruments/sar/applications/radar-courses/content-2/-/asset_publisher/qIBc6NYRXfnG/content/radar-course-2-real-aperture-radar#:~:text=Azimuth%20resolution%20describes%20the%20ability,motion%20vector%20of%20the%20sensor.

Elzakker, C. P. van (2004). *The use of maps in the exploration of geographic data.* Utrecht University.

Elzakker, C. P. van, Ormeling, F., Köbben, B. J., & Cusi, D. (2003). Dissemination of census and other statistical data through web maps. In *Maps and the internet*, 57-75.

Esri (2012). *ArcGIS 10.1 Geographic and Vertical Transformation Tables.* Retrieved on January 24, 2021, from https://resources.arcgis.com/en/help/main/10.1/003r/pdf/geographic_transformations.pdf.

Esri (2020). *ArcGIS for JavaScript.* Retrieved on 29 September, 2020, from https://developers.arcgis.com/javascript/.
Esri (2020). *Create Thiessen Polygons (Analysis)*. Retrieved on January 20, 2021, from https://pro.arcgis.com/en/pro-app/latest/tool-reference/analysis/create-thiessen-polygons.htm.
Esri (2020). *LAS Building Multipatch.* Rerieved on November 30, 2020, from https://pro.arcgis.com/en/pro-app/tool-reference/3d-analyst/las-building-multipatch.htm.
Esri Nederland (2012). *Topo RD*. Retrieved on February 16, 2021, from https://www.arcgis.com/home/item.html?id=1d1d425122e74d4d87695e163f3f10ce.
Esri Nederland (2018). *Elevation 3D (RD).* Retrieved on January 24, 2021, from arcgis.com/home/item.html?id=1da89d92880447129da0b02721ce9066.
Feringa, W. (2019). Data Visualization Chart. University of Twente.
Gagliardi, D., Schina, L., Sarcinella, M. L., Mangialardi, G., Niglia, F., & Corallo, A. (2017). Information and communication technologies and public participation: interactive maps and value added for citizens. *Government Information Quarterly*, *34*(1), 153-166.
Gehlot, S., Ketelaar, V. B. H., Verbree, E., & Hanssen, R. F. (2005). Conceptual framework for PS-insar deformation interpretation assisted by geo-information technology. In *High Resolution Earth Imaging for Geospatial Information*, 17-20.
Gehlot, S., & Verbree, E. (2006, September). Web-based sharing of a geo-processing chain: combination and dissemination of data and services. In *Proceedings of the International Symposium on Geospatial databases for Sustainable Development, eds. S. Nayak & SK Pathan, ISPRS TC Commitee IV Geo-databases and Digital Mapping, Goa, India*.
Gils, M. M. W. van, Stouthamer, E., & Groothuijse, F. A. G. (2020). Towards a legal strategy fitting today's challenge of reducing impacts of subsidence in the Netherlands. *Proceedings of the International Association of Hydrological Sciences*, *382*, 825-829.
Grus, L., Crompvoets, J., & Bregt, A. (2007). A Multi-View Framework to Assess Spatial Data Infrastructures. *International Journal of Spatial Data Infrastructures Research*, *2*, 33-53.
GSI (2020). *Monitorin the Earth Deformation from Space.* Retrieved on 19 October 2020 from https://vldb.gsi.go.jp/sokuchi/sar/qanda/qanda-e.html. Japan: Geospatial Information authority of Japan.
Haeberling, C., Bär, H., & Hurni, L. (2008). Proposed cartographic design principles for 3D maps: a contribution to an extended cartographic theory. *Cartographica: The International Journal for Geographic Information and Geovisualization*, *43*(3), 175-188.
Hanssen, R. F. (2001). *Radar interferometry: data interpretation and error analysis* (Vol. 2). Springer Science & Business Media.
Hu, Y., & Li, W. (2017). Spatial data infrastructures. *arXiv preprint arXiv:1707.03969*.
Javaheri, A., Brites, C., Pereira, F., & Ascenso, J. (2019). Point cloud rendering after coding: impacts on subjective and objective quality. *arXiv preprint arXiv:1912.09137*.
Knippers, R. (2019). E-lecture visualization: how to map data? [Powerpoint slides]. University of Twente. Retrieved from https://uu.blackboard.com/bbcswebdav/pid-3235022-dt-content-rid-28595332_2/courses/GEO-2019-JAAR-GEO4-GIMA1-V/GEO-2019-JAAR-GEO4-GIMA1-V_ImportedContent_20190715053432/GEO-2018-2-GEO4-GIMA1-V_ImportedContent_20180710040907/E-lecture%20Visualization%202017%20slides.pdf
Lavery, D. (2019). S*mart Choices for Basemaps and Color Ramps When Mapping Demographic Data*. Retrieved on Jauary 25, 2021, from https://www.esri.com/arcgis-blog/products/arcgis-online/mapping/smart-choices-for-basemaps-and-color-ramps-when-mapping-demographic-data/.
MacEachren, A.M. & M.J. Kraak (1997), Exploratory cartographic visualization: advancing the agenda. *Computers & Geosciences*, 23, 4, pp. 335-344.

Magnusson, M. (2009). *The three-dimensional normal-distributions transform: an efficient representation for registration, surface analysis, and loop detection* (Doctoral dissertation, Örebro universitet).

McCormick, M. P., & Leavor, K. R. (2013). Active lidar remote sensing. In *Aerosol Remote Sensing* (pp. 283-313). Springer, Berlin, Heidelberg.

Natijne, A. L. van, Lindenbergh, R. C., & Hanssen, R. F. (2018). Massive linking of PS-InSAR deformations to a national airborne laser point cloud. *International Archives of the Photogrammetry, Remote Sensing and Spatial Information Sciences - ISPRS Archives*, 42(2), 1137-1144.

Natijne, A.L. van (2018). Locating PS-InSAR derived deformation using LiDAR point clouds.

NCG (2020). *Actuele Bodemdalingskaart Nederland*. Retrieved September 1, 2020, from https://bodemdalingskaart.portal.skygeo.com/portal/bodemdalingskaart/u1/viewers/basic/?lang=nl/.

NCG (2020). *De fysische oorzaken van bodembeweding in Nederland.* Retrieved on September 16, 2020, from https://bodemdalingskaart.nl/nl/kennis-datacentrum/fysische-oorzaken/.

North Road (2020). *Announcing the Point Cloud Data in QGIS Crowdfunding Campaign*. Retrieved on January 20, 2021, from https://north-road.com/2020/08/24/announcing-the-point-cloud-data-in-qgis-crowdfunding-campaign/.

Overheid (2020). *Bodembeweging InSAR (harde topografie Nederland) - Sentinel-1 Baan 139 - 20150119-20191031.* Retrieved September 5, 2020, from https://data.overheid.nl/dataset/13130-bodembeweging-insar--harde-topografie-nederland----sentinel-1-baan-139---20150119-20191031.

PDOK (2020). *Dataset: Actueel Hoogtebestand Nederland (AHN3).* Retrieved September 5, 2020, from https://www.pdok.nl/introductie/-/article/actueel-hoogtebestand-nederland-ahn3-.

PDOK (2021). *Dataset: Bestuurlijke Grenzen.* Retrieved on February 8, 2021, from https://www.pdok.nl/geo-services/-/article/bestuurlijke-grenzen.

PDOK (2020). *Dataset: Bodemkaart van Nederland*. Retrieved on January 5, 2021, from https://www.pdok.nl/-/de-bodemkaart-van-nederland-beschikbaar-bij-pdok.

PDOK (2020). *Dataset: luchtfoto 2019 RGB*. Retrieved on January 5, 2021, from https://www.pdok.nl/-/nieuw-luchtfoto-2019-beschikbaar-bij-pdok.

Pettorelli, N., Schulte to Buehne, H., Shapiro, A. & Glover-Kapfer, P. (2018). *Conservation Technology Series Issue 4: SATELLITE REMOTE SENSING FOR CONSERVATION.* 4. United Kingdom: WWF United Kingdom.

Poux, F. (2019). *The Smart Point Cloud: Structuring 3D intelligent point data* (Doctoral dissertation, Université de Liège, Liège, Belgique).

Poux, F. (2020). *How to represent 3D Data?* Retrieved on October 28, 2020, from https://towardsdatascience.com/how-to-represent-3d-data-66a0f6376afb.

Pradhan, B., & Sameen, M. I. (2020). *Laser Scanning Systems in Highway and Safety Assessment*. Springer International Publishing.

Rubalcava, R. (2017). *Introducing ArcGIS API 4 for JavaScript: Turn Awesome Maps Into Awesome Apps*. Apress.

Schans, R. van der. (2001). GIS-Kartografie: opbouw en gebruik van landschapsmodellen en visualizatiemodellen. In E. Verbree (Ed.), *CT1130 Inleiding Geoinformatie.*

Schmitt, M., Tupin, F., & Zhu, X. X. (2017). Fusion of SAR and optical remote sensing data—Challenges and recent trends. *2017 IEEE International Geoscience and Remote Sensing Symposium (IGARSS)*, 5458-5461.

Schoffelen, J., Claes, s., Huybrechts, L.., Martens, S., Chua, A. & Van de Moere, A. (2015): *Visualising things. Perspectives on how to make things public through visualisation*, CoDesign, DOI: 10.1080/15710882.2015.1081240

SkyGeo (2020). De 3 stappen van bodemdalingskaart naar een succesvolle InSAR implementatie [Webinar].

Accessed on November 3, 2020.
SkyGeo (2020). *InSAR Technical Background.* Retrieved on September 2, 2020, from https://skygeo.com/insar-technical-background/.
Stouthamer, E., Erkens, G., Cohen, K.M., Hegger, D.L.T., Driessen, P.P.J., Weikard, H.P., Hefting, M., Hanssen, R.F., Fokker, P.A., den Akker, J. van and Groothuijse, F.A.G. (2020). Dutch National Scientific Research Program on Land Subsidence: Living on Soft Soils-Subsidence and Society. *Proceedings of the International Association of Hydrological Sciences*, 382, 815-819.
Tre Altamira (2020). *SAR Imagery.* Retrieved on 19 October 2020 from https://site.tre-altamira.com/insar/.
Tupin, F. (2010). Fusion of optical and SAR images. *Radar Remote Sensing of Urban Areas, Springer*, 133–159
Van der Marel, H. (2014). Reference systems for surveying and mapping. Lecture notes, Faculty of Civil Engineering and Geosciences Delft University of Technology, Delft, The Netherlands.
Van Oosterom, P., Martinez-Rubi, O., Ivanova, M., Horhammer, M., Geringer, D., Ravada, S., Tijssen, T., Kodde, M. and Gonçalves, R., (2015). Massive point cloud data management: Design, implementation and execution of a point cloud benchmark. *Computers & Graphics*, 49, pp.92-125.
Verbree, E. and Van Oosterom, P. (2015). *Exploratieve puntenwolken*. GISt Rapport No. 68. Delft: Delft University of Technology.
Webster, T.L. and Forbes, D.L. (2006) "Airborne laser altimetry for predictive modeling of coastal storm-surge flooding." *Remote sensing of aquatic coastal ecosystem processes*. Springer, Dordrecht. 157-182.
Welle Donker, F. (2020). User needs analysis. [Powerpoint slides]. Retrieved from https://uu.blackboard.com/webapps/blackboard/content/listContent.jsp?course_id=_123690_1&content_id=_3427894_1.
Wolniak, R. (2017). The Design Thinking method and its stages. *Systemy Wspomagania w Inżynierii Produkcji*, *6*(6), 247-255.
Yu, T. Y. (2008). A new way to investigate dynamics in a storm using Doppler spectra from weather radar. In *24th Conference on IIPS*.
Zhang, L., van Oosterom, P., & Liu, H. (2020). Visualization of point cloud models in mobile augmented reality using continuous level of detail method. *The International Archives of Photogrammetry, Remote Sensing and Spatial Information Sciences,* 44, 167-170.
Zlatanova, S., Rahman, A. A., & Shi, W. (2004). Topological models and frameworks for 3D spatial objects. *Computers & geosciences*, *30*(4), 419-428.

Appendix A. Bertin's theory on visual variables (Feringa, 2019)

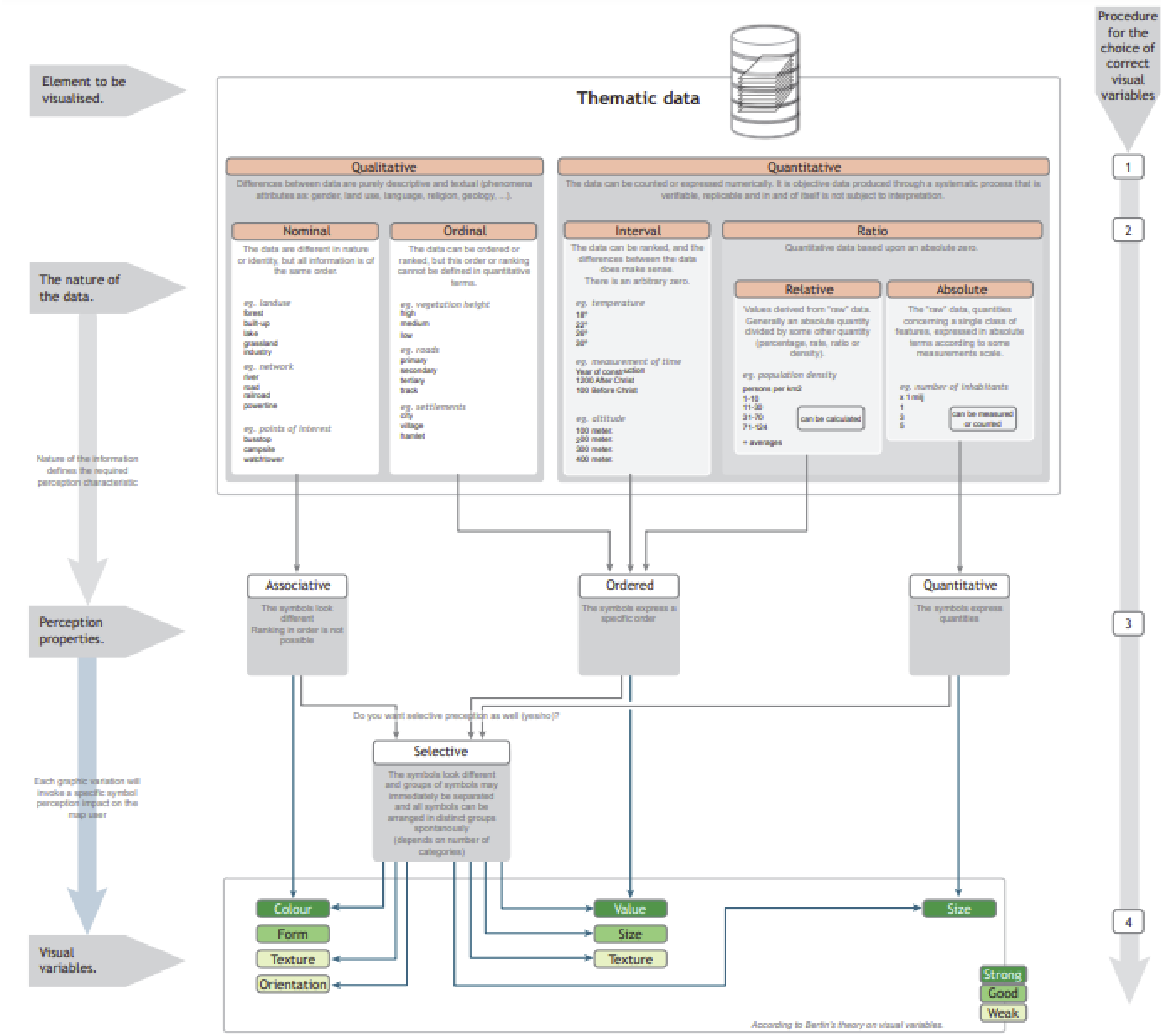

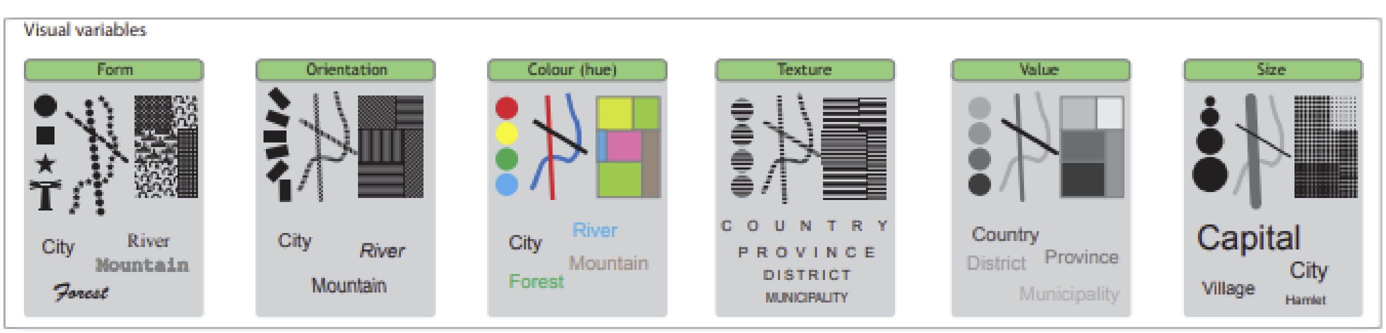

Appendix B. Legend subsurface properties

- AAK Afgegraven kleigronden
- AAP Aangemaakte petgaten
- ABk Kleiige beekdalgronden
- ABl Lossige beekdalgronden
- ABv Venige beekdalgronden
- ABz Zandige beekdalgronden
- AD Duin- en kweldergronden
- AEk9 Geegal. en verw. zeekleigronden zonder veen binnen 120 cm; zw. zavel en l. klei
- AEm5 Geegal. en verw. zeekleigronden met plaats. veen binnen 120 cm; zavel
- AEm8 Geegal. en verw. zeekleigronden met plaats. veen binnen 120 cm; klei
- AEm9 Geegal. en verw. zeekleigronden met plaats. veen binnen 120 cm; zw. zavel en l. klei
- AEm9A Geegal. en verw. zeekleigronden met plaats. veen binnen 120 cm of met niet-ger. ondergrond; zw. zavel en l. klei
- AEp6A Geegal. en verw. zeekleigronden (eerd- en vaaggronden met ger. ondergrond); zavel en l. klei,kalkrijk
- AEp7A Geegal. en verw. zeekleigronden (eerd- en vaaggronden met ger. ondergrond); zw. zavel en klei,kalkrijk
- AFk Roodoornige kleiige Vechtdalgronden
- AFz Roodoornige zandige Vechtdalgronden
- AGm9C Hollebollige, gemoerde zeekleigronden; zw. zavel en l. klei
- AHa Glauconiethellinggronden
- AHc Loss-, terras- en kalksteenhellinggronden
- AHk Kalksteenhellinggronden
- AHl Loss- en terrashellinggronden
- AHs Vuursteenhellinggronden
- AHt Terrashellinggronden
- AHv Terras-,tertiair-,kalksteen- en veenhellinggronden
- AHz Loss-,tertiair- en terrashellinggronden
- AK Kreekbeddingen
- ALu Linge-uiterwaardgronden
- AM Mengelgronden
- AMm Gronden in oude maasmeanders
- AO Overslaggronden
- AP Petgaten
- AQ Met huisvuil opgehoogde gronden
- AR Roergronden
- AS Stuifzandgronden
- AVk Veenafbraakgebied
- AVo Veen in ontginning
- AWg Warmoezerijgronden (gerijpt)
- AWo Warmoezerijgronden (ongerijpt)